USE OF

RADIAL AND VERTICAL MAGNETIC FIELD COMPONENTS

IN

TIME - DOMAIN

ELECTROMAGNETIC SOUNDING.

by

Ofiafate Ofrey.

A thesis submitted to the Faculty and the Board of Trustees of the Colorado School of Mines in partial fulfillment of the requirements for the degree of Master of Science (Geophysical Engineering).

Signed ______________________
Ofiafate Ofrey

Golden, Colorado

Date: April 17, 1975.

Approved : ______________________
Dr. G. V. Keller,
Thesis Advisor and
Head of Department.

TO MY PARENTS.

ACKNOWLEDGEMENT.

I express appreciation to Drs. G.V. Keller, R.C. Holmer, and Phil Romig for their helpful suggestions. I also wish to express my thanks to Dr. Cathy Skokan of C.S.M.

Support for the study was under Colorado School of Mines, Office of Research Services project P - 308, with funds from National Science Foundation.

CONTENTS

LIST OF FIGURES

LIST OF FIGURES (Continued)

LIST OF TABLES

ABSTRACT

In the investigation of a geothermal prospect, it is often necessary to use some vertical sounding technique to determine the depths to the boundaries of the various layers in the earth. One method of determining the electrical properties of the earth as a function of depth consists of measuring the electromagnetic coupling between a current-carrying wire and an induction loop receiver.

In this study, a time-domain electromagnetic (TDEM) survey was carried out in the Black Rock Desert area of Nevada, using a sensitive three component magnetometer to measure the vertical and radial components of the electromagnetic field generated by the current in a grounded wire source.

The vertical component was interpreted first by the early time asymptote method, and then by comparing with theoretical curves for a layered earth model generated by linear filter theory. In the interpretation, a two-layered earth model along with a conductive surface layer was assumed. The surface layer has resistivity values ranging from 0.5 to 1 ohm-meter, and thickness from 80 to 200 meters. The second layer which is the one of

interest as a possible geothermal reservoir has resistivity values from 1 to 15 ohm-meters and thickness from 300 to 900 meters. The basement resistivity values range from about 50 ohm-meters to 550 ohm-meters

In case of the radial field, it was discovered that good interpretations for resistivity cannot be easily obtained. However, the radial field is a sensitive indicator of lateral changes. A qualitative interpretation was done using the distortions on the recorded transients to locate a major fault.

The results obtained agree fairly well with those obtained in other concurrent geophysical studies.

In conclusion, this interpretation has demonstrated the usefulness of measuring the radial component of the electromagnetic field and the usefulness of the three-component magnetometer in time-domain electromagnetic sounding.

INTRODUCTION

An electromagnetic survey of the Black Rock Desert area of Nevada is part of a geothermal research project being conducted by the Department of Geophysics, Colorado School of Mines. Other concurrent studies include Dipole (resistivity) mapping, microseimicity, and Infra red imagery.

In the investigation of a geothermal prospect, it is often necessary to use some vertical sounding technique to determine depths to the boundaries of the various layers in the earth. Recent research at the Colorado School of Mines indicates that the electromagnetic sounding method is useful for this purpose.

One method of measuring the electrical properties of the earth as a function of depth consists of measuring the electromagnetic coupling between a current-carrying wire and an induction loop receiver. In time-domain electromagnetic sounding, an electromagnetic field is generated by reversing the direction of current in a grounded wire abruptly. Recordings of the transient magnetic field generated are then made at stations around the grounded wire.

The field work was done in June 1974.

LOCATION AND GENERAL GEOLOGY

The Black Rock Desert is situated in the North-western part of Nevada (Figure 1 is a location map and Figure 2 shows an index map with the area of investigation marked)

The geology of the Black Rock Desert area is inadequately known, hence only a brief general description is presented. Figure 3 is a generalised geologic map.

The Black Rock prospect is in the Basin and Range province of Northwestern Nevada. It has long been recognized that the Basin and Range province is characterised by extensive normal faulting with associated major vertical displacements. The Black Rock Desert area is no exception, major faults occur in this area with vertical displacements in the order of a few thousand feet (Bonham, 1969)

According to Osmond (1960), the Basin and Range province was elevated during the late Tertiary and Quarternary. The uplifted areas are composed of Cretaceous granodiorite, Tertiary volcanics and Permian metavolcanics. The lower area are filled with Quarternary material. This includes alluvium and Lake Lahortan sediments which consists of clays, silts, algal material and minor sands.

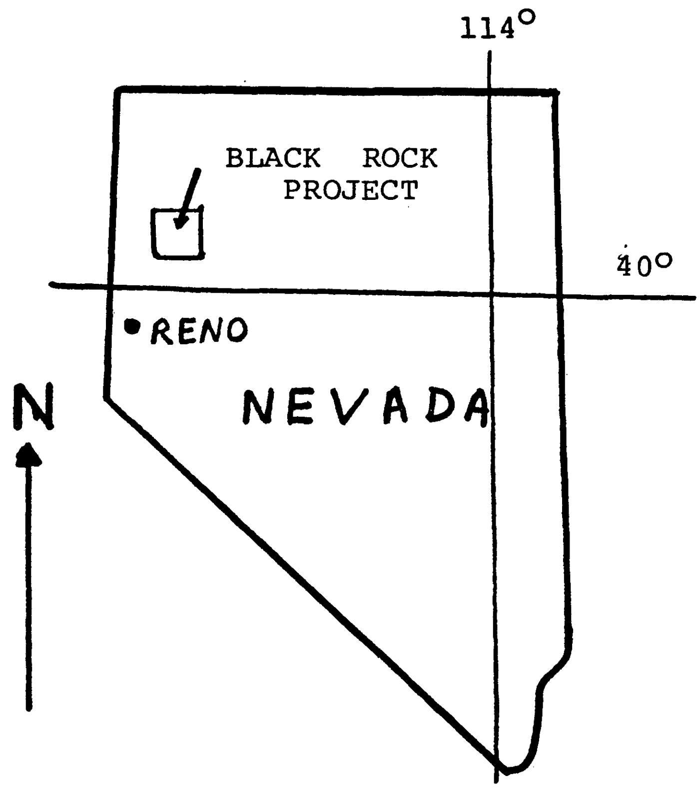

BLACK ROCK PROJECT

WASHOE, HUMBOLT,
PERSHING COUNTIES,
NEVADA.

Figure 1

Location map showing area of Black Rock project.

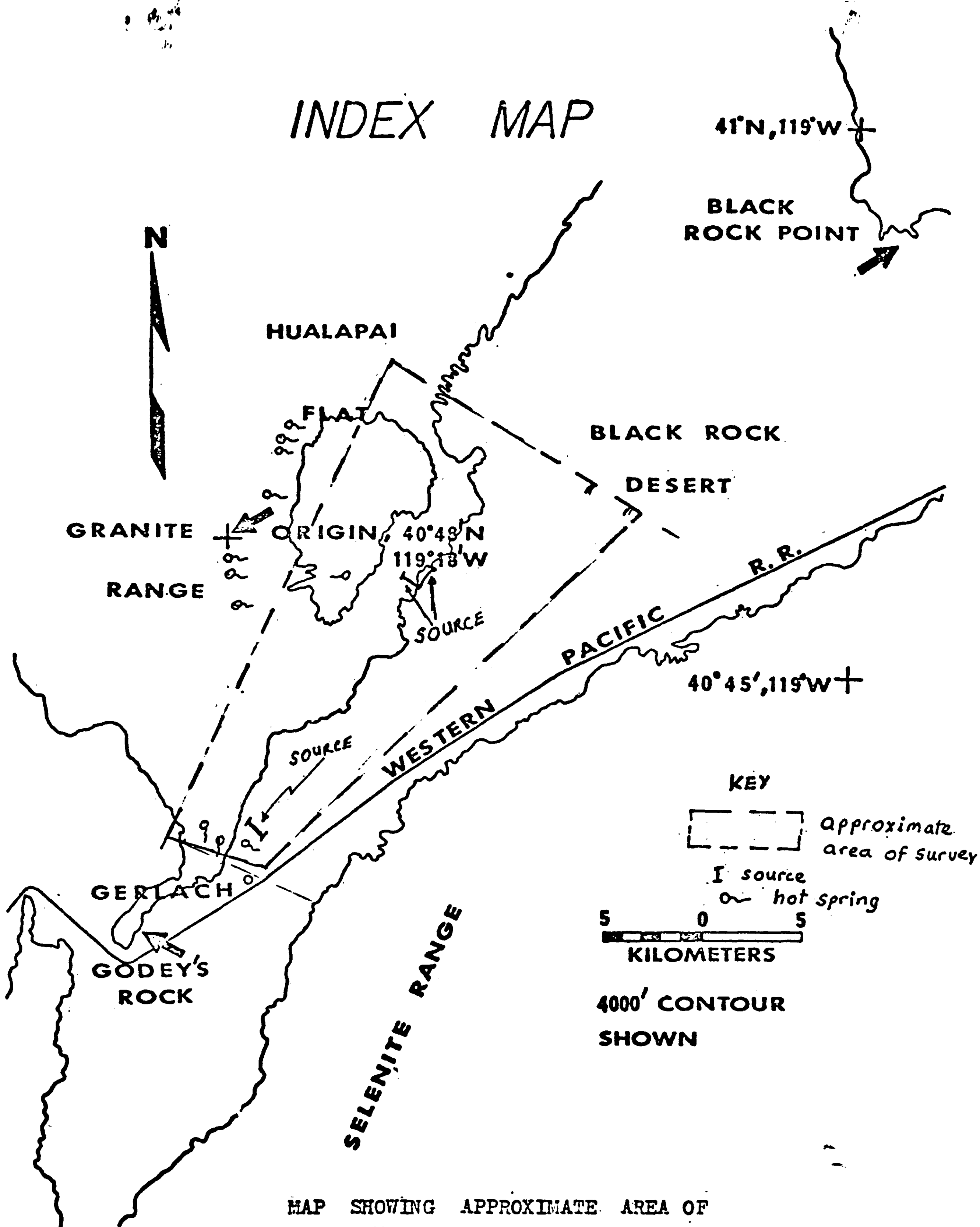

MAP SHOWING APPROXIMATE AREA OF SURVEY AND LOCATION OF SOURCES AND HOT SPRINGS.

---Figure 2

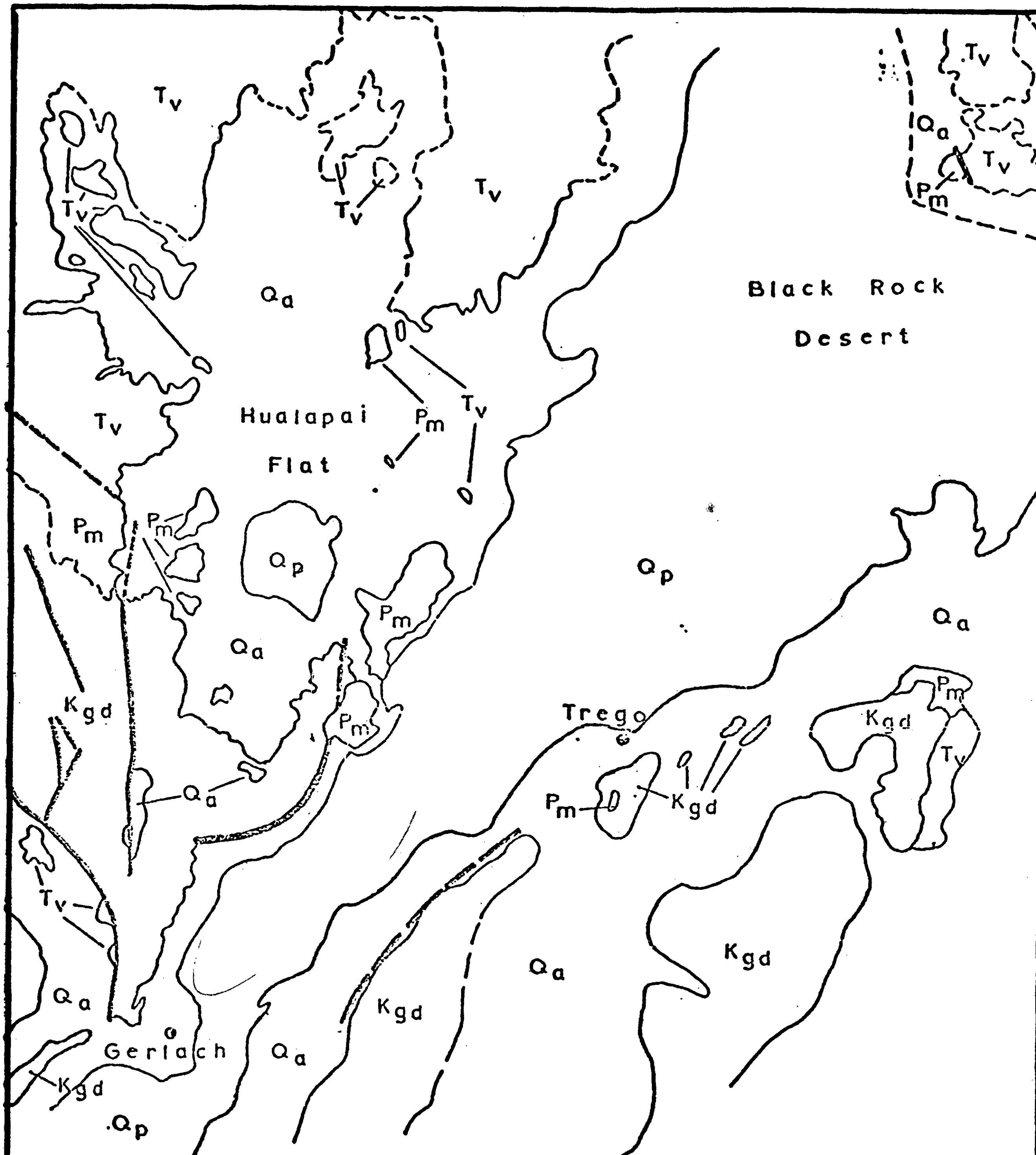

Figure 3

GEOLOGY of the BLACK ROCK AREA

Qa	Quaternary alluvial	Qp	Quaternary Playa
Tv	Tertiary Volcanics		Recent Faults
Kgd	Cretaceous Granodiorite		0 5 kilometers
Pm	Permian Metamorphics		

The topography of the Black Rock Desert area is typical of the Basin and Range province. The Granite Range is the predominant topographic feature in the area. Parallel to it is the low lying Black Rock Desert itself and the Hualapi Flat.

DETECTION OF MAGNETIC FIELD COMPONENTS

Normally, a large induction loop laid on the ground is used to detect the electromagnetic field at a receiver site. Such receiver coils are commonly 1000 to 2000 feet lengths of multi-conductor wire laid in the form of a square. An induction coil of this type has the advantage of being an extremely simple means for detecting small magnetic field over the frequency range of interest--0.1 to 30 hertz, but has several limitations. Vibrations of the induction coil cause electrical noise to be generated and so it is necessary to seek out locations where the coil can be laid flat on the earth so that wind will not cause it to move. Often such locations are difficult to find where a survey is to be made. Another limitation of large induction coils is that only the vertical component of magnetic field can be measured. This is a major limitation, as measurement of the horizontal field components give indications of lateral changes in the resistivity, and thereby locating vertical boundaries caused by faults and other lateral discontinuities.

In this survey a sensitive three-component magnetometer manufactured by Superconducting Technology Incorporated of San Francisco, California was used. This magnetometer also contains induction coils as the sensing elements but each coil is one centimeter in diameter and is superconducting, being maintained in a liquid helium environment at a temperature of about 4°K.

The basic detector in this magnetometer is the SQUID (Superconducting QUantum Interference Device). There are two types of SQUID, the direct-current (dc) SQUID and the radio frequency (rf) SQUID. The magnetometer used in this survey has a rf SQUID.

The rf SQUID was developed by Zimmerman and his co-workers, Mercereau and Nisenoff (Clarke, 1974). It consists of a single Josephson Junction mounted on a superconducting ring. A Josephson Junction can be described as follows. Two super conductors separated by a thin (10 to 20 angstroms) insulating barrier at normal temperatures will have barrier resistance of several ohms. However, at very low temperatures when the metals are superconducting, the barrier resistance vanishes. It is thus possible to pass a small supercurrent through the junction without developing any voltage across the barrier. This process is known as the d-c Josephson effect. The maximum value of current that can flow as a supercurrent is I_c, known as the critical current. The value of I_c depends upon junction parameters and temperature. If the external current exceeds I_c, a voltage appears across the junction. When there is a voltage across a Josephson Junction, the supercurrent still exists but oscillates with time. This phenomenon is the a-c Josephson effect. The frequency of the oscillation is related in a simple way to the voltage V across the junction by the Josephson voltage-frequency relation (Clarke, 1974) which is as follows:

$$f = \frac{2eV}{h}$$

where

f is frequency of oscillation

e is electronic charge

V is the voltage across the Josephson Junction

and h is Planck's constant

Figure 4 is a diagram of a Josephson Junction and Figure 5 shows a rf SQUID.

A steadily increasing magnetic field induces quantum transitions in the SQUID. If the junction is repetitively driven into a voltage-supporting state at superconducting temperatures, there will be an average circulating supercurrent that is periodic in the applied flux. This current is detected by coupling the SQUID to the inductance of a resonant inductance-capacitance (LC) circuit. (Figure 5) An alternating current at the resonant frequency of

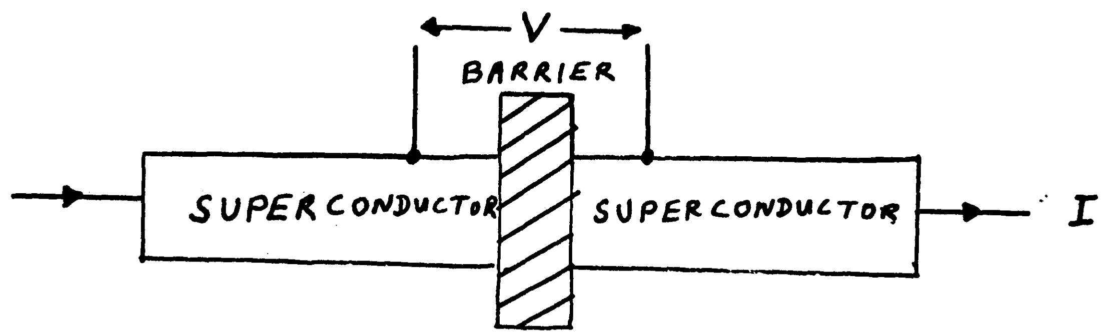

Figure 4 A Josephson Junction.

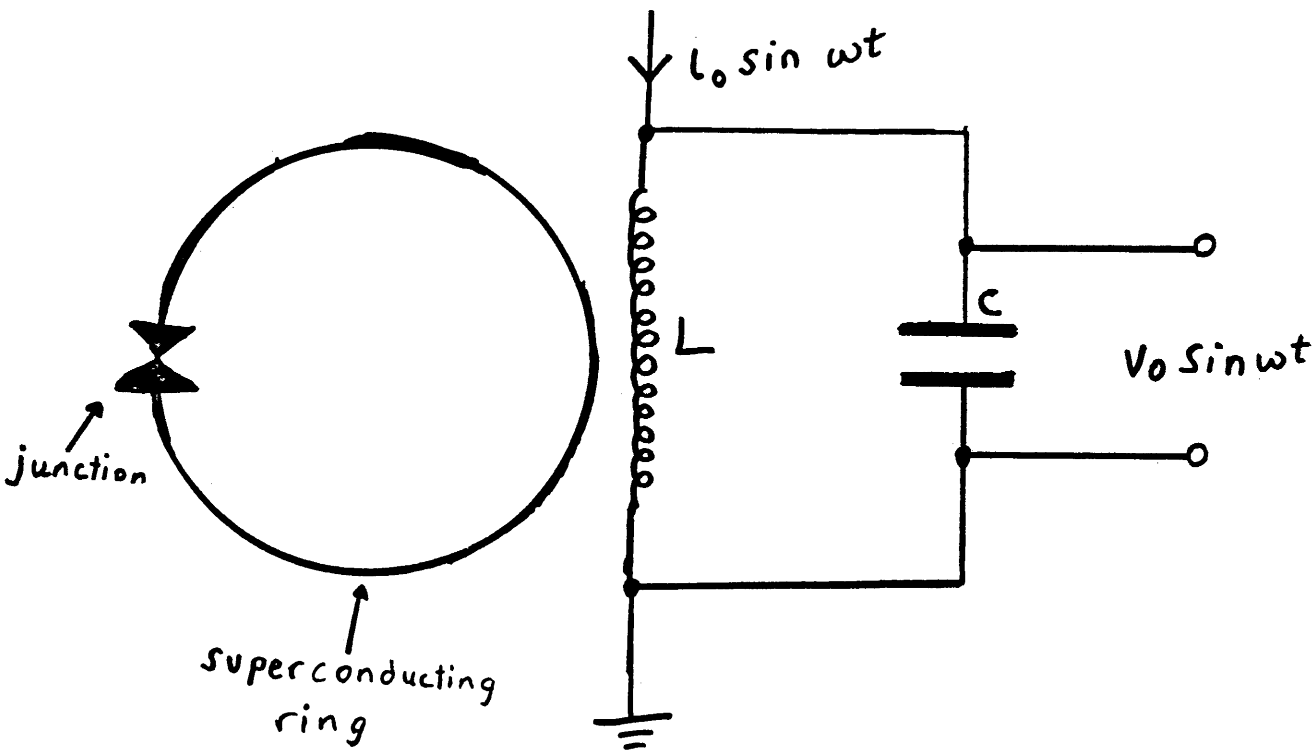

Figure 5 A rf SQUID.

after Clarke(1974)

30 mega-hertz generates an alternating voltage across the resonant circuit The amplitude of this rf voltage depends on the circulating supercurrent in the SQUID and is therefore periodic in the flux applied to the SQUID. The rf voltage is amplified and rectified using conventional electronic circuitry.

The rf SQUID produces a voltage that is periodic in the flux applied to it. The SQUID is a digital magnetometer in that one only has to count the oscillations in voltage to measure any change in the applied field. However, in practice the SQUID is incorporated in a feedback circuit, the whole system producing a voltage output that is linearly proportional to changes in the applied flux. The principle is illustrated in Figure 6.

The SQUID is biased with a current I_o as described earlier. The voltage applied across the SQUID is amplified by conventional electronic circuitry. The output from the amplifier is fed via a resistance R_f into a coil L_f which is coupled to the SQUID. Suppose a small field dH is applied to the SQUID, the change in the SQUID voltage is amplified and fed back as a current I_f into the coil L_f. The flux produced by this current opposes and exactly cancels dH. The total flux threading the SQUID is therefore zero, and the output voltage $V_o = I_f R_f$ is linearly proportional to dH. The SQUID is thus the null detector in a feedback system.

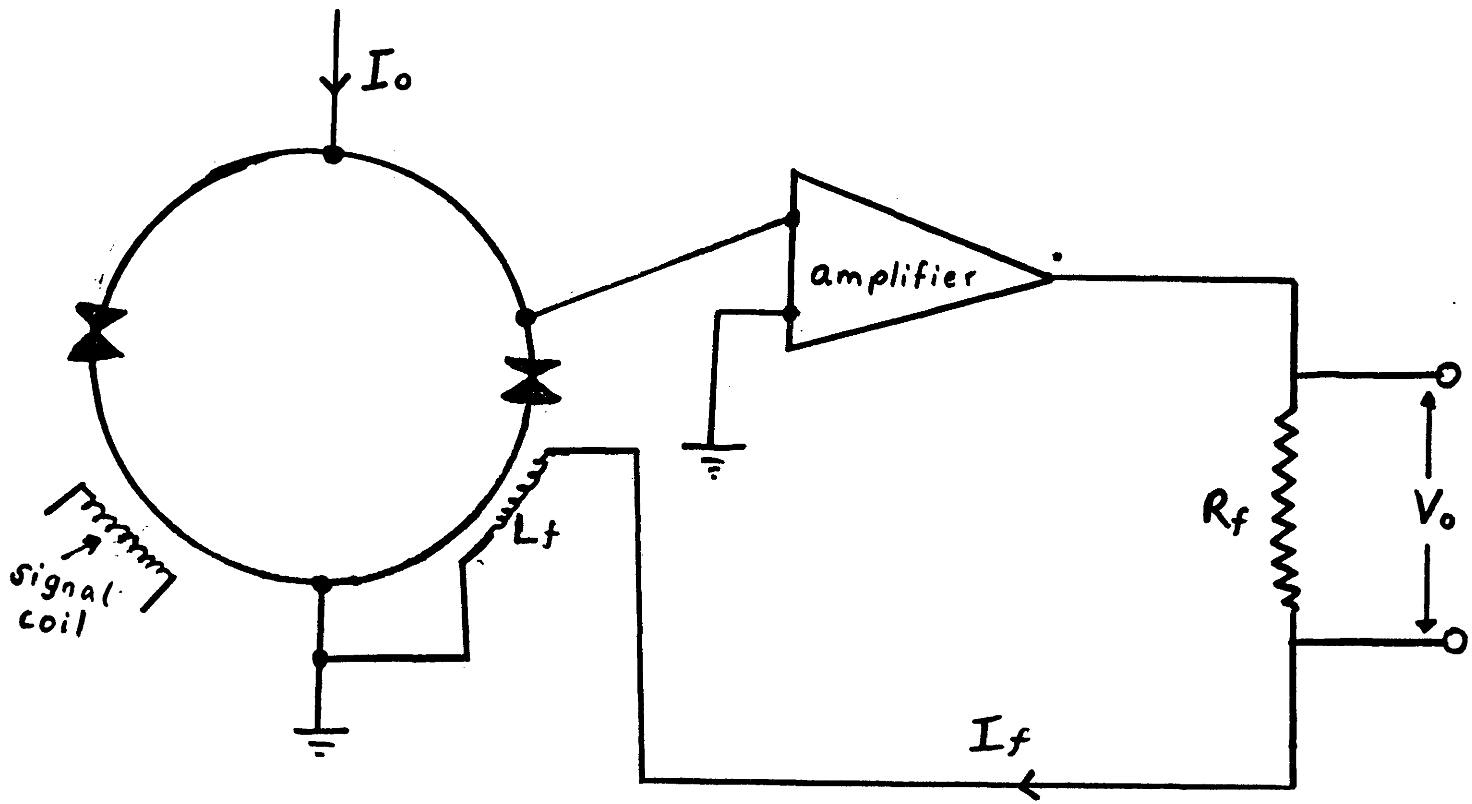

Figure 6 Feedback circuit for a SQUID.

after Clarke (1974)

The threshold sensitivity in the equipment used in this survey is about 2×10^{-3} gammas with a flat frequency response from DC. Selectable filters of 10, 100 and 1000 hertz were available for the upper frequency limit.

FIELD PROCEDURE AND DATA PREPARATION

Current Source

Figure 7 is a schematic block diagram of the source equipment. In this survey, the power source used is a 30 KVA Onan generator with an output of 220 volts, 60 cycle A-C. The generator output was stepped up to 440, or 880 volts with a three phase transformer and run through a Variac to keep a steady current.

The A.C. voltage from the transformer was rectified and an asymetrical square wave was applied to the source which consisted of a length of copper wire grounded at both ends. The current between the electrodes was recorded on an Esterline Angus T - 171 - B chart recorder.

Three source locations were used with lengths 1850, 1615, and 1463 meters.

Receiver

The receiver equipment consisted of a cryogenic three-component magnetometer with accompanying electronics and a Gould Brush Mark 250 chart recorder.

Magnetic field detected by the magnetometer is fed into an accompanying amplifier which is set to have a frequency response from DC to 100 hertz. The amplified

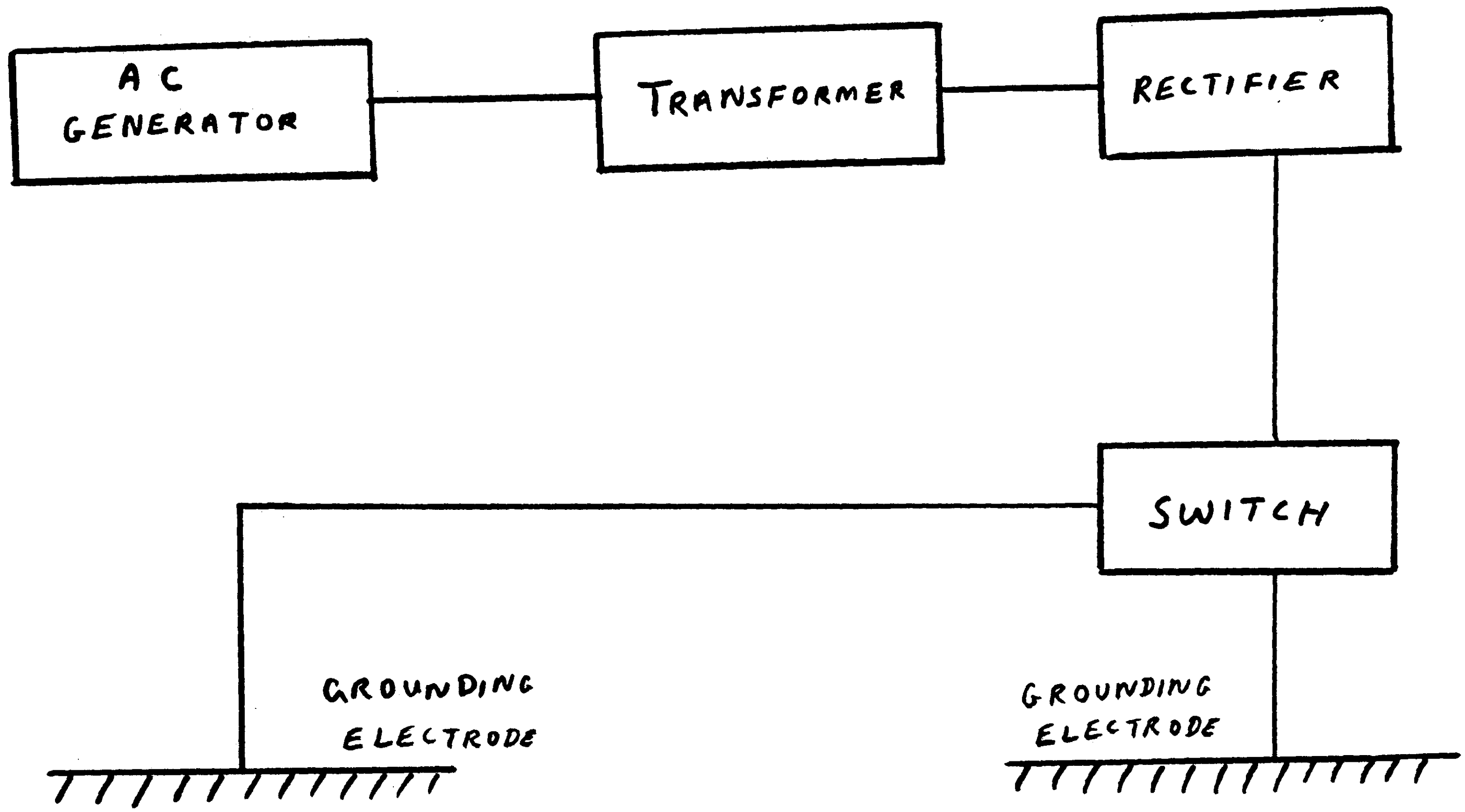

Figure 7 Schematic block diagram, showing source equipment.

signal is then recorded on the Gould Brush chart recorder which has a frequency response from DC to 30 hertz.

With a short line source, measurements are taken at distances (usually about five source lengths) such that the source appears to be a dipole. It was observed that at distances five source lengths away, the electromagnetic field is too small to be detected by the equipment in use, measurements were therefore made at distances less than five source lengths. Figure 8 shows the location of the sources and stations.

Vanyan (1967) stated that the dipole approximation worked well for distances from the source which are a few times the depth to a boundary, therefore a dipole approximation was used in the interpretation of the data.

A square wave with a 14 second period introduced between 120 and 140 amperes of current into the ground. Measurements of the transient magnetic field resulting from the current step were then made with the receiver equipment already described. Recordings were made for the vertical magnetic field and the radial magnetic field except for cases where the signal was below noise. At each of the forty-eight stations, six to eight recordings were made.

Data Preparation

After the data were collected they were prepared

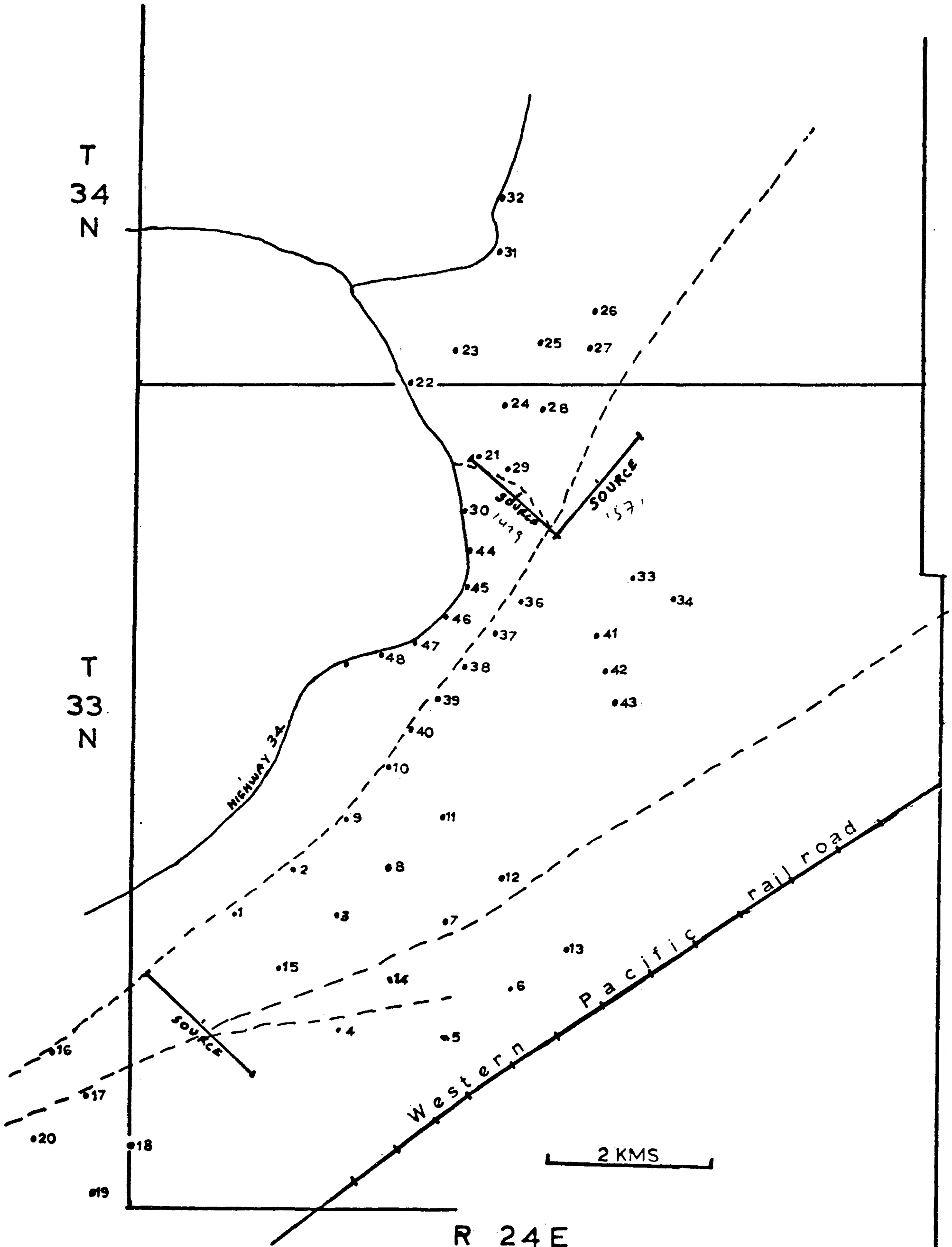

Figure 8 Map showing location of stations and sources.

for interpretation. Between 0.8 and 1.0 second length of each record was digitized at an interval of 0.02 second in some cases and 0.025 second in others. For each receiver station one to six records were digitized depending on the quality of the record.

The data from the noisier signals were stacked three to six fold to reduce the error in transient representation. When stacking, a statistical test was applied to insure that each data point is within a reasonable distance of the average signal. If the value is more than two standard deviations from the average, it is rejected. Table 1 shows the stacked data for Station EM18. The field in amperes HENRY per meter is under AV - H, the standard deviation for the different points is shown under STD - DV Figure 9 shows the record from Station EM15 which does not require any stacking and Figure 10 shows one of the records from Station EM18.

A deconvolution process was carried out on the data to remove the response of the system, thereby leaving only the response due to the earth. Due to the fact that gradients were used in this interpretation scheme, gradients from the system response were deconvolved with gradients from the digitized and stacked records. The program SYSTEM.F4 originally written by Keller (1972) was modified and used along with a modified version of

Table 1.

TIME = Cumulative time
NUMBER = Number of points used in stacking
AV-H = Average field in Henrys/meter
ST. DEV. = Standard Deviation at each point.

EDITED AND STACKED DATA STATION EM18

TIME	NUMBER	AV-H	ST. DEV.
.025	4	0.105E-01	0.520E-03
.050	4	0.102E-01	0.584E-03
.075	4	0.986E-02	0.586E-03
.100	4	0.951E-02	0.573E-03
.125	4	0.927E-02	0.534E-03
.150	4	0.891E-02	0.508E-03
.175	4	0.859E-02	0.505E-03
.200	4	0.820E-02	0.487E-03
.225	4	0.777E-02	0.550E-03
.250	4	0.723E-02	0.587E-03
.275	4	0.681E-02	0.491E-03
.300	4	0.640E-02	0.485E-03
.325	4	0.596E-02	0.432E-03
.350	4	0.552E-02	0.331E-03
.375	4	0.514E-02	0.186E-03
.400	4	0.469E-02	0.162E-03
.425	4	0.431E-02	0.134E-03
.450	4	0.388E-02	0.164E-03
.475	4	0.348E-02	0.178E-03
.500	4	0.497E-02	0.320E-02
.525	4	0.498E-02	0.373E-02
.550	4	0.443E-02	0.324E-02
.575	4	0.439E-02	0.359E-02
.600	4	0.198E-02	0.725E-04
.625	4	0.174E-02	0.145E-03
.650	4	0.161E-02	0.911E-04
.675	4	0.135E-02	0.663E-04
.700	4	0.125E-02	0.367E-04
.725	4	0.113E-02	0.494E-04
.750	4	0.917E-03	0.789E-04
.775	4	0.796E-03	0.121E-03
.800	4	0.619E-03	0.699E-04
.825	4	0.519E-03	0.957E-04
.850	4	0.519E-03	0.849E-04
.875	4	0.376E-03	0.142E-03
.900	4	0.276E-03	0.164E-03
.925	4	0.133E-03	0.129E-03
.950	4	0.553E-04	0.725E-04
.975	4	0.000E+00	0.000E+00

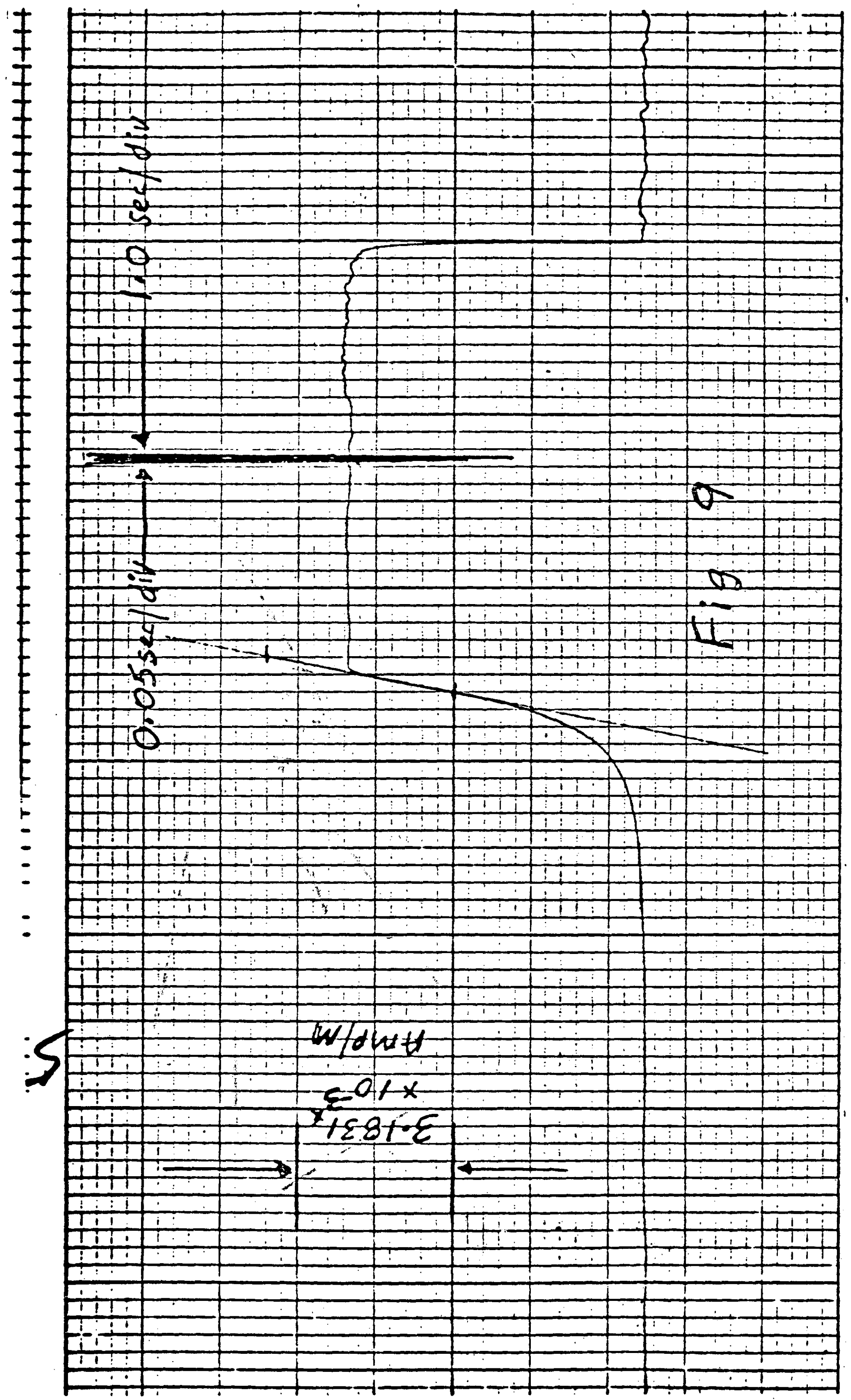

Figure 9 H_z field record, Station EM15.

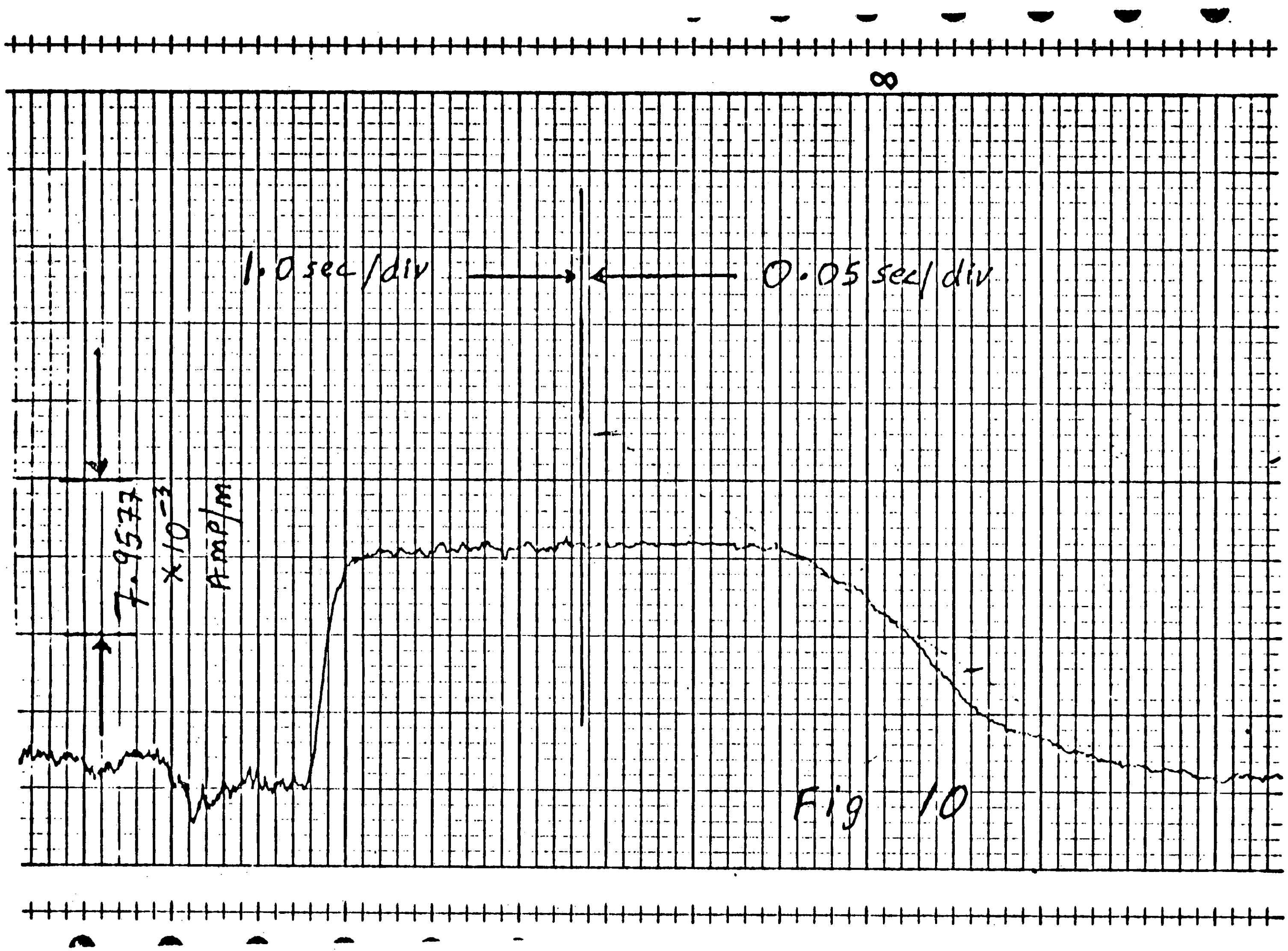

Figure 10 H_z field record, Station EM18.

the program STACK2.F4 to carry out the deconvolution process

The flow for the program SYSTEM.F4 which generates the system function is as follows:

1. Read in number of digitized points (NUM) and sampling interval (DT)
2. Read in digitized points from step response.
3. Find gradients from one point to the next (Y_k)
4. Calculate a "frequency" - (π/NUM)*i, i = 1.
5. Calculate real part of transform for that "frequency"

$$AR_i = \sum_{k=1}^{NUM} Y_k * C_k + 1$$

where $C_{k+1} = C_k * \cos(w) - S_k * \sin(w)$

$C_1 = \cos(w)$

$S_1 = \sin(w)$

6. Calculate the imaginary part of the transform for that "frequency"

$$AI_i = \sum_{k=1}^{NUM} Y_k * S_k + 1$$

where $S_{k+1} = S_k * \cos(w) + C_k * \sin(w)$

7. Calculate amplitude and phase correction factors:

$$\text{Amplitude}_i = \frac{(AR_i^{\ 2} + AI_i^{\ 2})^{1/2}}{(AR_i^{\ 2} + AI_i^{\ 2})^{1/2}}$$

$$\text{Phase}_i = \pi/2 - \text{Tan}^{-1} \frac{AI_i}{AR_i}$$

8. Increase i by one and repeat steps 4 through 7 until i = NUM, print out each amplitude and phase correction factor.

The program STACK5.F4 after performing the stacking removes the step response of the recording system by multiplying the amplitude and amplitude correction factors and by adding the phase and phase correction factors. The program STACK5.F4 which is a modified version of the program STACK2.F4 is listed in Appendix B.

The deconvolved fièld data are then curve matched as described later.

INTERPRETATION TECHNIQUES

Vertical Field

For the vertical component of magnetic field H_z, two interpretation methods were employed.

1. Early-time asymptote method.
2. Theoretical layered-earth model curve matching method.

Early-time Asymptote Method

Vanyan (1967) has demonstrated that the voltage detected with a vertical-axis induction loop can be used to calculate an apparent resistivity with the formula

$$\rho a = \frac{2\pi R^4 V}{3IAL \cos\theta}$$

where

ρa is apparent resistivity

R is distance from source to receiver

V is voltage received

I is current in source

L is length of source

A is the area of the receiver loop

θ is angle away from the equator for the radius vector from the transmitter to the receiver.

and all quantities are measured in M.K.S. units

Some assumptions were made to arrive at this equation. They are:

1. Displacement currents were small enough to be neglected.
2. μ is a constant for all media.
3. The air layer above the surface of the earth is ignored.
4. The system displays cylindrical symmetry.

It is emphasized that this equation is valid only for early time; i.e., condition that

$$\frac{\mu \sigma R^2}{2t} < 4\pi^2 \approx 16$$

where

t is recorded time

μ is magnetic permeability, $4\pi \times 10^{-7}$

σ is conductivity.

The equation above was modified before being used in this interpretation due to the fact that magnetic field intensities can be obtained directly from the data in this survey. The equation was modified as follows:

$$V_{Loop} = \frac{\partial \phi}{dt} \text{ flux}$$

$$= A \frac{\partial B}{dt}$$

$$= A\mu \frac{\delta H}{dt}$$

$$\rho_a = \frac{2\pi R^4 \mu}{3IL\cos\phi} \cdot \frac{dH}{dt}$$

where all variables are as defined earlier.

The gradient of the early part of the transients were therefore obtained and used in the calculation of apparent resistivities. Table 2 shows the apparent resistivities obtained for the records which were interpretable. Figure 11 is an apparent resistivity map obtained using this method of interpretation.

The apparent resistivity obtained from this equation is related to the resistivity of the first layer. If there is a conductor below the first layer, the early time resistivity is equal to the resistivity of the first layer, but in the case of a resistive second layer, the early-time resistivity is slightly greater than the first layer resistivity. In the Black Rock Desert, a model of a conductive first layer over a resistive second layer is suitable, so the early time resistivities obtained are slightly higher than the first layer resistivities.

Theoretical Layered-earth Model Curve Matching Method

Computer programs for electromagnetic interpretation were developed by Daniel (1974). One of the programs which is used in this interpretation utilizes linear filter theory to evaluate numerically an electromagnetic

Table 2

Apparent resistivities obtained from early time asymptote method of interpretation.

Station No.	Apparent resistivity ohm - m
EM03	6.80
EM04	0.19
EM05	44.28
EM06	11.59
EM07	7.17
EM08	4.51
EM09	66.01
EM11	22.88
EM12	5.54
EM14	1.95
EM15	0.094
EM16	0.23
EM17	1.29
EM19	1.69
EM20	1.89
EM21	0.028
EM22	7.18
EM23	6.23
EM24	-1.60
EM25	6.78
EM26	9.99
EM27	4.45
EM28	7.59
EM30	-5.43
EM31	12.00
EM32	17.74
EM33	1.18
EM34	0.92
EM37	7.29
EM38	5.61
EM39	53.35
EM41	3.28
EM42	1.93
EM44	1.08
EM45	3.25
EM46	13.74
EM47	5.21
EM48	50.8

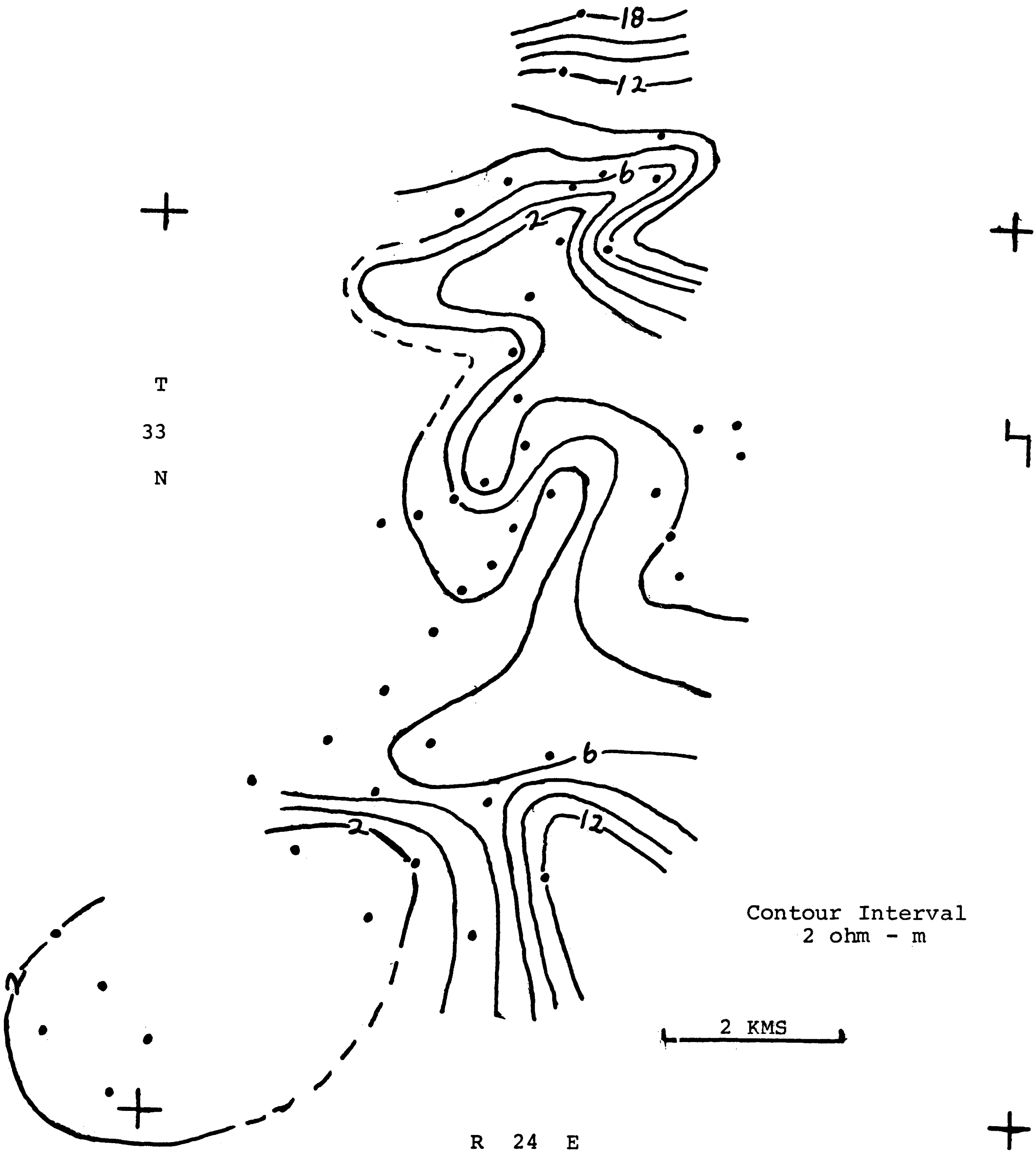

Figure 11 Apparent resistivity map obtained from early time asymptote method.

field for a dipole source over a layered earth. The convolution technique was used to calculate theoretical frequency domain curves. These curves are then Fourier transformed into the time-domain using the polygonal approximation method (Papoulis, 1962). The step response for these curves is calculated and then the results obtained are compared with curves obtained by plotting time against apparent resistivity. The apparent resistivities plotted are obtained from the formula given earlier.

In this case, the gradient between each successive point on the digitized transient is taken and the apparent resistivity obtained by substituting this value in the formula given earlier is plotted against cumulative time in the logarithm domain. The curves were smoothed by applying a flat seven point filter. The program STACK5.F4 which carries out the stacking and smoothing is given in Appendix B.

A two layer earth model was subsequently assumed in the interpretation. The plots of the apparent resistivities were compared with a catalog of theoretical curves prepared by Silva (1969) to obtain first estimates. Theoretical curves were then computed from these first estimates, compared to the observed data and adjustments were made to the parameters.

The program EMFWD8.F4 which is a modified version of the one written by Daniel (1974), was used to generate the theoretical curves in the frequency domain. These were then Fourier transformed into the time domain using the polygonal approximation method using the program TRANS3.F4 The curves in some cases have to be scaled to bring them to the level of the observed curves. The programs are listed in Appendix B.

It was discovered that to obtain suitable fits, a conductive surface layer had to be included. A surface layer with resistivity values from 0.5 to 1 ohm-meter and thickness varying from 80 to 200 meters had to be used before suitable fits were obtained.

Theoretical matches were not obtained for some of the nearer stations; this is due to the fact that the dipole approximation as earlier mentioned is only suitable for stations which are at distances a few times the depth to a boundary. Generally at distances less than one and a half source lengths, computed theoretical fits were not possible. Some of the stations in this category were interpreted empirically by matching with theoretical curves compiled by Silva (1969)

Some of the matched curves and deconvolved field curves are given in Appendix A.

RESULTS

Table 3 shows the values of resistivities and thicknesses obtained from the interpretation scheme. Values in parentheses are those for stations with source-receiver separations less than one and a half source length.

The results show a conductive surface layer with resistivity ranging from 0.5 to 1 ohm-meter and thickness varying from 80 to 200 meters, underlain by a less conductive layer with thickness ranging from 300 meters to 900 meters and resistivity ranging from 1 ohm-meter to 15 ohm-meters, and then a resistive basement with resistivity values starting from 50 ohm-meters.

TABLE 3

APPARENT RESISTIVITY OBTAINED FROM H_z

Station	P_1 ohm-m	H_1 meters	P_2 ohm-m	H_2 meters	P_3 ohm-m
EM03	1	200	5	300	160
EM05	1	125	12	760	450
EM07	1	125	4	600	140
EM08	1	125	5	800	250
EM11	1	100	11	600	350
EM12	1	80	9	700	100
EM14	1	150	11	600	350
EM15			(2)	(300)	(80)
EM16			(6)	(450)	(56)
EM17			(3)	(410)	(50)
EM18			(1)	(100)	(500)
EM21			(5)	(380)	(150)
EM22	1	130	11	300	250
EM23	1	150	11	300	350
EM24			(1)	(190)	(500)
EM25	1	200	7	500	270
EM26	1	150	8	600	265
EM27			(3)	(220)	(500)

TABLE 3 (Continued)

Station	P_1 ohm-m	H_1 meters	P_2 ohm-m	H_2 meters	P_3 ohm-m
EM28			(5)	(900)	(48)
EM30			(3)	(225)	(85)
EM31	1	100	10	800	550
EM32	1	150	15	900	500
EM33			(1)	(158)	(250)
EM34			(1)	(220)	(250)
EM37	1	125	4	400	100
EM38	1	125	5	300	250
EM41	0.5	200	2	600	50
EM42	0.7	200	2	600	550
EM44			(2)	(220)	(56)
EM45			(7)	(800)	(220)
EM46	1	80	10	400	350
EM47	1	80	15	400	500

Radial Field Component

An expression for the radial component of the electromagnetic field generated by a time varying source is given in Vanyan (1969) It is as follows:

$$H_r = - \frac{M}{4 \quad R^3} [(\gamma R)^2 (I_1 k_1 - I_o k_o) + 4 \quad R(I_1 k_o - I_o k_1)$$

$$+ 16 I_1 k_1]$$

$$\gamma = (i \mu \sigma w)^{1/2}$$

where

H_r is radial component of magnetic field

M is moment of source

R is source-receiver separation

μ is magnetic susceptibility

σ is conductivity

w is frequency

and

I_o, K_o, I_1, K_1 are modified Bessel functions of order zero and one.

Argument of modified Bessel functions is $\gamma R/2$.

It is apparent that this equation cannot be solved for conductivity in terms of the other quantities which are measurable.

An approach used in the determination of conductivity is to find limit of this expression as γR becomes very large; i.e., large separations.

An expression for the radial component of the magnetic field for large separations was given in a paper by Wait (1961) and in Vanyan (1967). This is:

$$H_r = - \frac{Ids \operatorname{Sin} \theta}{\pi \gamma R^3}$$

where

H_r, γ, and R are as defined earlier

I is the current step

ds is source length

θ is the angle which the radius vector makes with the source.

Finding the derivative of this expression with respect to time (t) and transforming into the time domain, we obtain:

$$\frac{dH}{dt} = - \frac{Ids \operatorname{Sin} \theta}{2\pi^{3/2} (\mu\sigma)^{1/2} R^3 t^{3/2}}$$

apparent resistivity p_a is then given by

$$\rho a = \frac{4\pi\mu R^6 t^3}{I^2 ds^2 \operatorname{Sin}^2 \theta} \cdot \left(\frac{dH}{dt}\right)^2$$

Apparent resistivity curves were computed and using the maximum field gradient approach, the maximum resistivity value for each station was obtained. These are given on Table 4.

The values obtained show a significant range. This is expected since (1) the radial field component is very sensitive to lateral variations due to vertical boundaries

Table 4

Apparent resistivities from radial component of magnetic field.

Station No.	Apparent resistivity ohm - m
EM01	0.59
EM02	7.92
EM03	3.68
EM04	0.81
EM05	211.09
EM07	10.48
EM09	8.87
EM14	0.22
EM16	0.0065
EM17	0.00054
EM18	0.00043
EM19	0.000076
EM20	0.00071
EM21	6.04
EM22	0.012
EM23	0.20
EM24	0.0025
EM25	0.019
EM26	0.21
EM27	0.38
EM28	0.00011
EM29	0.000012
EM30	0.034
EM31	0.091
EM33	0.15
EM34	0.000066
EM36	1.95
EM37	0.93
EM38	0.55
EM39	0.52
EM40	0.0012
EM41	10.85
EM42	2.99
EM43	1.57
EM44	0.022
EM45	0.29
EM46	0.74

(i.e. faults), and (2) as can be seen from the expression for apparent resistivity, the field is proportional to the square root of resistivity which is not the case for the vertical component.

A plot of the resistivities obtained from the radial field curves and the vertical field curves was made to see if any relationship exists. This plot is given on Figure 12. As can be seen from the plot which is in the logarithm domain, the scatter is significant, so a reasonable conclusion is that no such relationship exists, and that suitable resistivities cannot be obtained from measurements of the radial component of the magnetic field.

However, because of its sensitivity to lateral variations, measurements of the radial field component are useful in locating vertical boundaries caused by faults and other lateral variations. This is due to the fact that recordings of the transient when a station is near a vertical boundary show significant distortions in form of an overshoot. This is further discussed under Geological Interpretation.

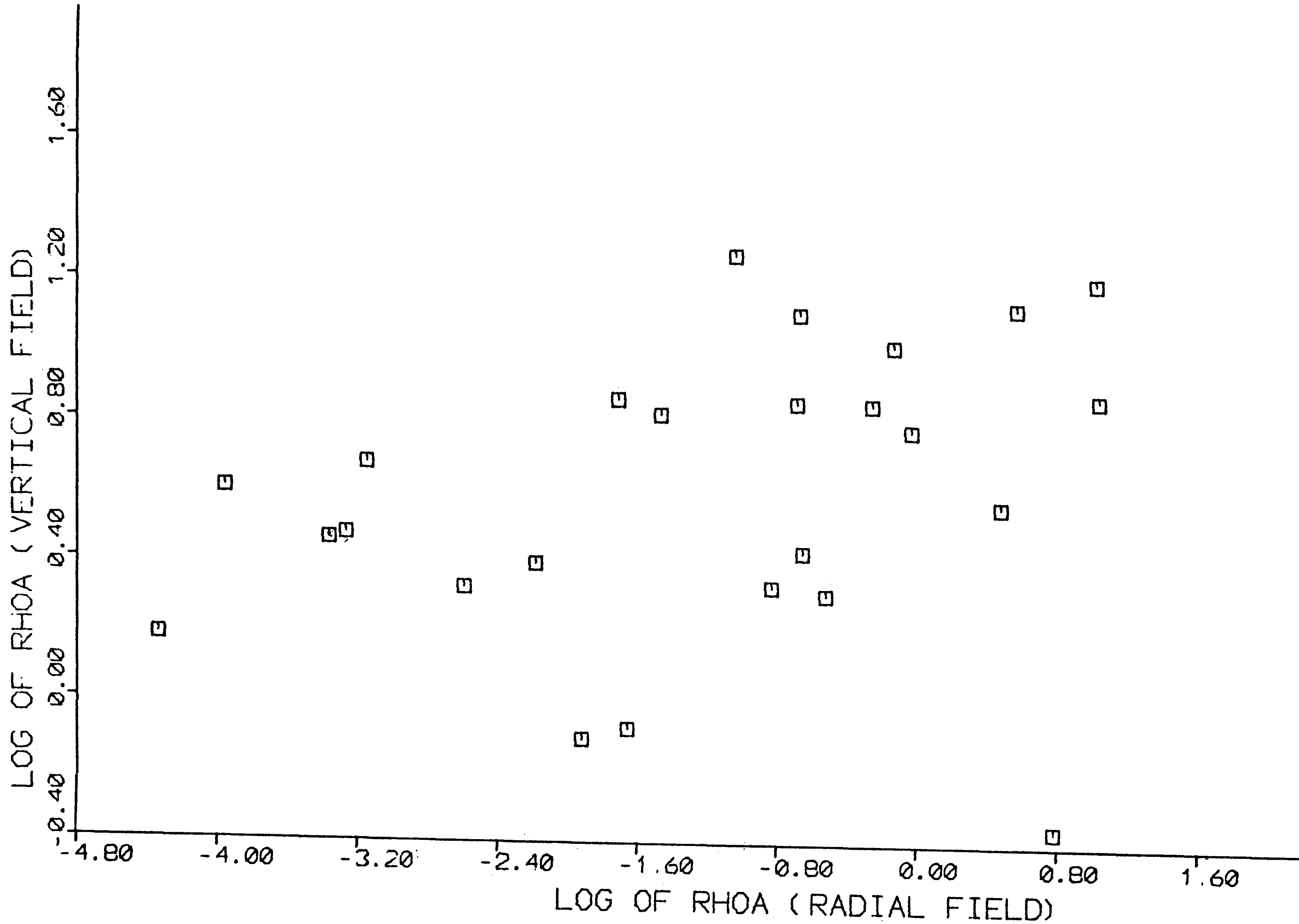

Figure 12 Plot of apparent resistivities obtained from H_z & H_r

GEOLOGICAL INTERPRETATION

The surface layer as shown on the geologic map on Figure 3 consists of Quaternary playa, accounting for the high conductivity. The second layer is the one of interest as a possible geothermal reservoir. Its low resistivity can be explained by the fact that it consists of lake sediments and large areas of this layer may have been penetrated by geothermal waters, evidence of which can be seen on the surface in form of the numerous hot springs found in the general area. Basement resistivities have a lower limit of about 50 ohm-meters; these relatively low basement resistivity values are due to the presence of Tertiary volcanics in this area. These agree fairly well with values obtained by Morris (personal communication) in a concurrent study using the more conventional dipole mapping technique.

Cross sections along stations EM03 - EM07 - EM12 and along stations EM22 — EM23 — EM25 — EM26 are shown on Figures 14 and 15. The location of the sections is shown on Figure 13. These sections show a general thickening of the second layer in the direction of the center of the Black Rock Desert.

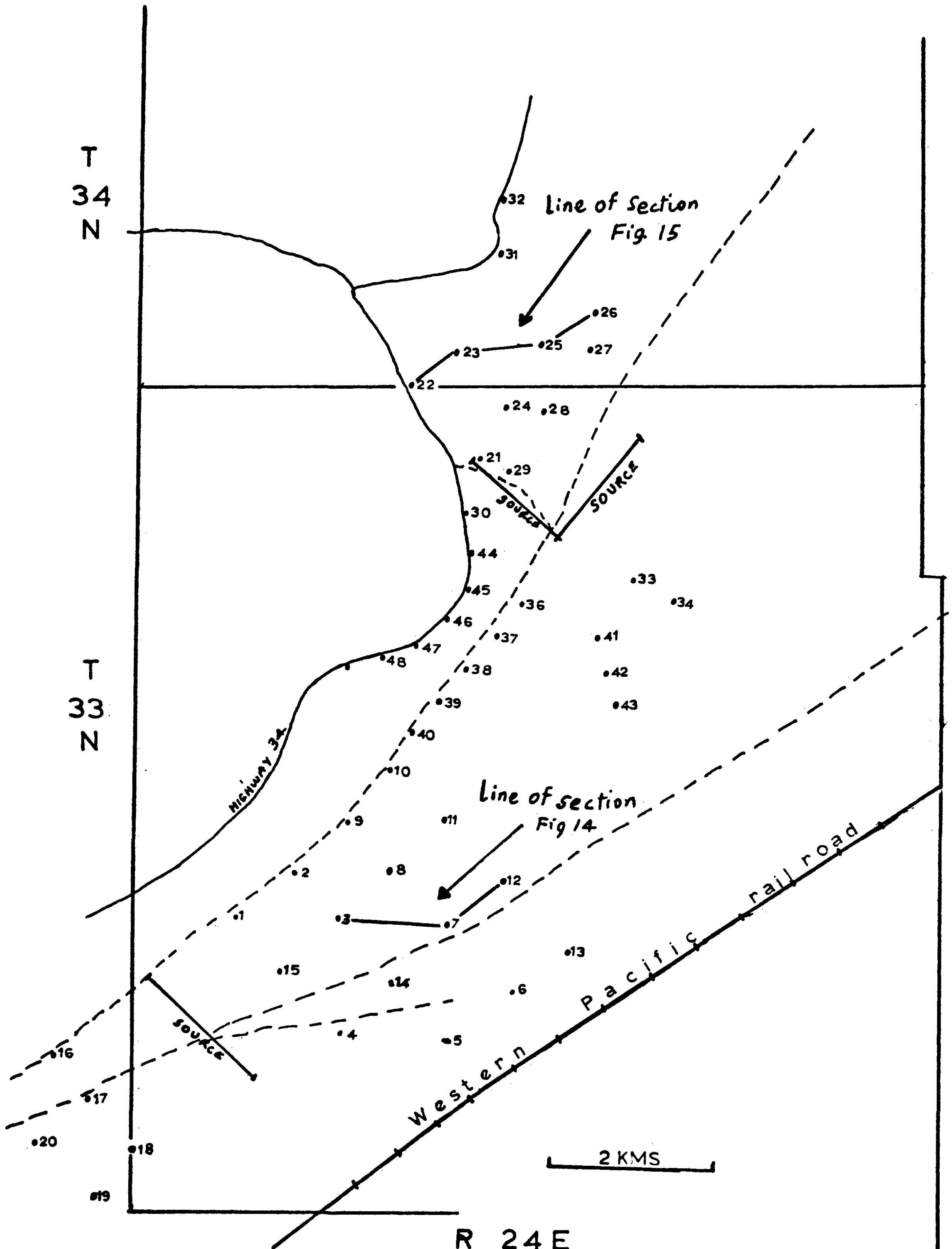

Figure 13 Map showing line of section, Figures 14 & 15.

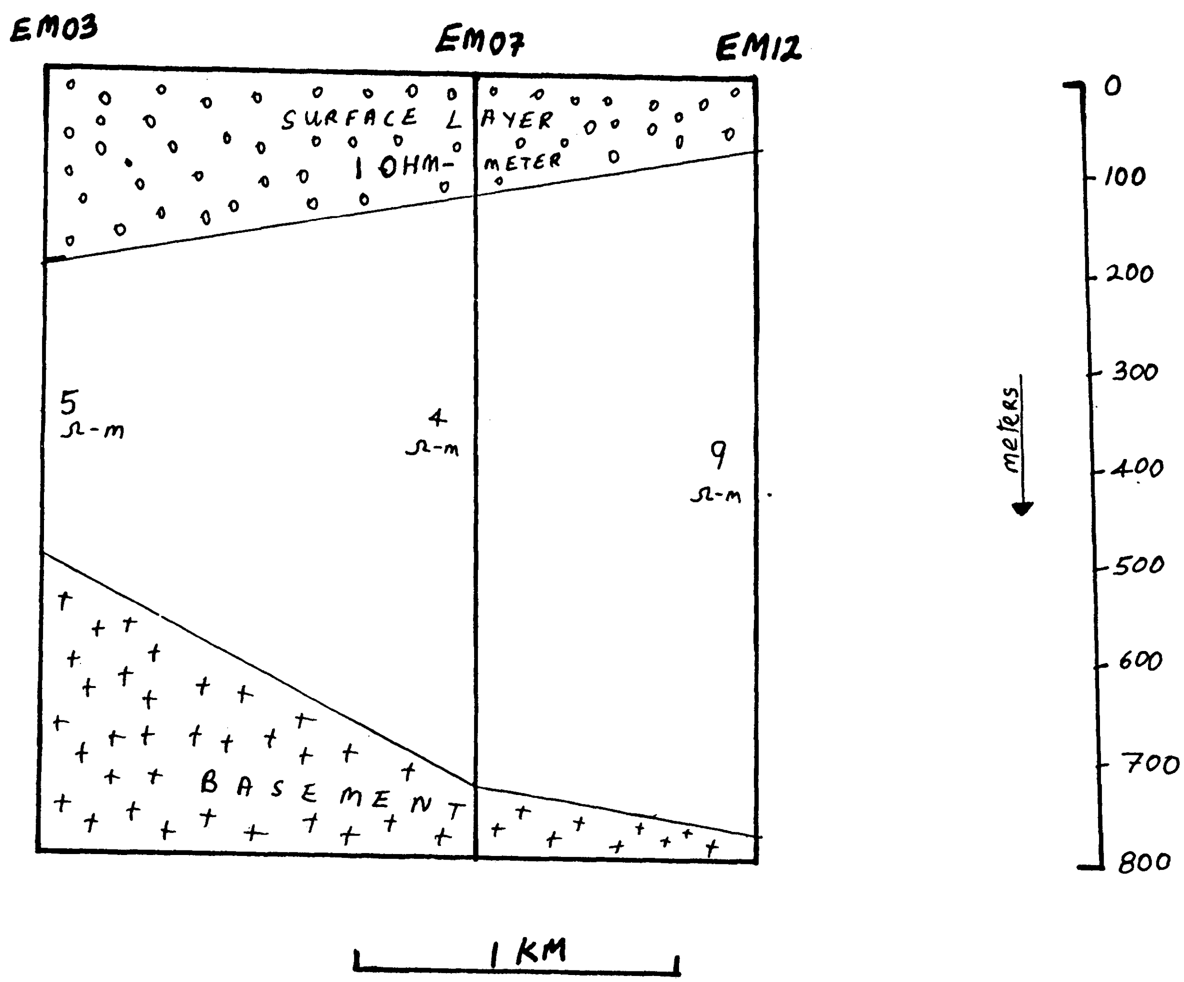

Figure 14 Geologic section, Stations EM03 - EM07 - EM12.

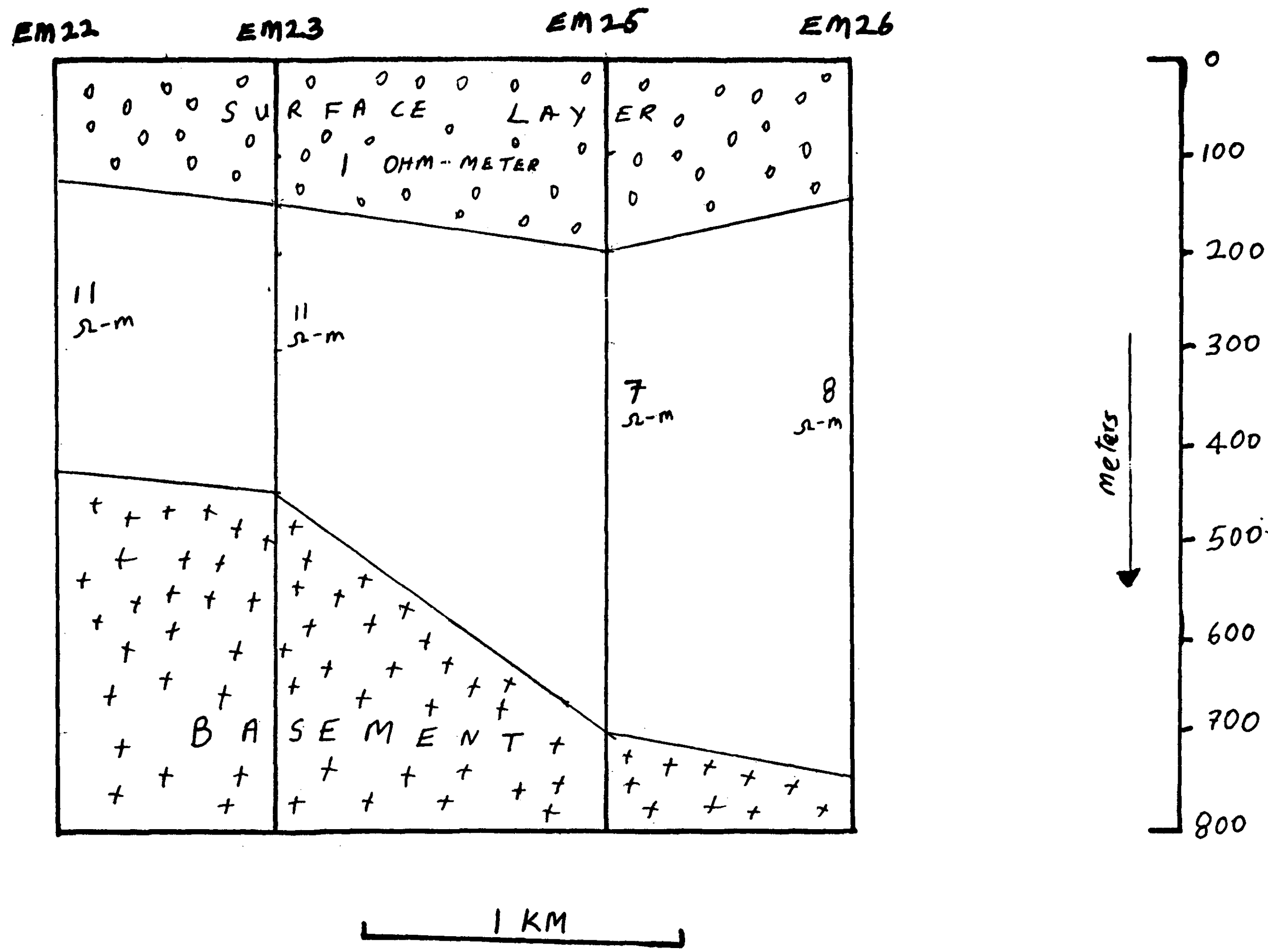

Figure 15 Geologic section, Stations EM22 - EM23 - EM25 - EM26.

As have been mentioned earlier, major faults occur in the Black Rock Desert area. The approximate location of these faults can be obtained from the recordings of the transient. This is due to the fact that when recordings are made near a vertical discontinuity (fault), an edge effect in the form of an overshoot show up on the recording of the transient. When the direction of current in the source wire is reversed, one expects a gradual decay of the electromagnetic field, thus producing the transient. Instead, a sharp reversal and overshoot is obtained which then gradually decays to the level of the steady-state electromagnetic field. A set of these overshoots can give an approximate location of a major fault.

On the recordings of the vertical electromagnetic field component, overshoots are found on the records for stations EM24 and EM30. Figure 16 is the record for station EM24. It can be observed that the transient is in the wrong direction in the early part of the record.

The radial component of the electromagnetic field is more sensitive to lateral variations; because of this, more overshoots were found. These are on the records for stations EM21, EM22, EM23, EM24, EM25, EM26, EM27, EM28, EM29, EM30, EM36, and EM37. Figures 17 and 18 are records from stations EM21 and EM23 respectively. A

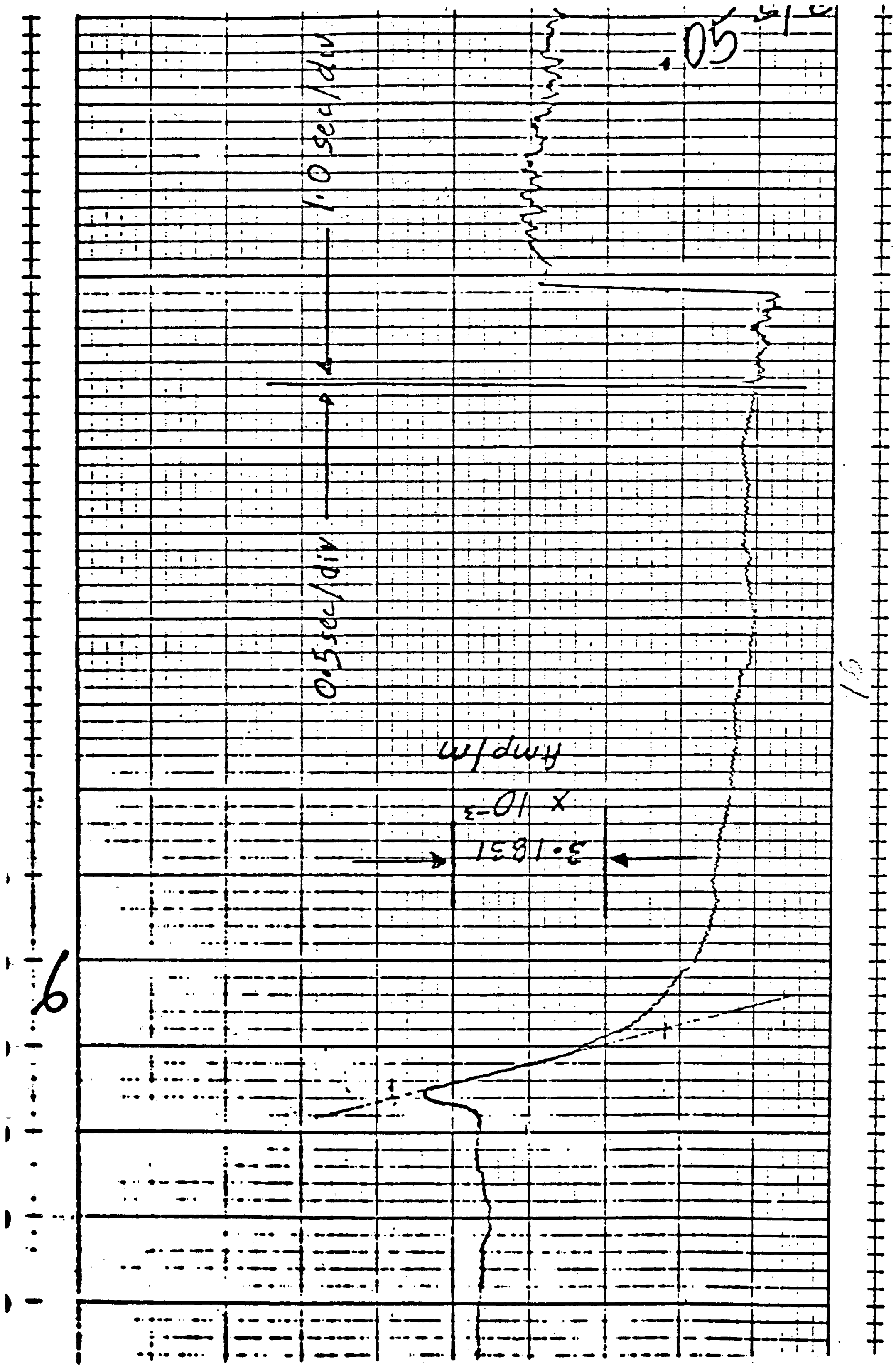

Figure 16 H_z field record, Station EM24.

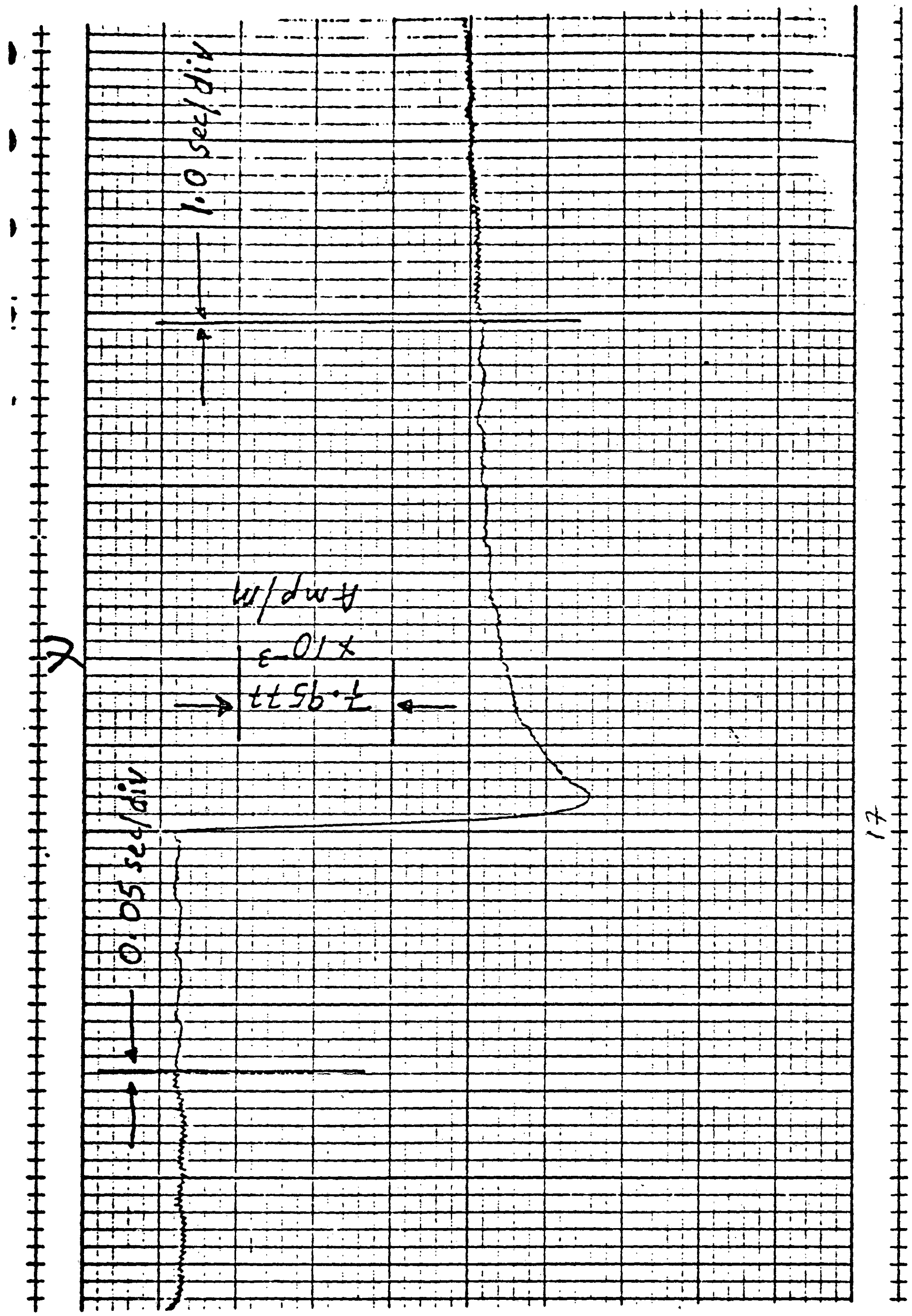

Figure 17 H_r field record, Station EM21.

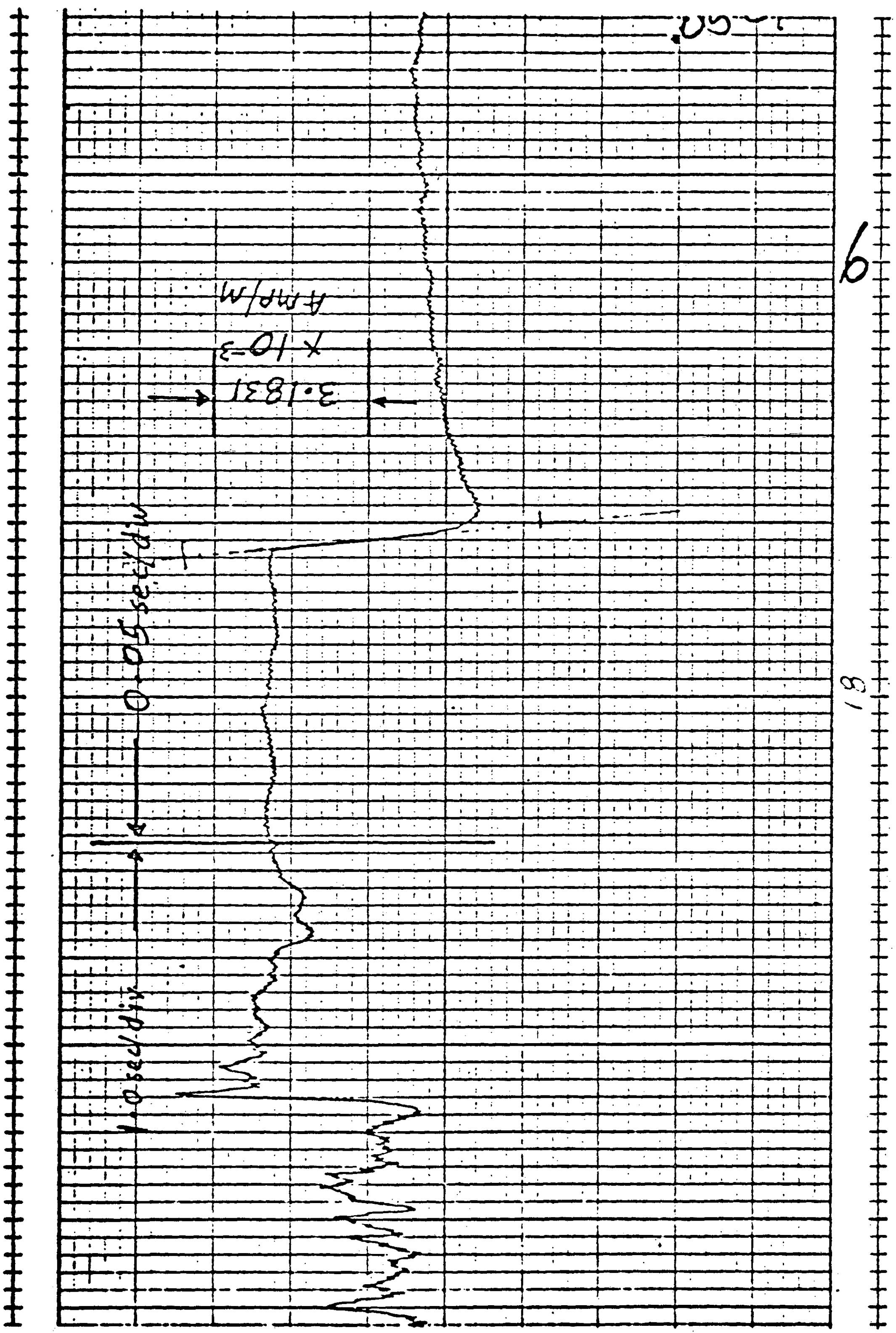

Figure 18 H_r field record, station EM23.

probable location for the fault causing these anomalies is shown on Figure 19. This is supported by the fits obtained for the vertical component. The second layer boundary for stations EM22 and EM23 is at about 450 meters, and the second layer boundary on stations EM25 and EM26 is at about 750 meters. This indicates a change of about 300 meters from the first set of stations to the second. Thickening in the depositional basin can probably not reach this order of magnitude in such a distance, so it is reasonable to conclude that there is a fault causing this displacement. Furthermore, evidence from the seismic monitoring done in this area supports the location of this fault. Figure 20 shows an epicenter map obtained from the seismic monitoring program. The cluster of epicenters which correspond to a fault zone agrees fairly well with this interpretation.

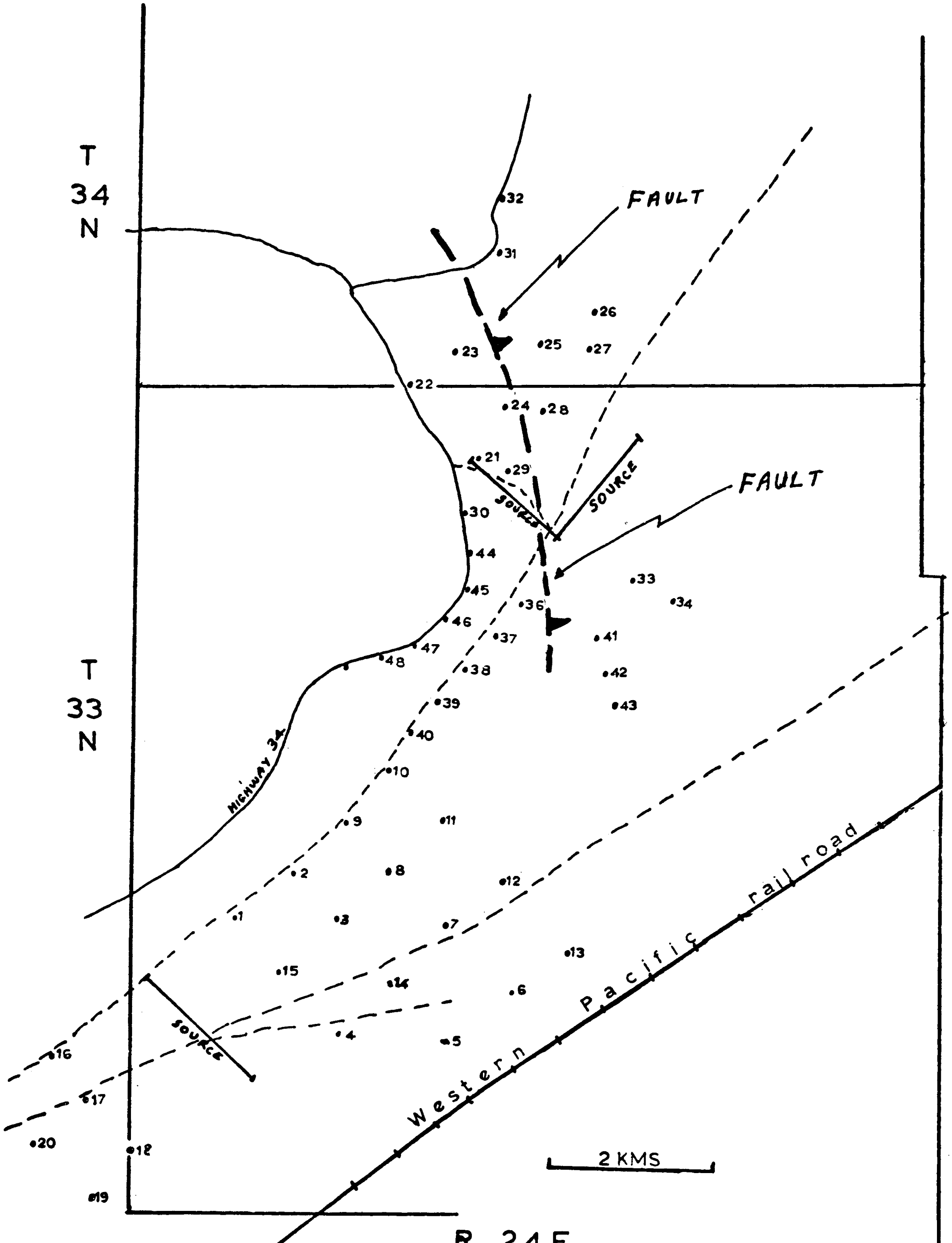

Figure 19 Map showing location of fault.

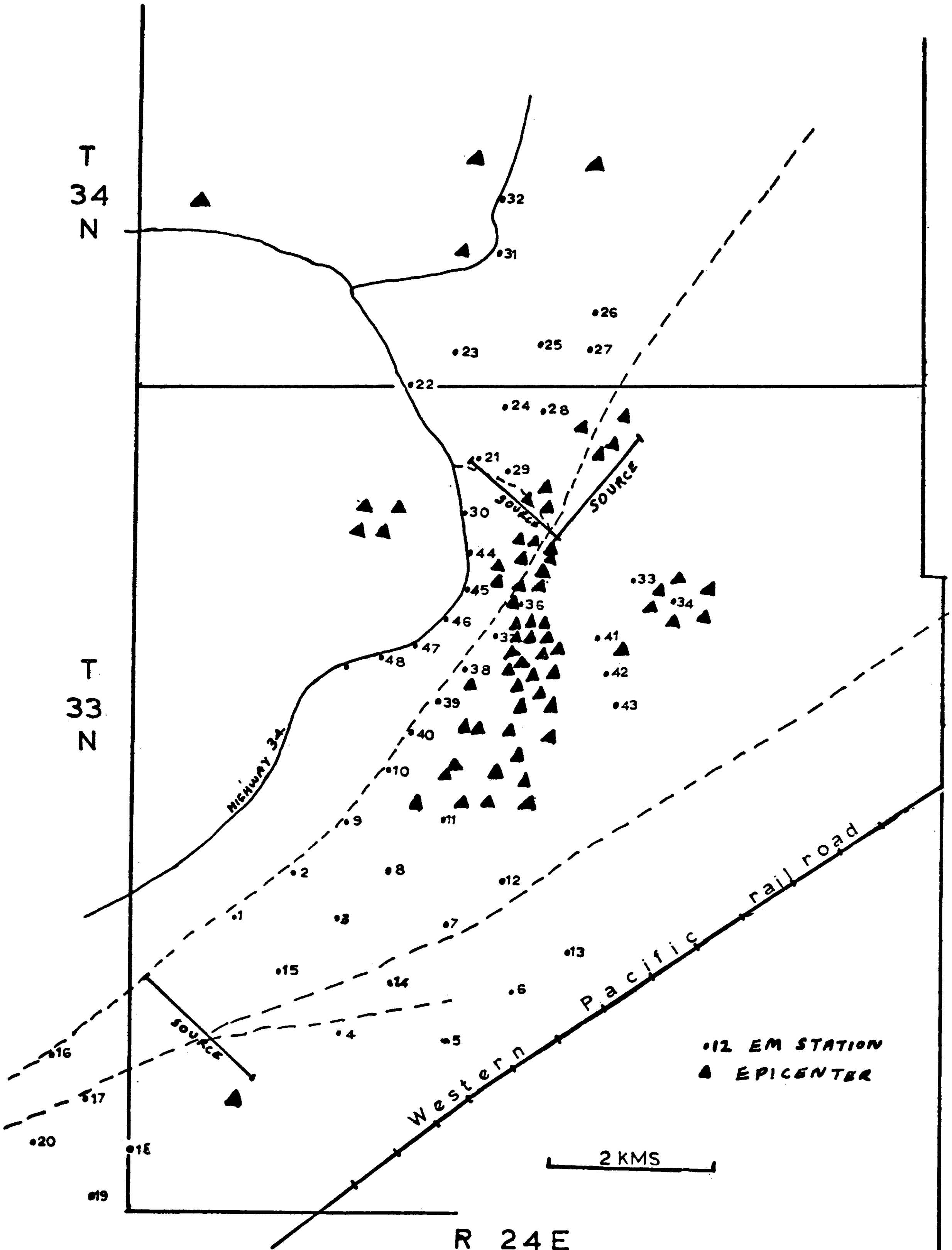

Figure 20 Map showing epicenter locations.

DISCUSSION AND CONCLUSIONS

Figure 21 is a contour map of the apparent resistivities obtained for the second layer (the surface layer being the first) The values range from 1 ohm-meter to 15 ohm-meters. These resistivity values agree fairly well both in the order of magnitude and trend with apparent resistivities obtained by the more conventional dipole mapping technique. Figure 22 is an apparent resistivity map obtained from the dipole mapping method by Morris (personal communication). This map covers the general area considered in this interpretation. Figure 23 is a composite apparent resistivity map for the whole Black Rock Desert area.

The second layer of this interpretation is a possible geothermal reservoir. The low resistivities are typical of a geothermal environment and the faults in this area are probably the conduits for the geothermal waters. Hot springs and other geothermal activity on the surface which are abundant in this area probably occur in places where the faults reach the surface.

The dipole approximation is quite adequate for this type of interpretation if all stations are maintained at distances at least one and a half source lengths away.

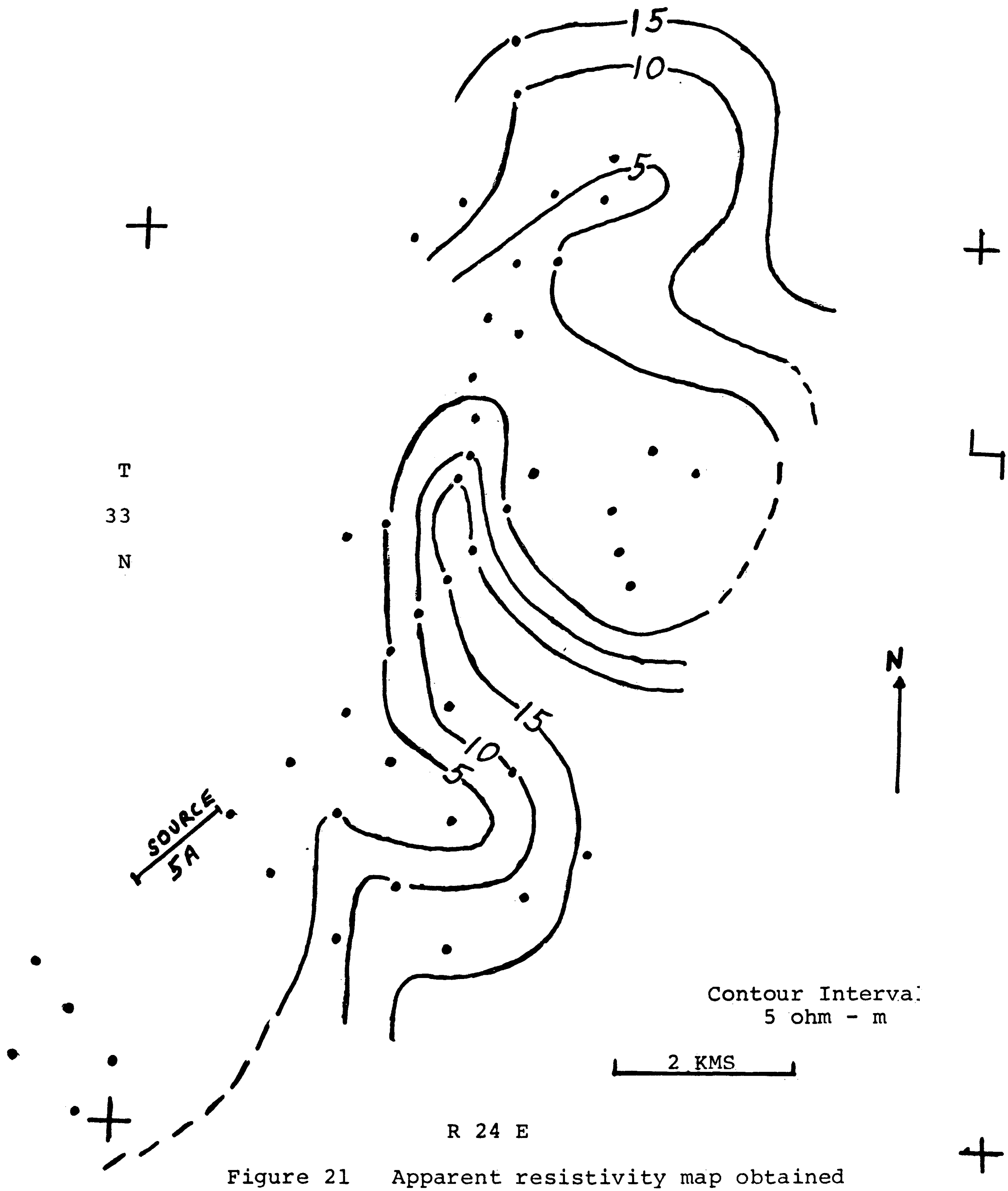

Figure 21   Apparent resistivity map obtained from theoretical layered earth curve matching.

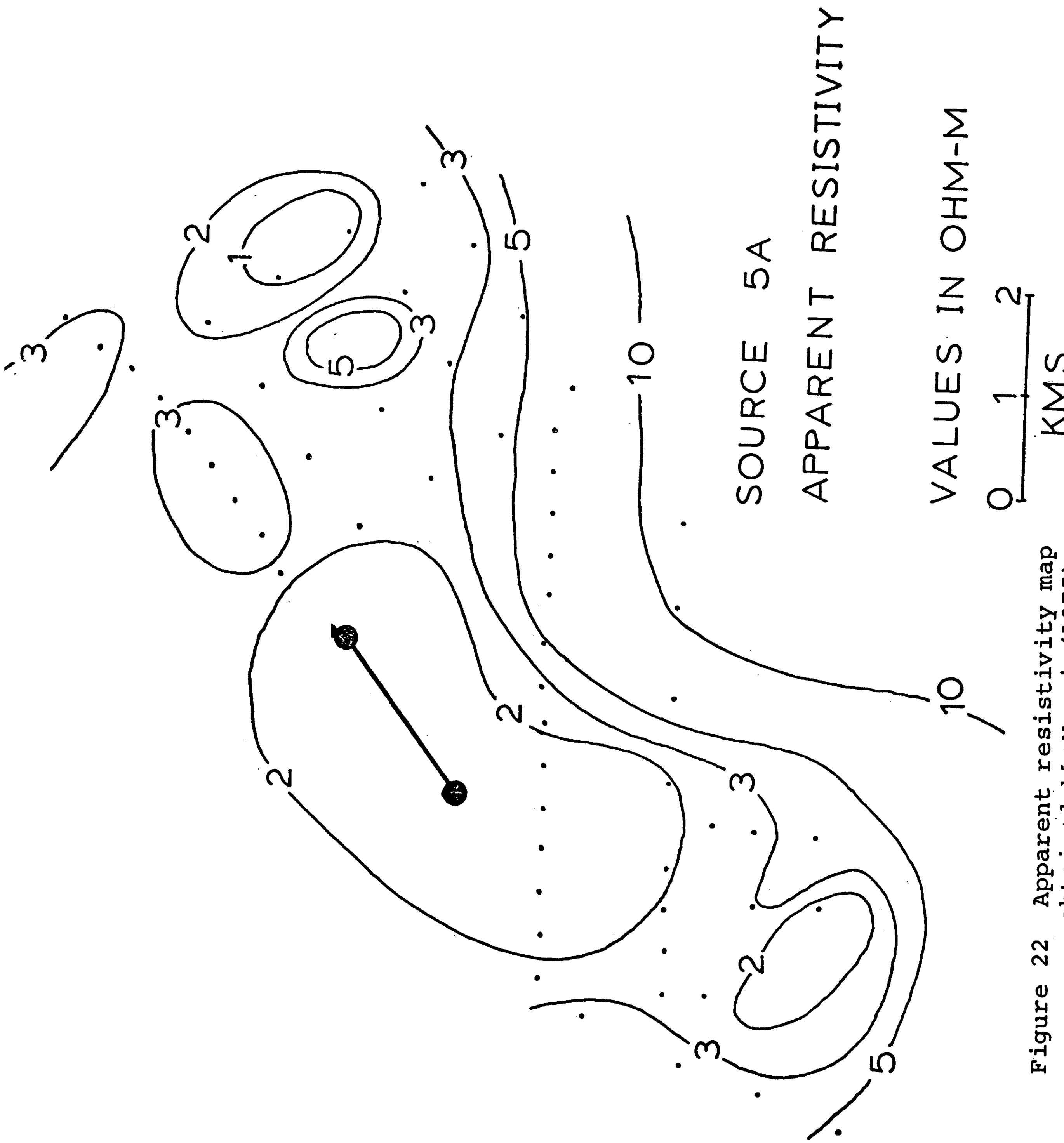

Figure 22 Apparent resistivity map obtained by Morris(1975)

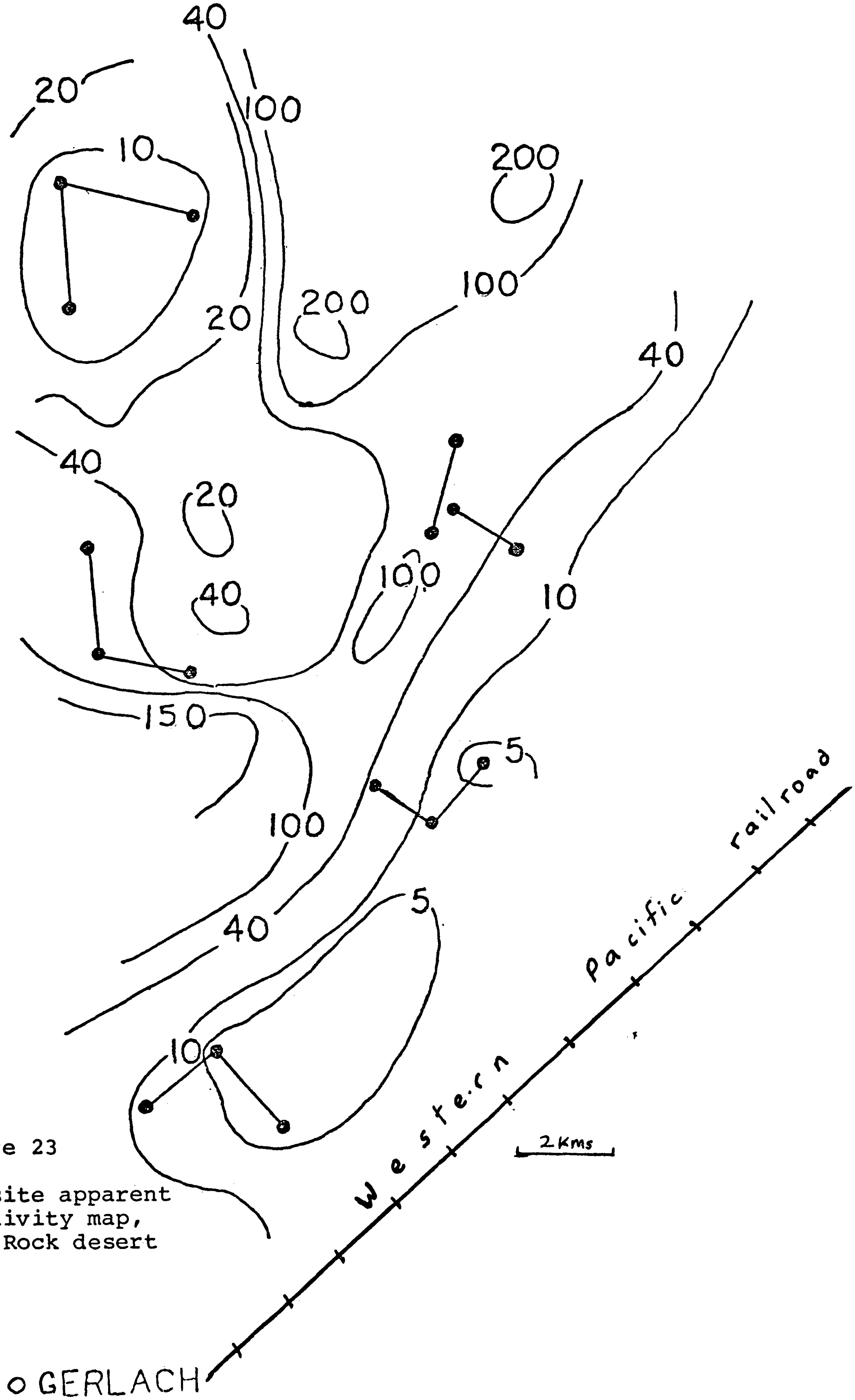

Figure 23

Composite apparent resistivity map, Black Rock desert area.

In conclusion, this interpretation has demonstrated the usefulness of measuring the radial component of the electromagnetic field and the usefulness of the three-component magnetometer in time domain electromagnetic sounding (TDEM)

Although suitable resistivities cannot be obtained from the recordings of the radial field, its sensitivity to lateral variations and the diagonistic transients obtained near lateral discontinuities provide a powerful tool in the location of faults and other vertical boundaries. The recordings of the radial field component as with all geophysical measurements becomes more useful when used in conjunction with available geologic data and other geophysical techniques.

A P P E N D I X A

Deconvolved field curves.

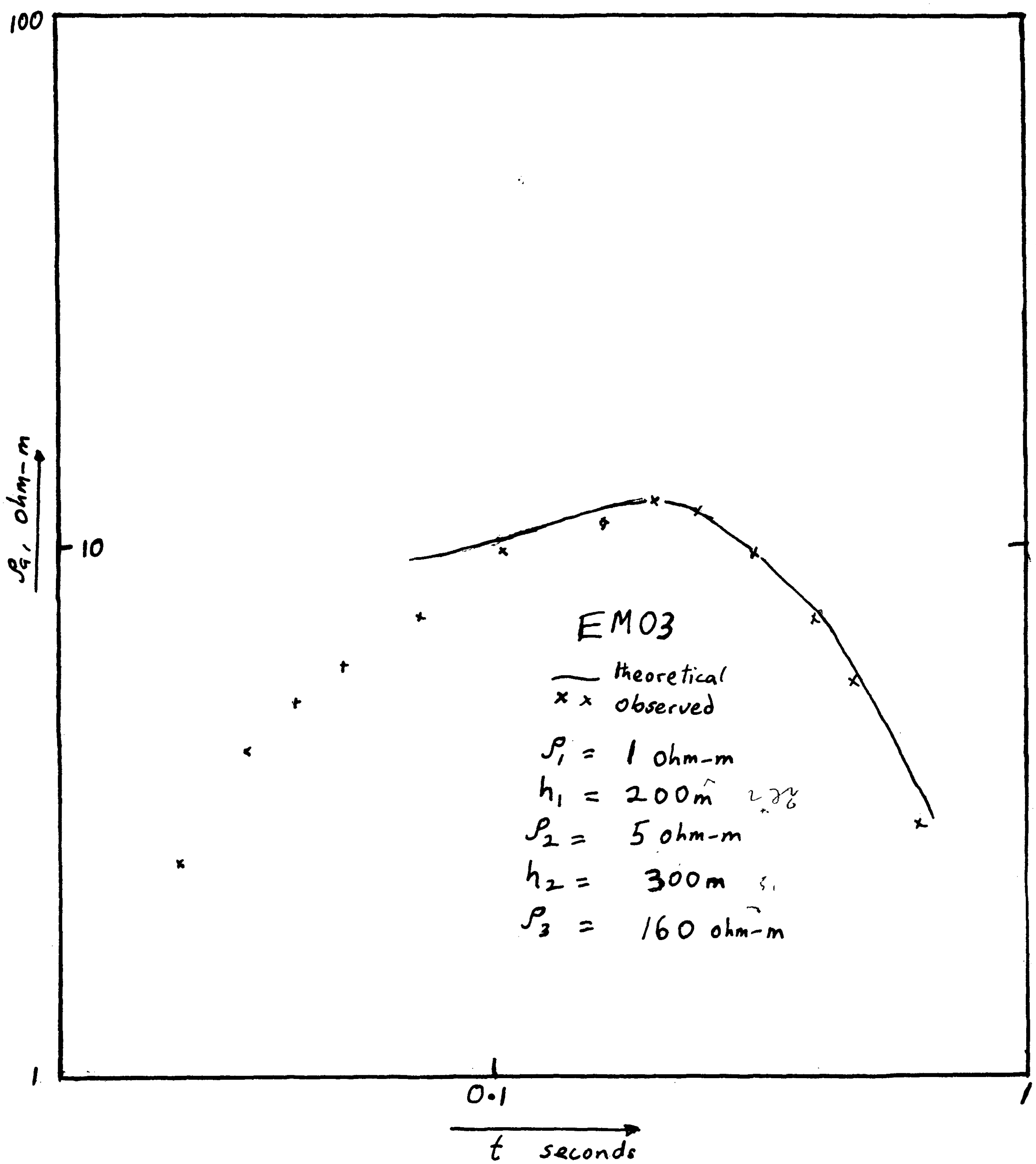

Deconvolved field curve and theoretical match,
Station EM03

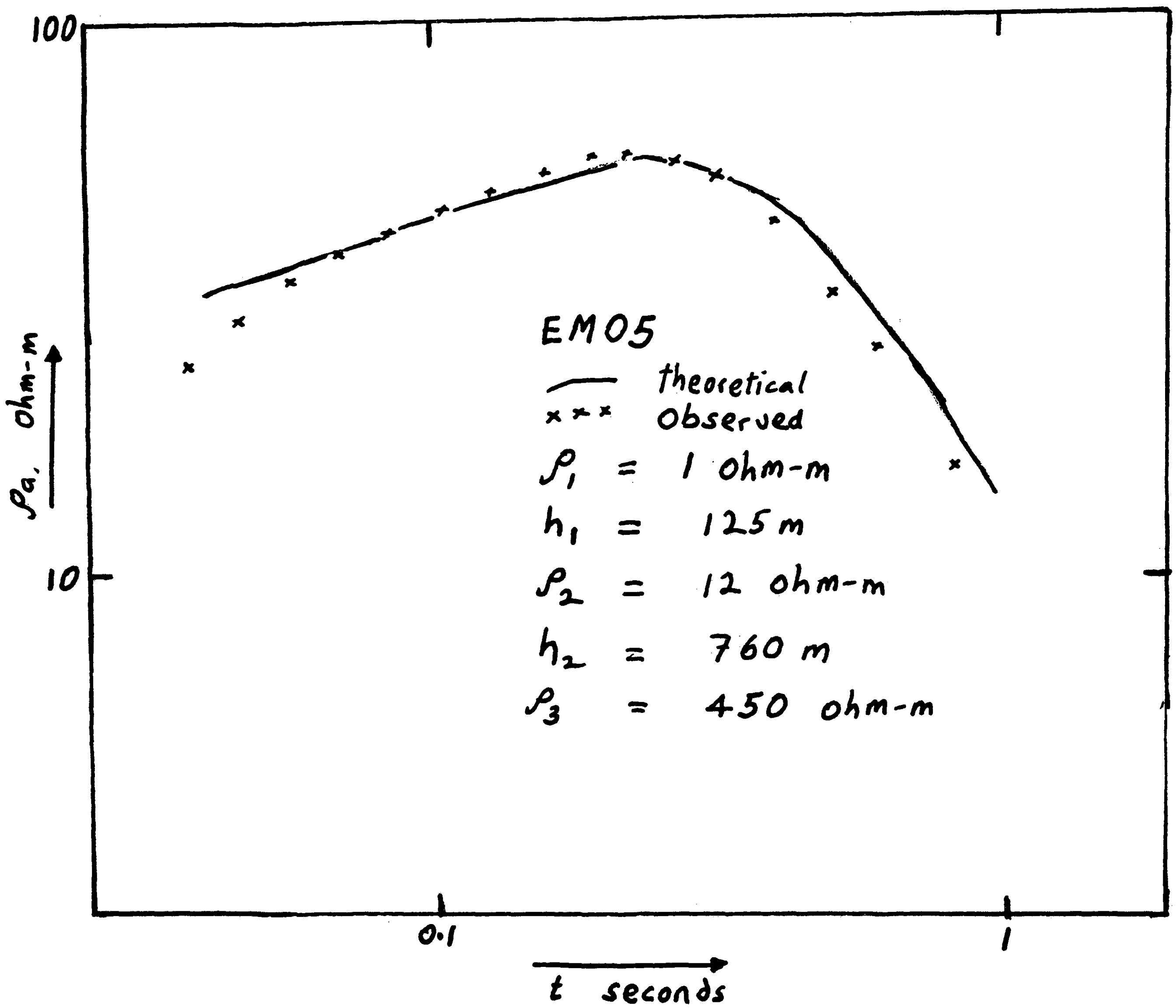

Deconvolved field curve and theoretical match, Station EM05

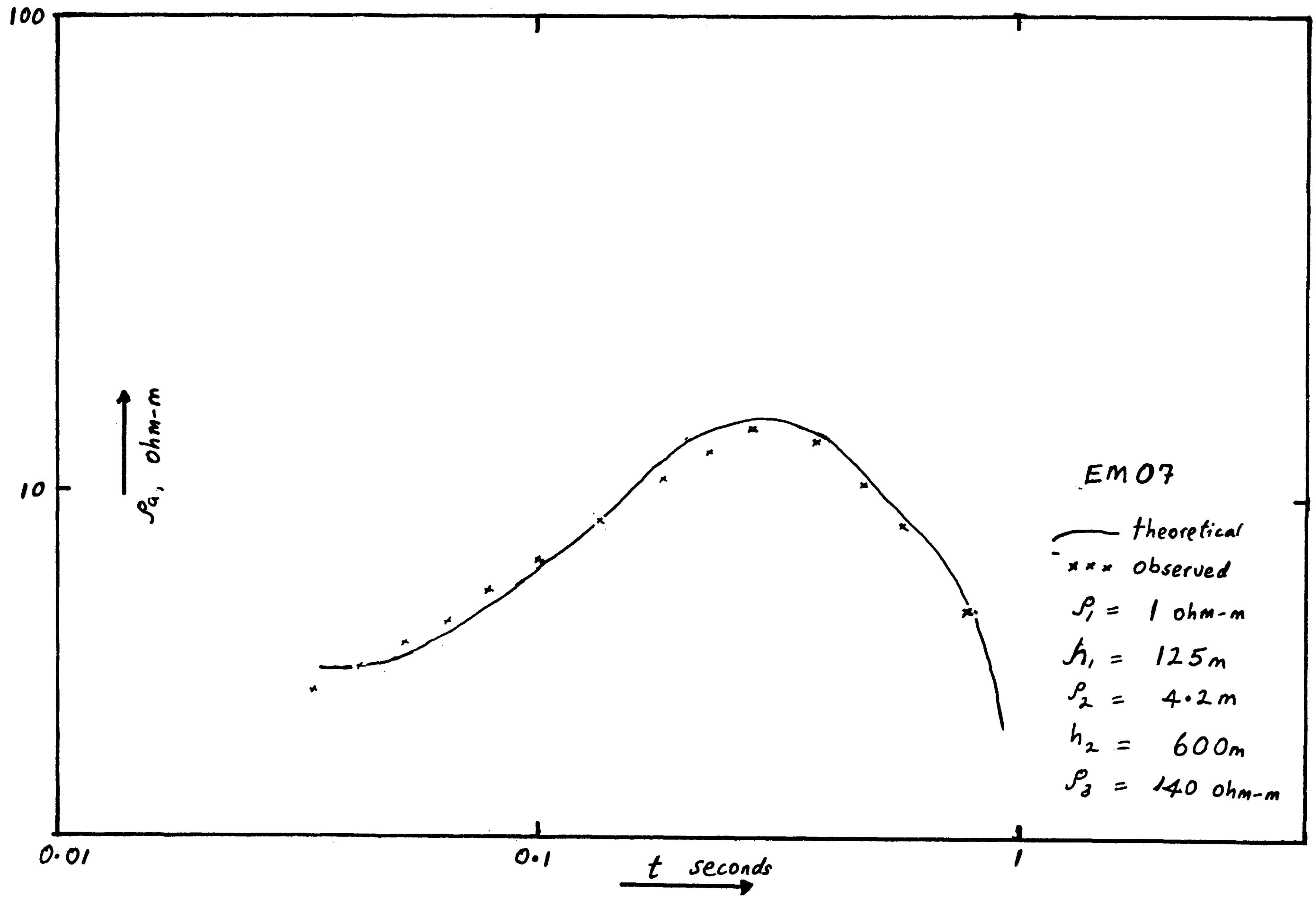

Deconvolved field curve and theoretical match, Station EM07.

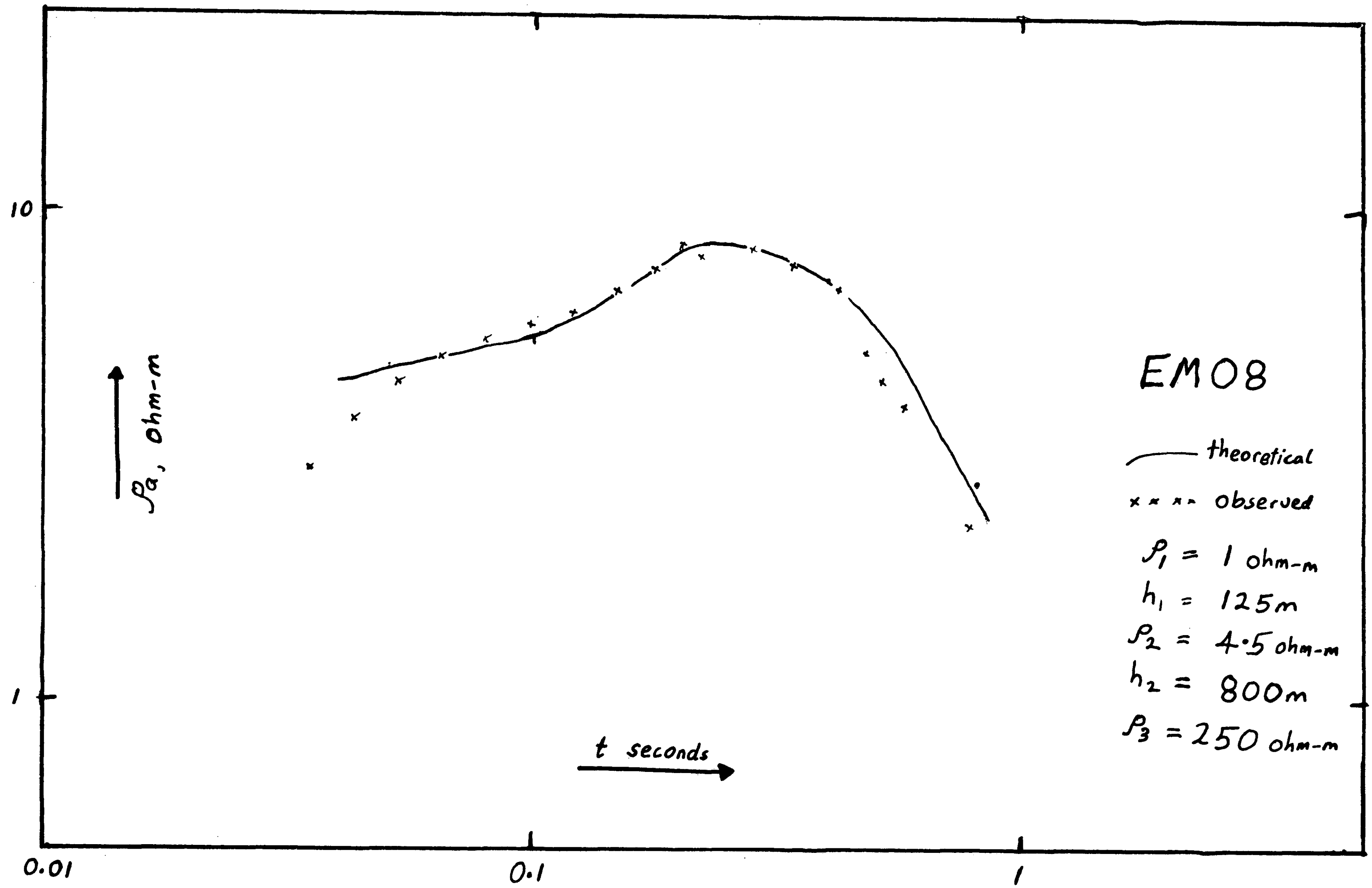

Deconvolved field curve and theoretical match, Station EM08.

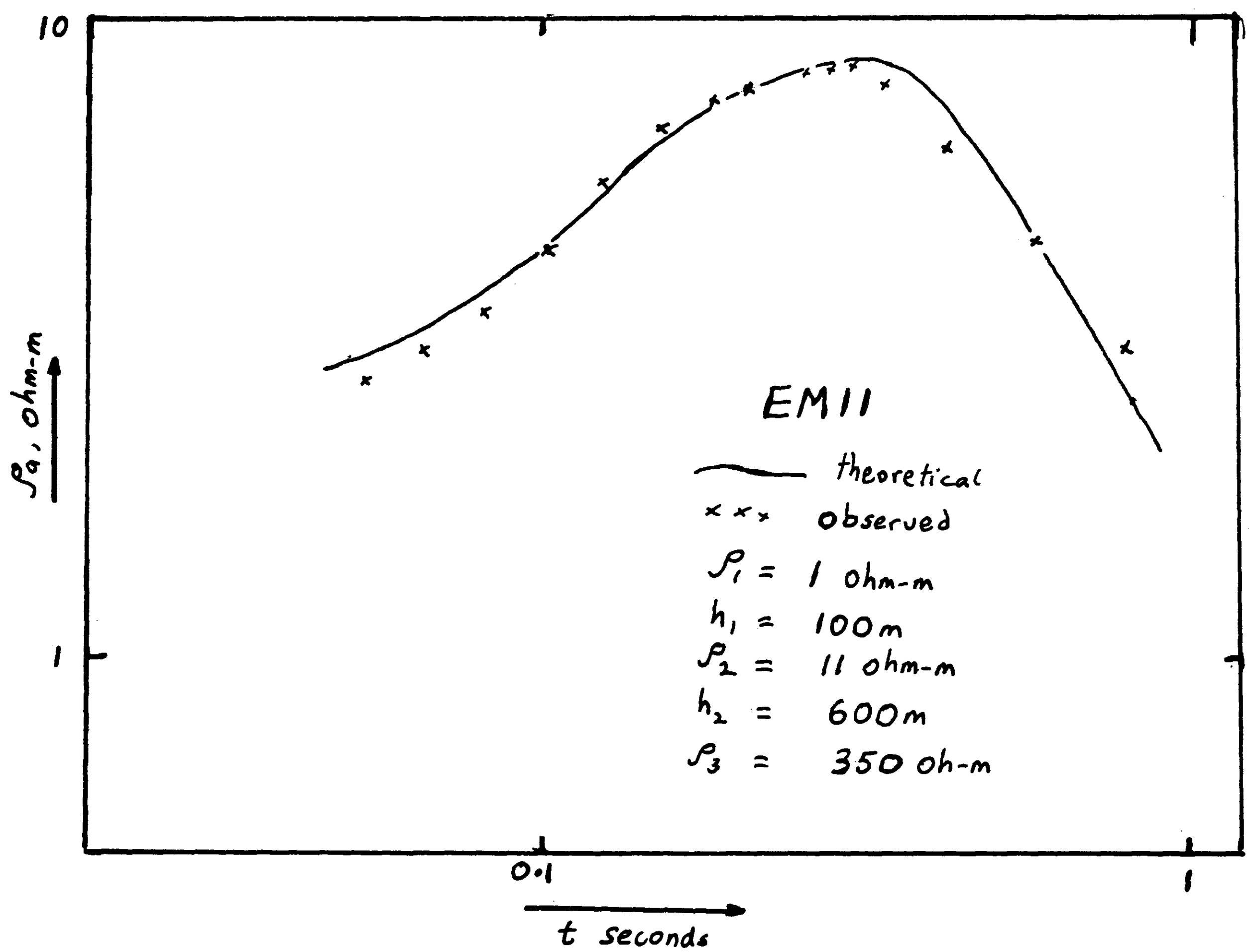

Deconvolved field curve and theoretical match, Station EM11.

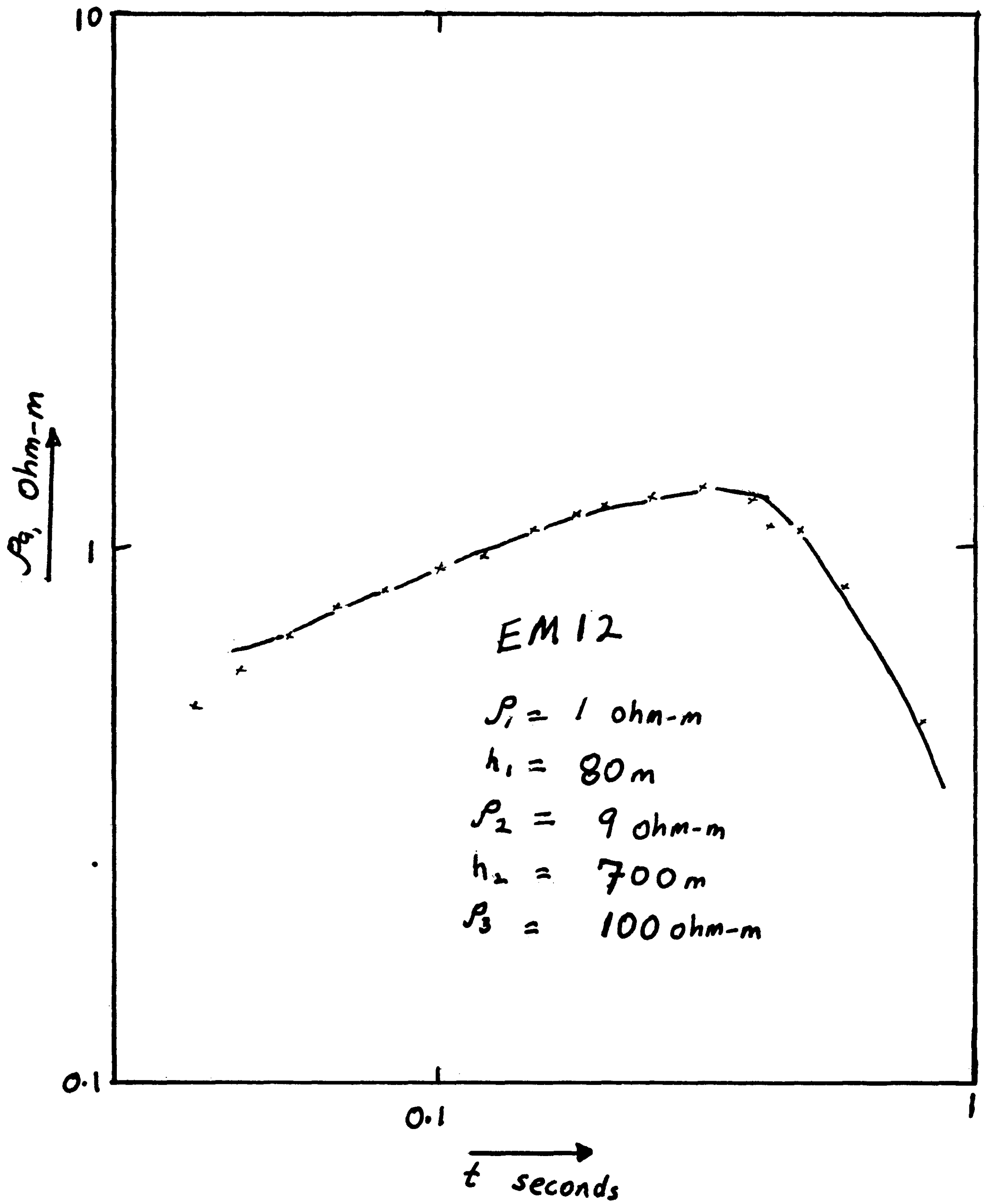

Deconvolved field curve and theoretical match, Station EM12.

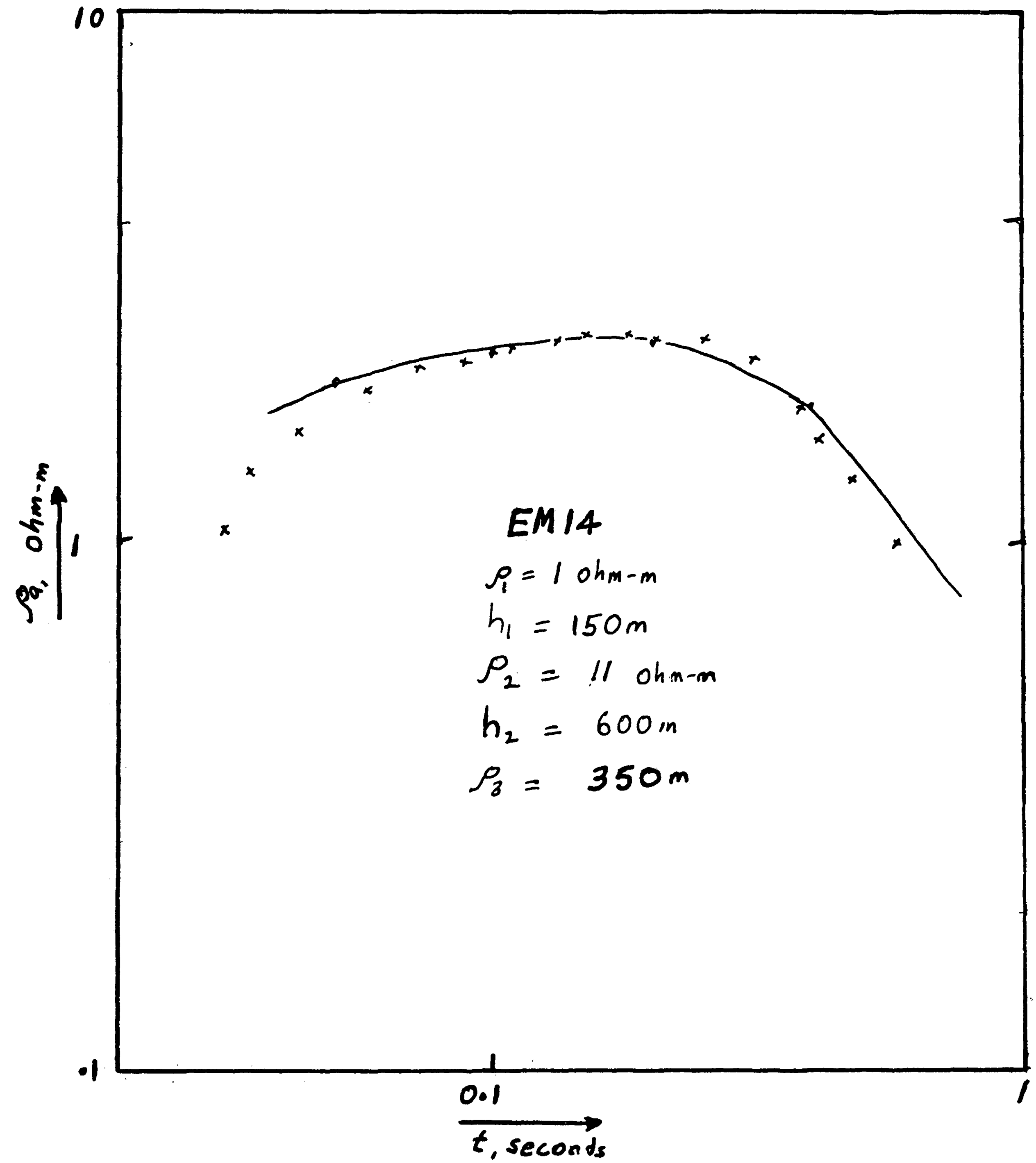

Deconvolved field curve and theoretical match, Station EM14.

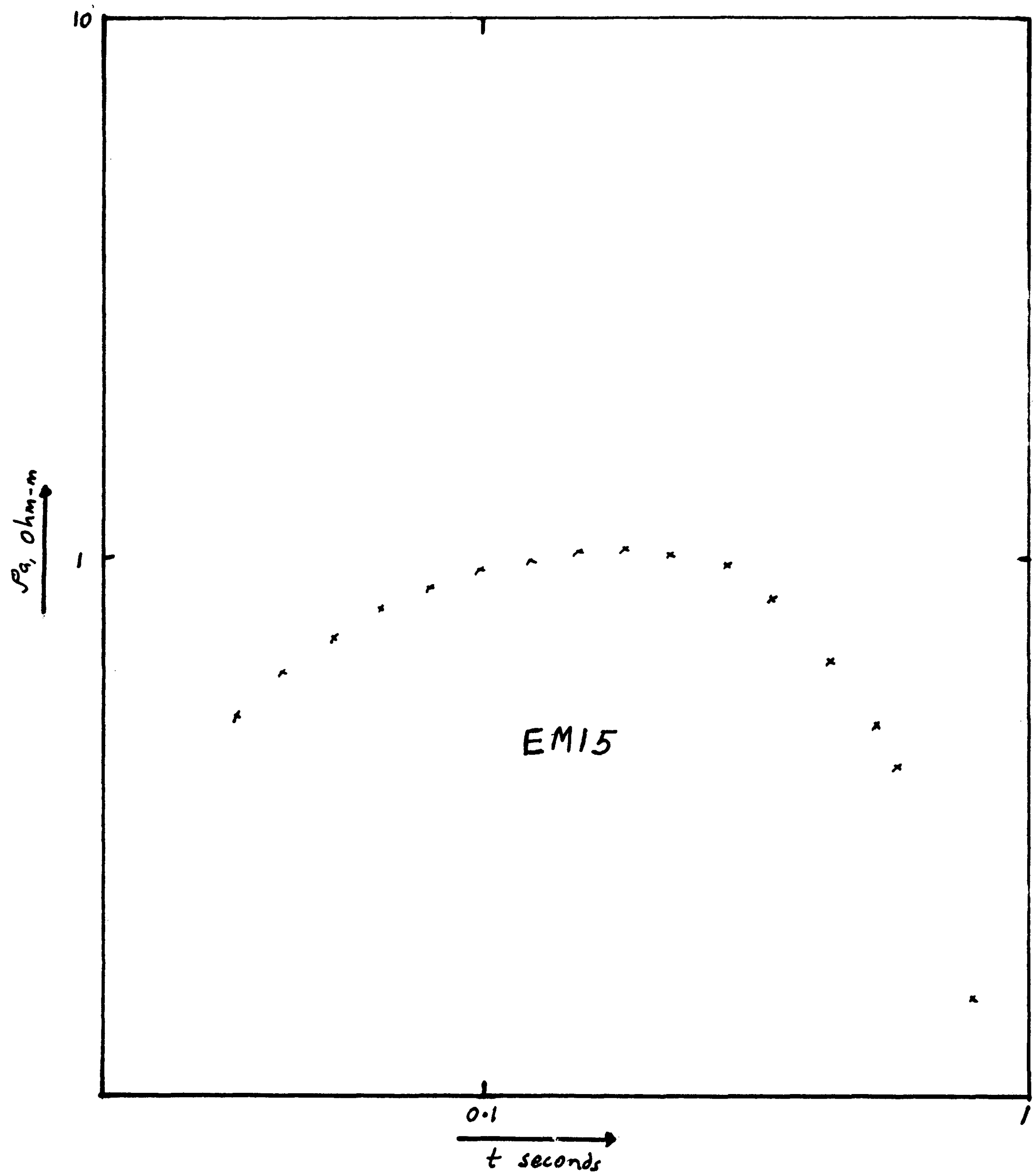

Deconvolved field curve, Station EM15.

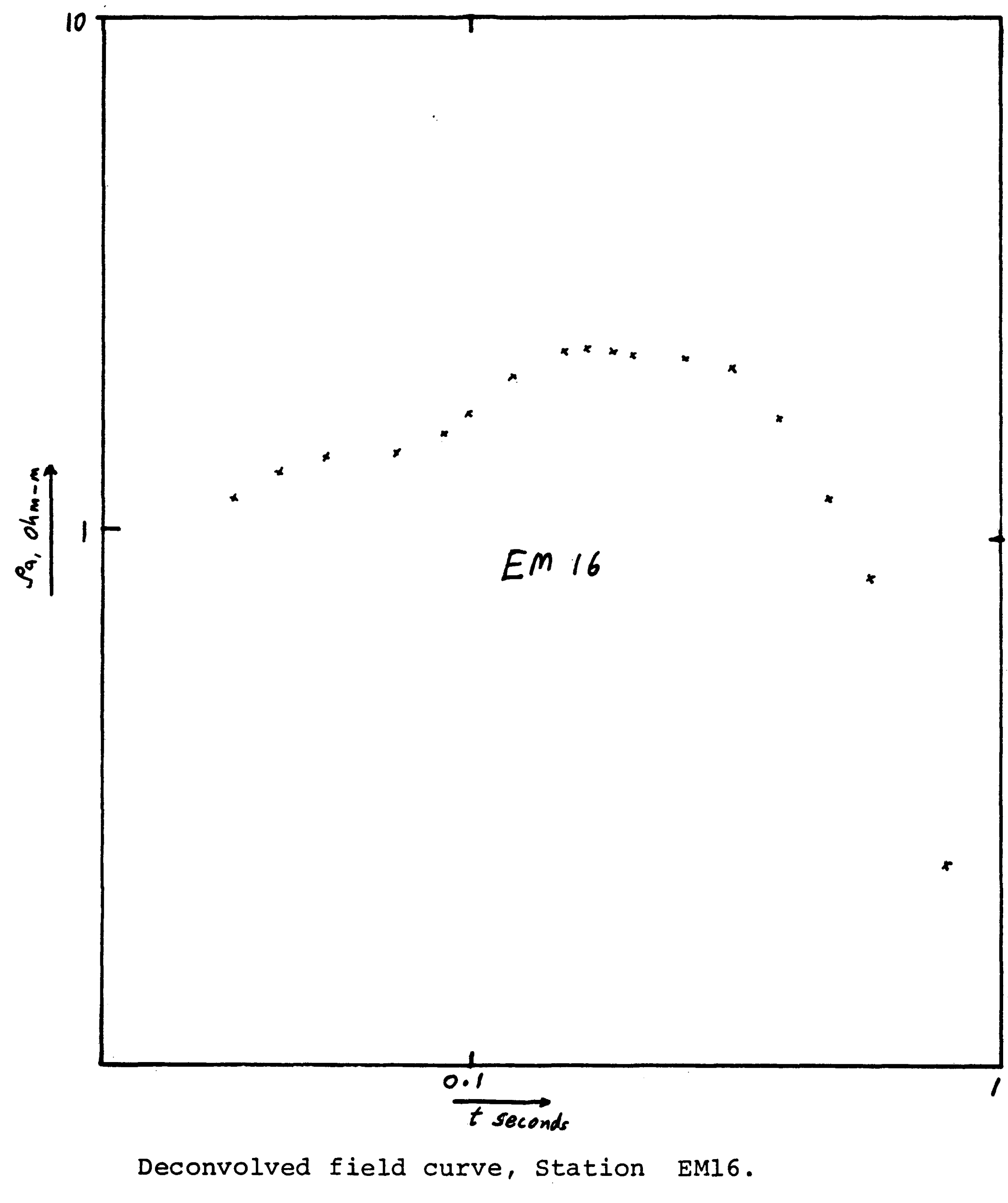

Deconvolved field curve, Station EM16.

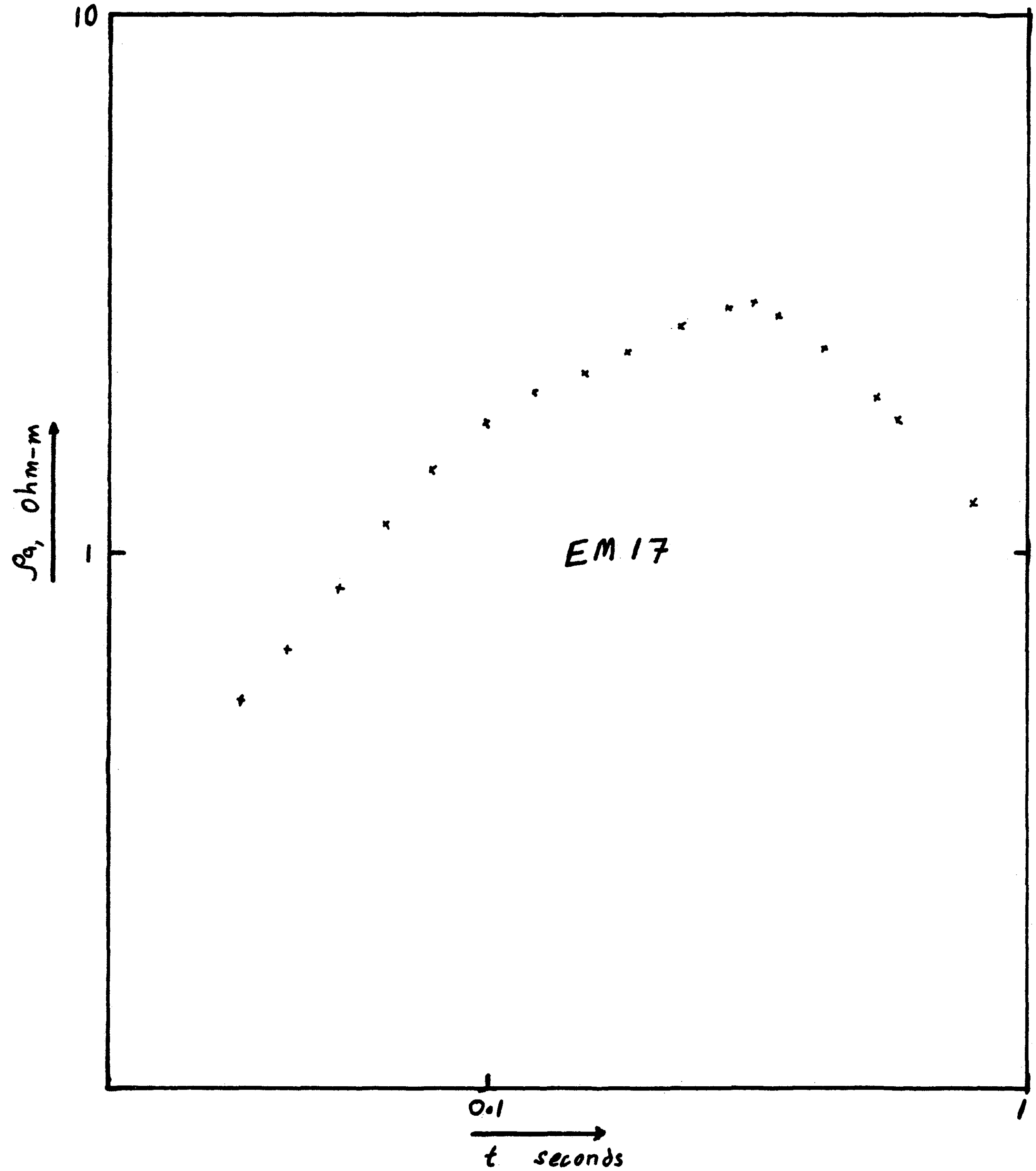

Deconvolved field curve, Station EM17.

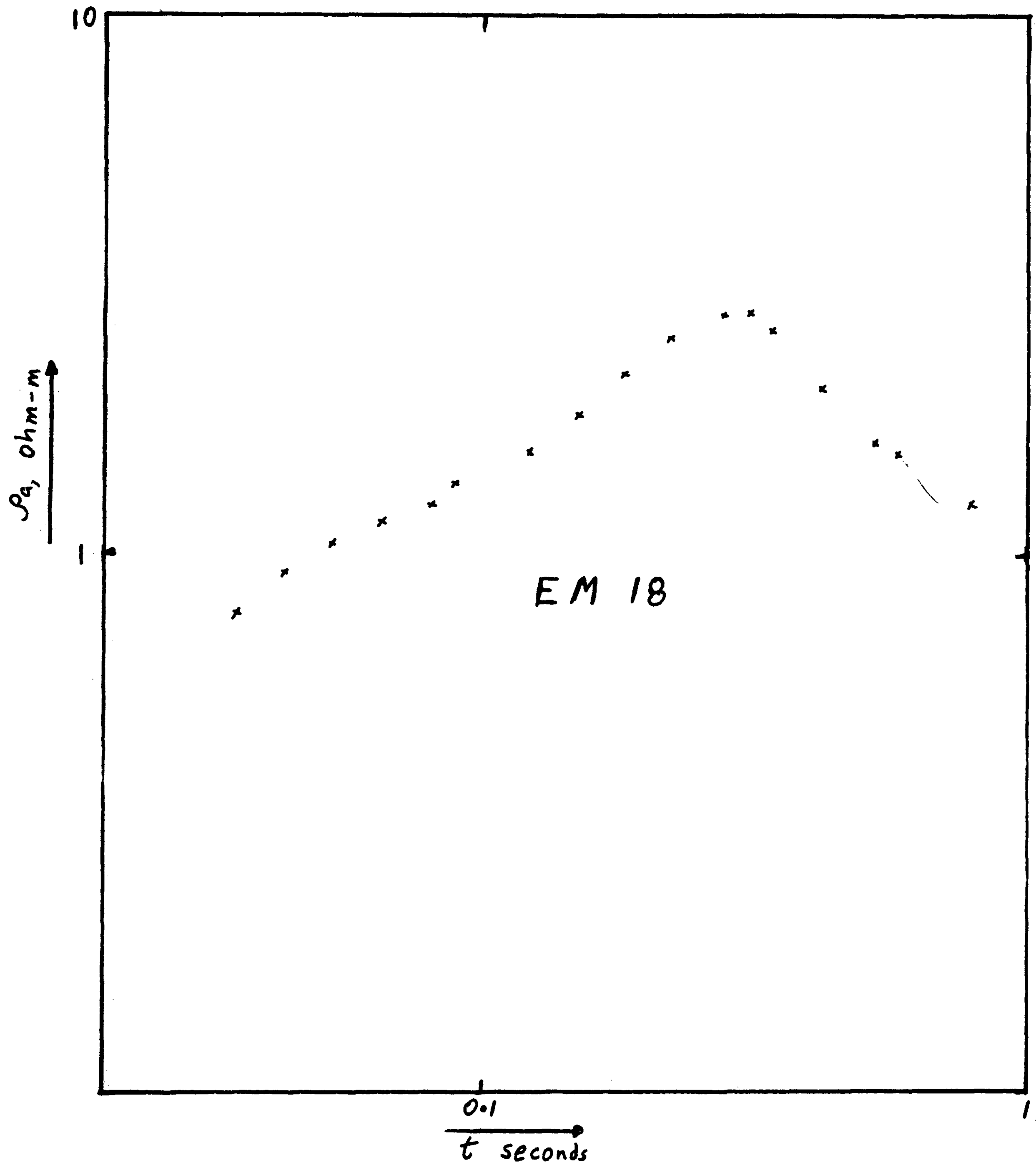

Deconvolved field curve, Station EM18.

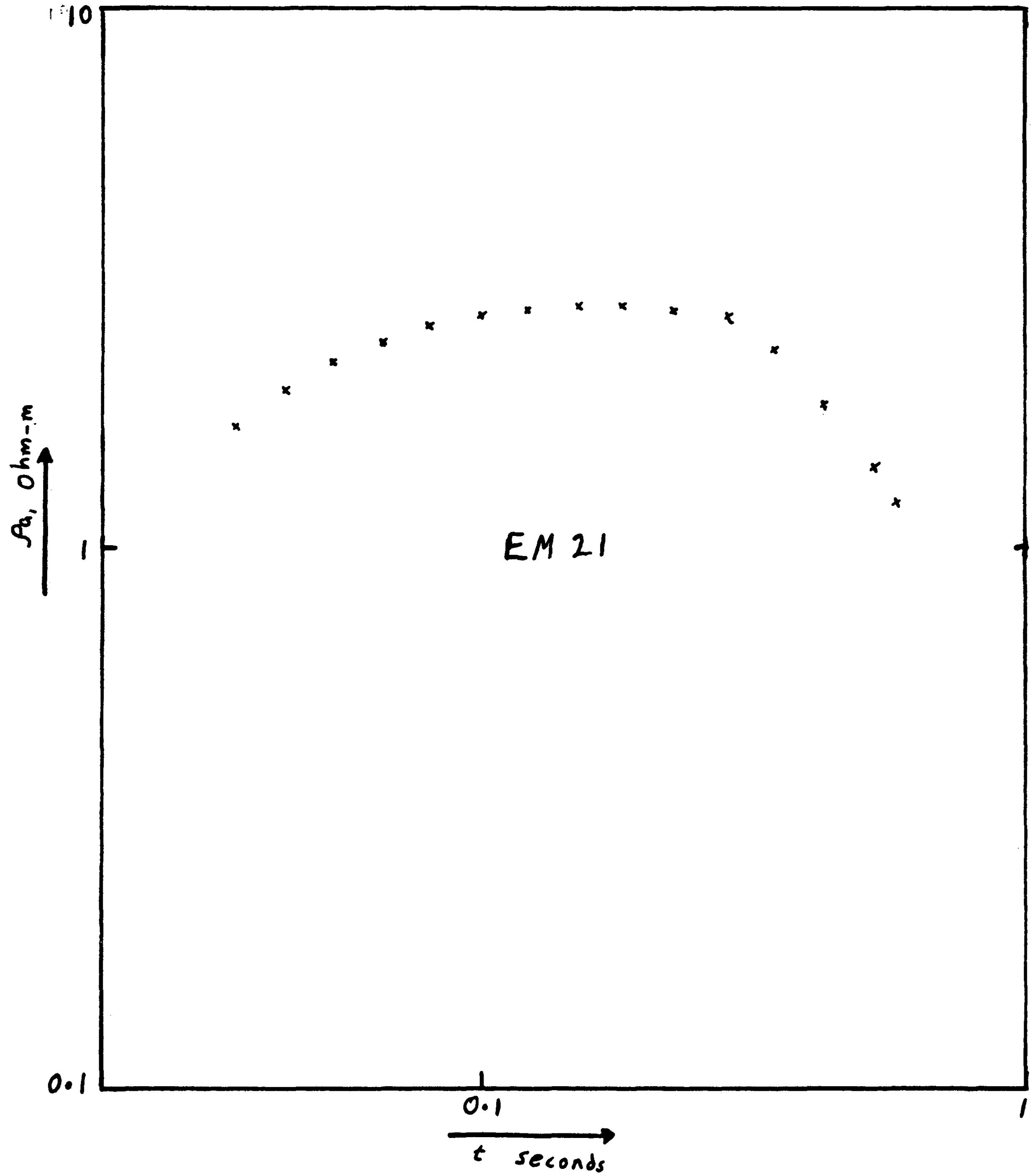

Deconvolved field curve, Station EM21.

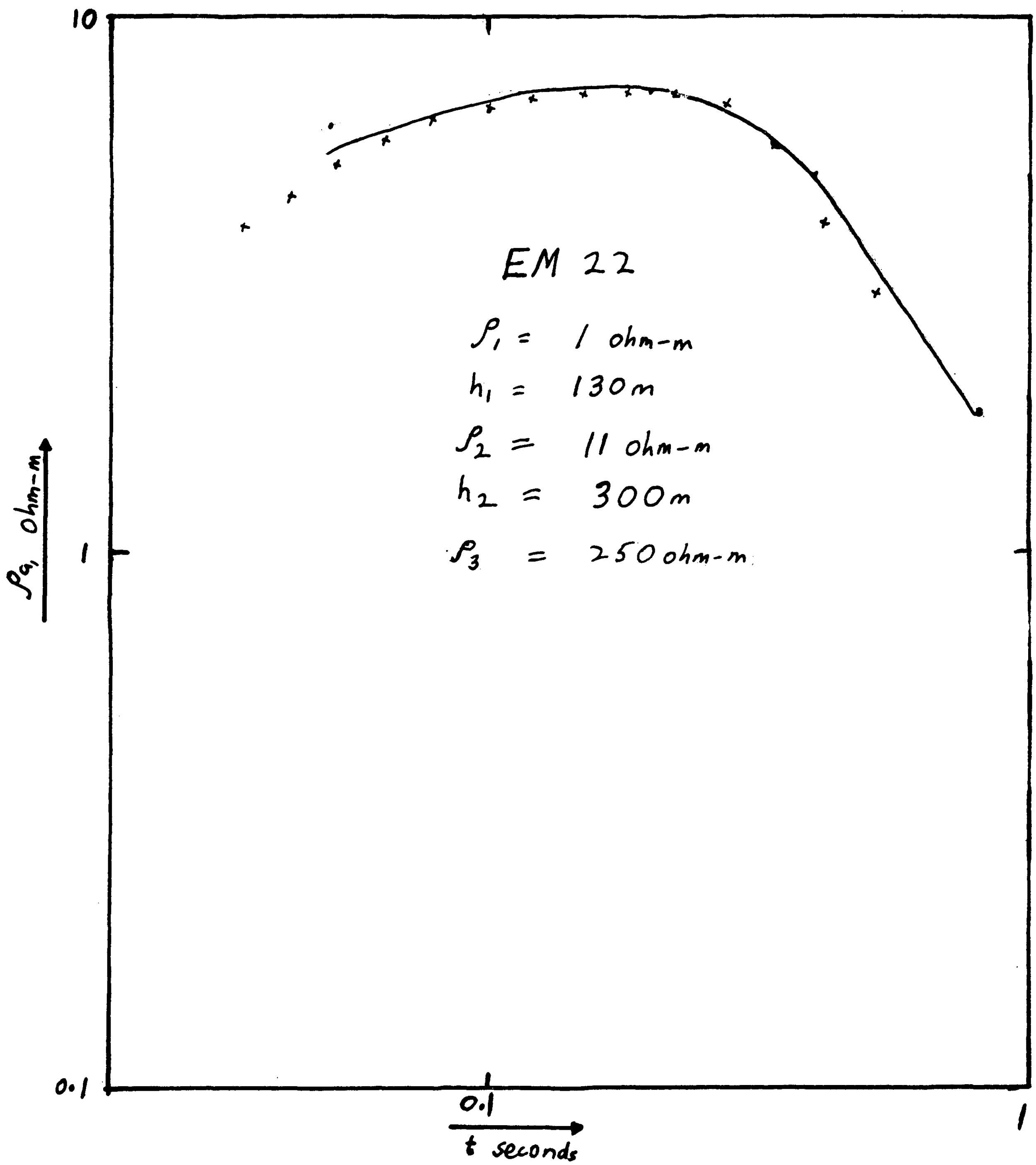

Deconvolved field curve and theoretical match, Station EM22.

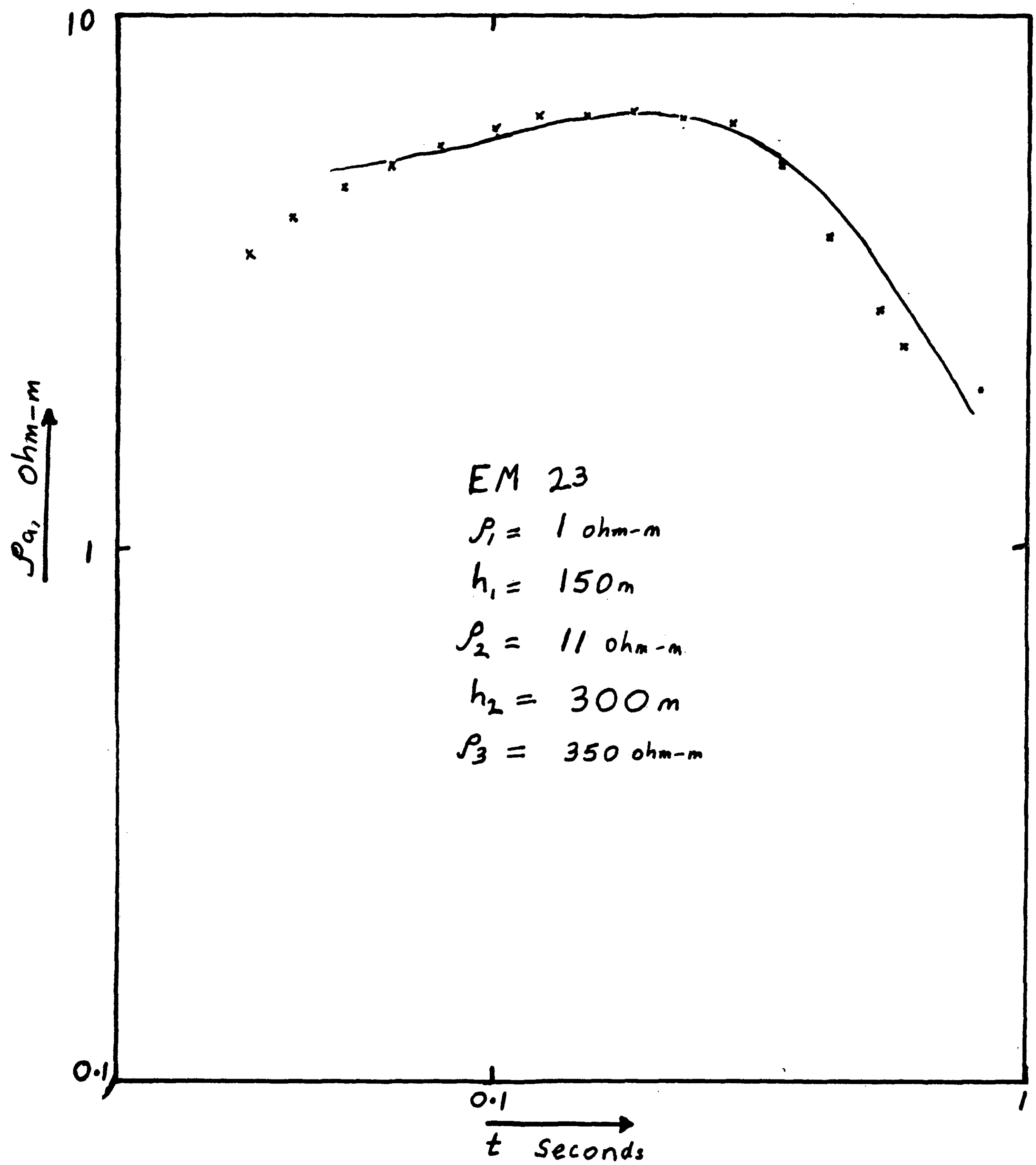

Deconvolved field curve and theoretical match, Station EM23.

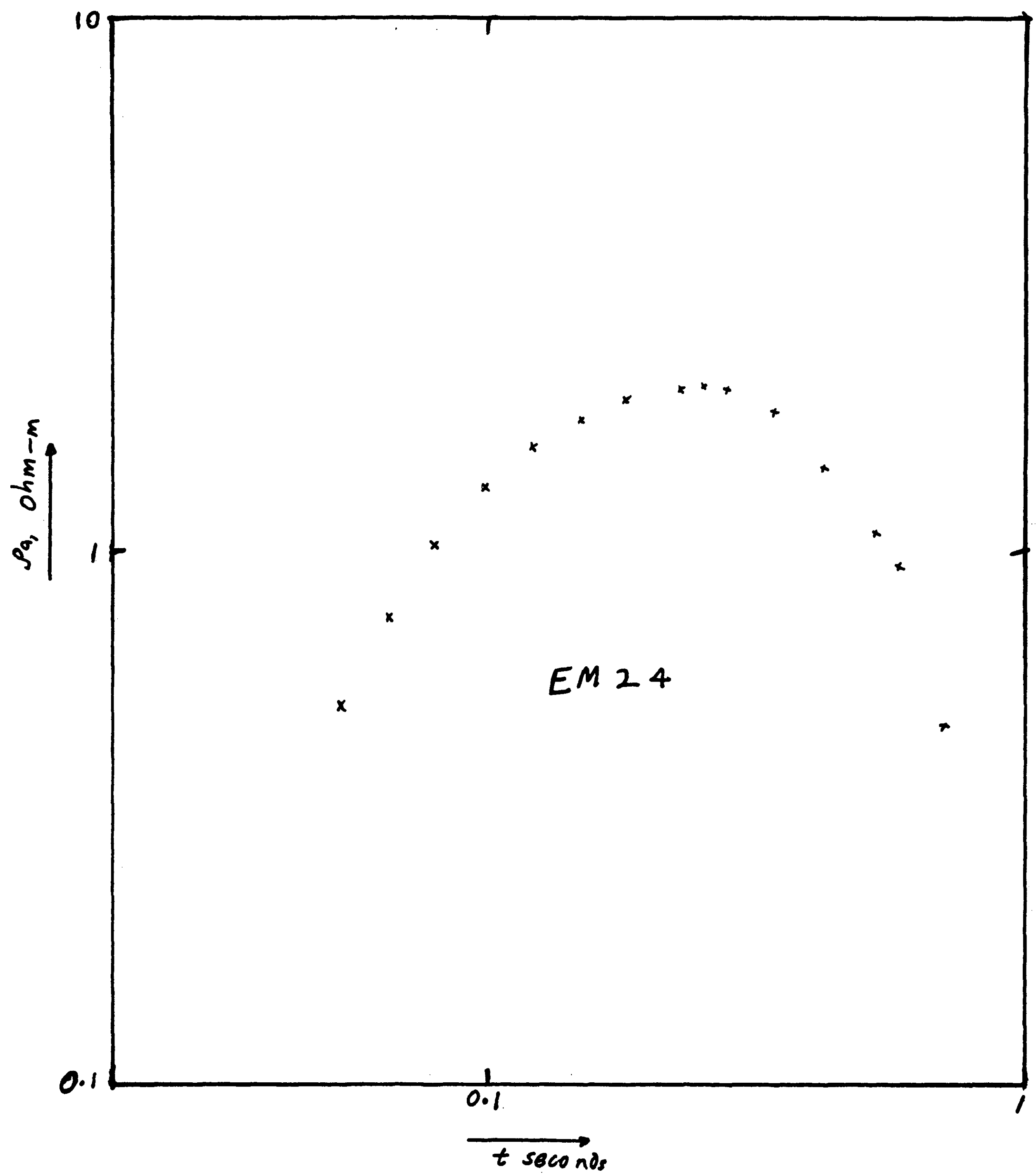

Deconvolved field curve, Station EM24.

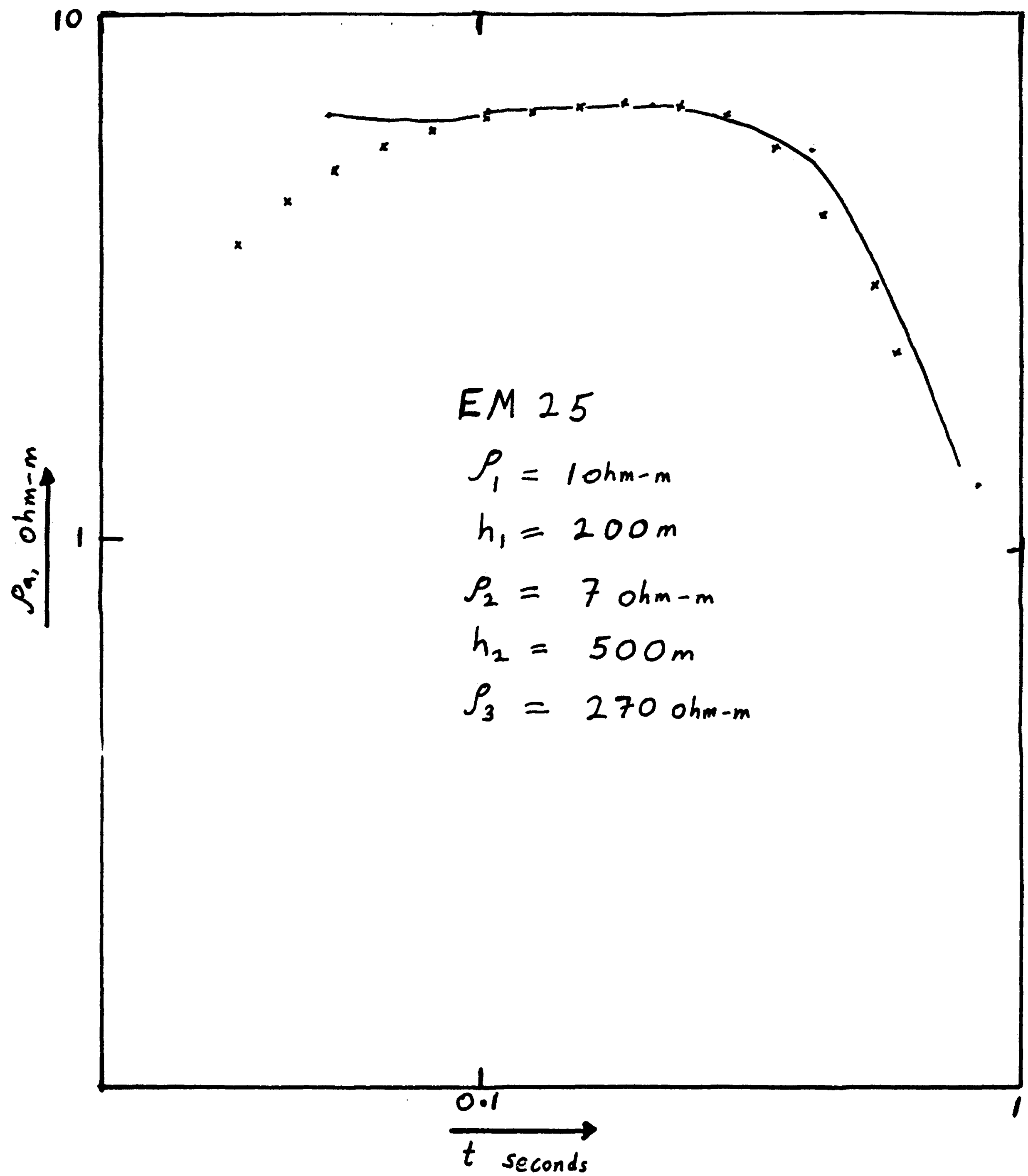

Deconvolved field curve and theoretical match, Station EM25.

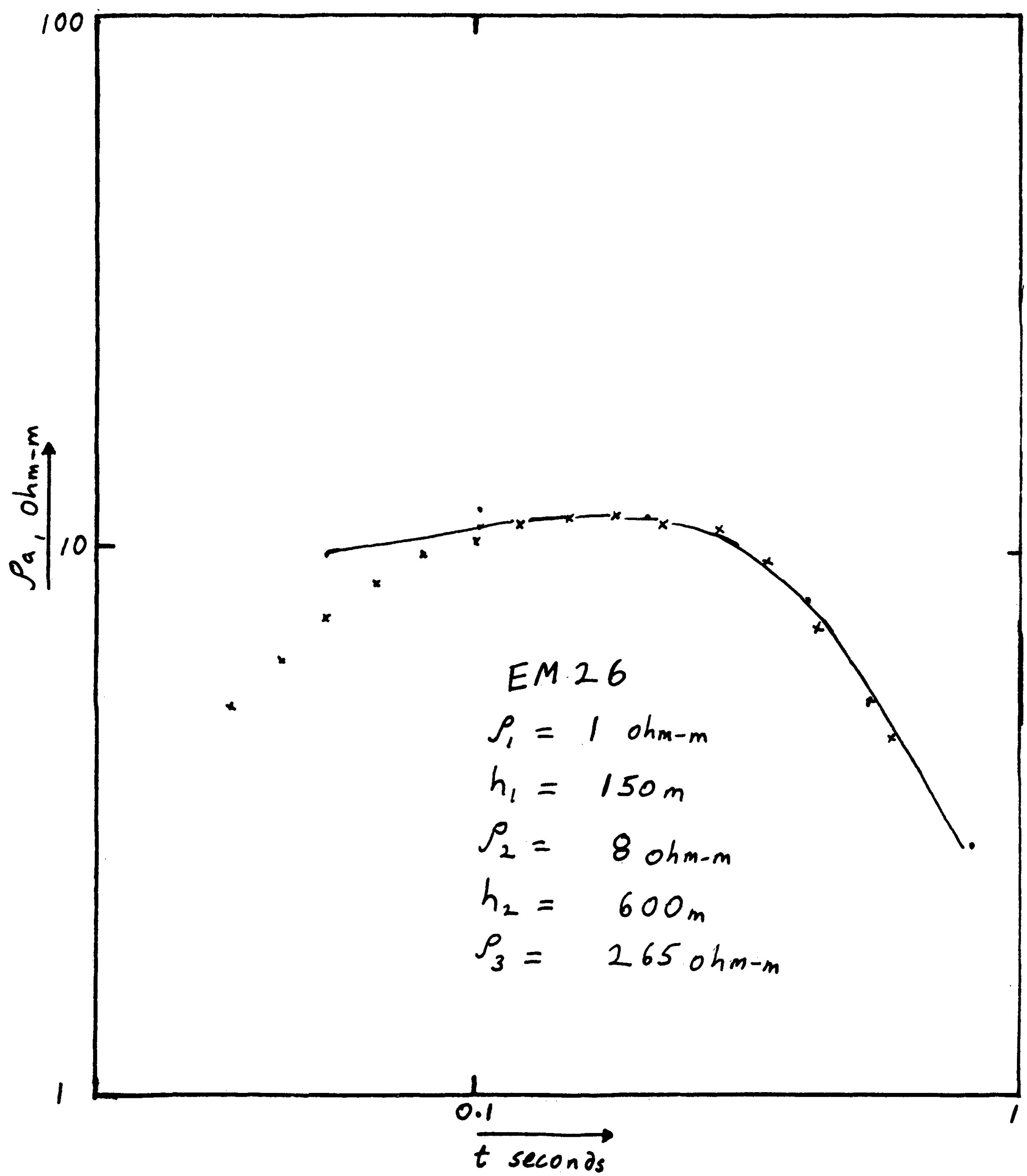

Deconvolved field curve and theoretical match, Station EM26.

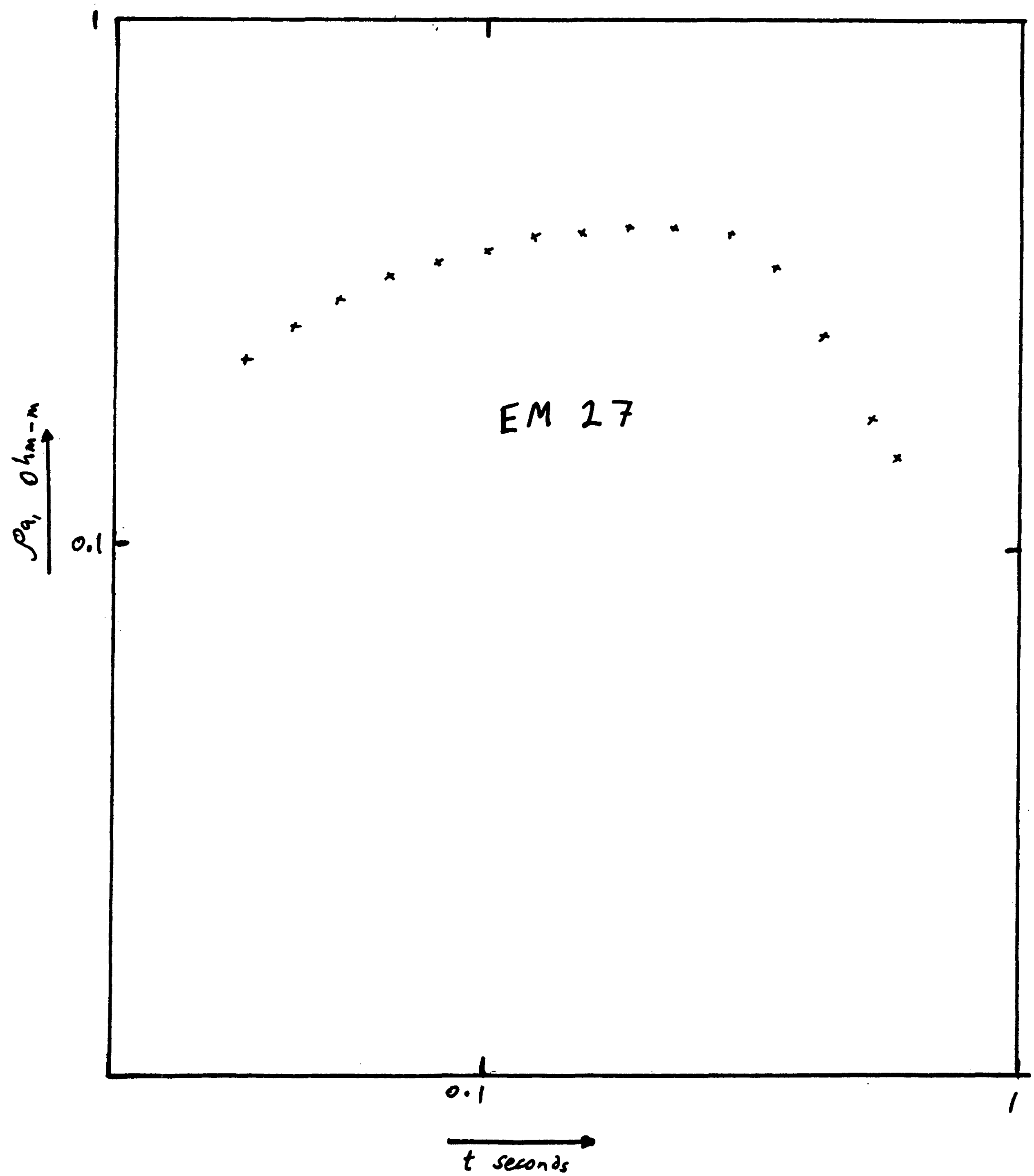

Deconvolved field curve, Station EM27.

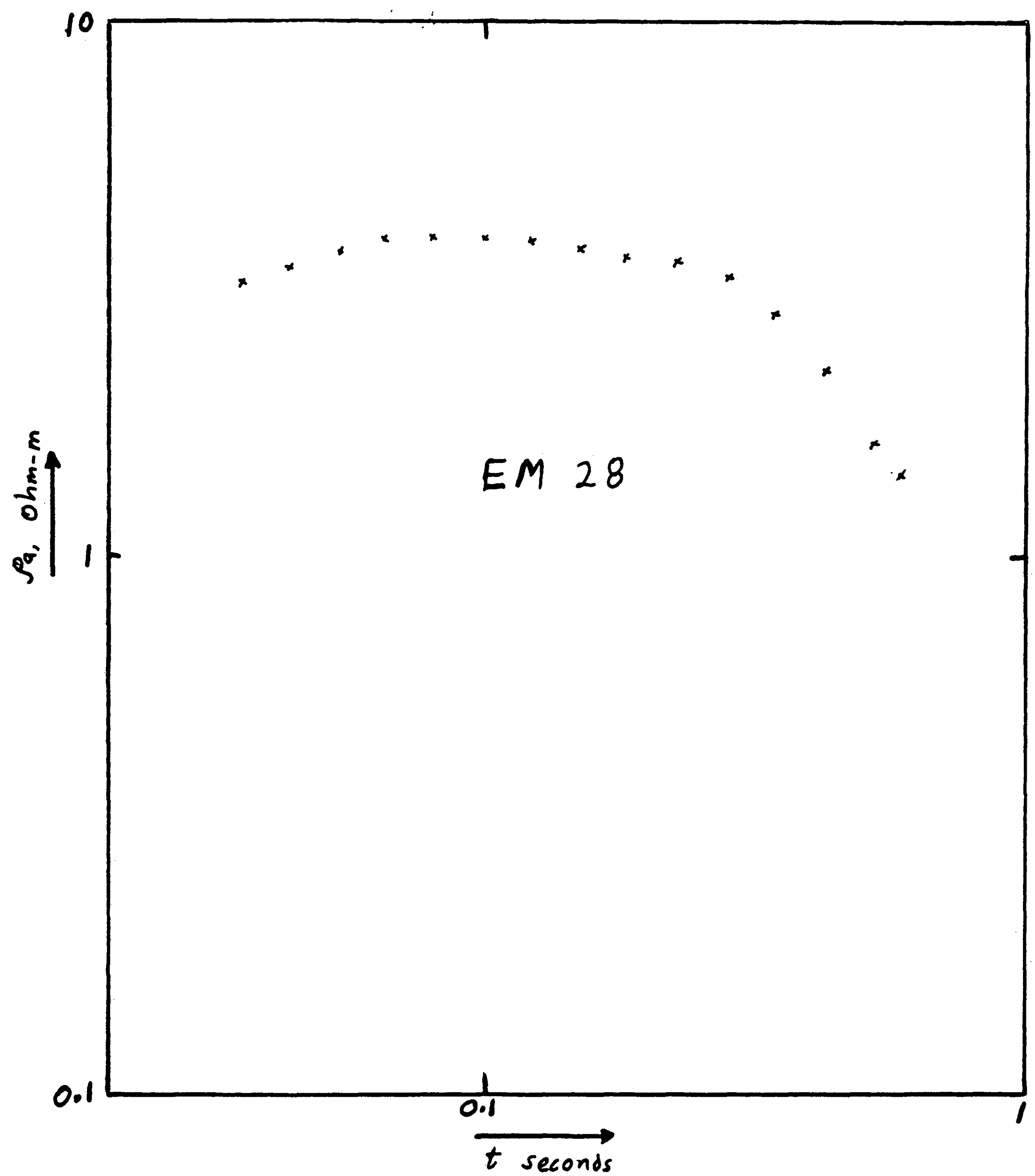

Deconvolved field curve, Station EM28;

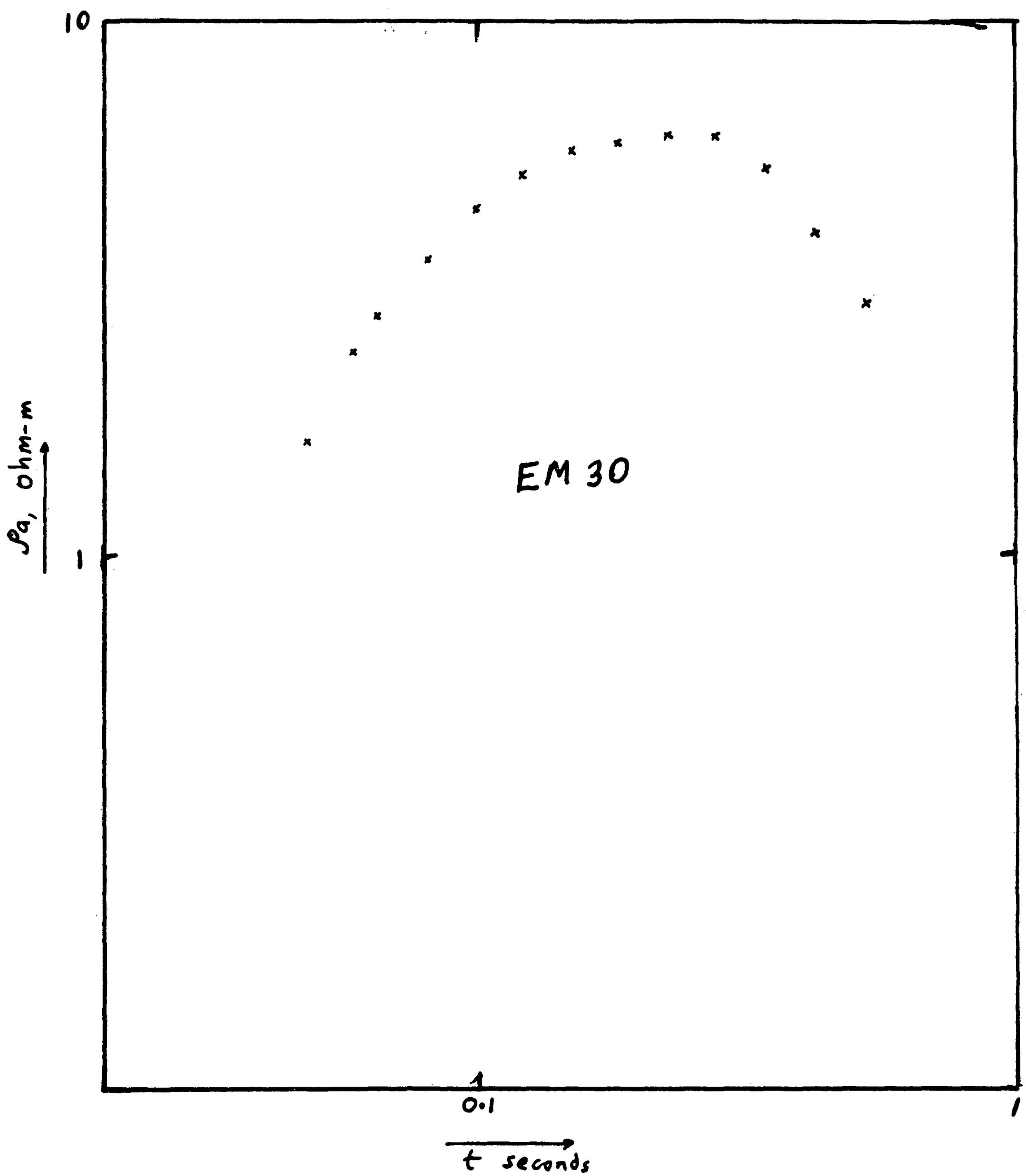

Deconvolved field curve, Station EM30.

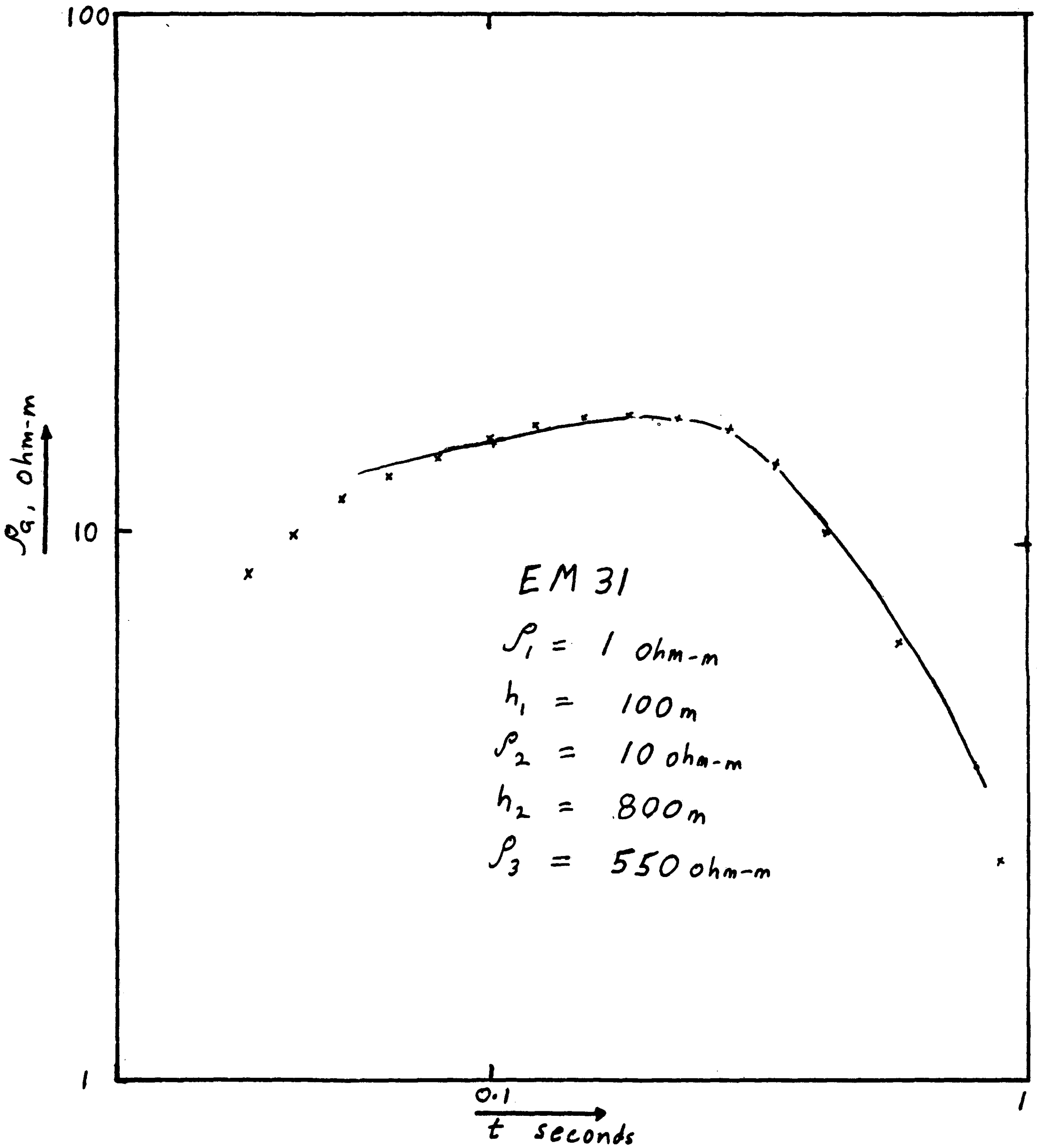

Deconvolved field curve and theoretical match, Station EM31.

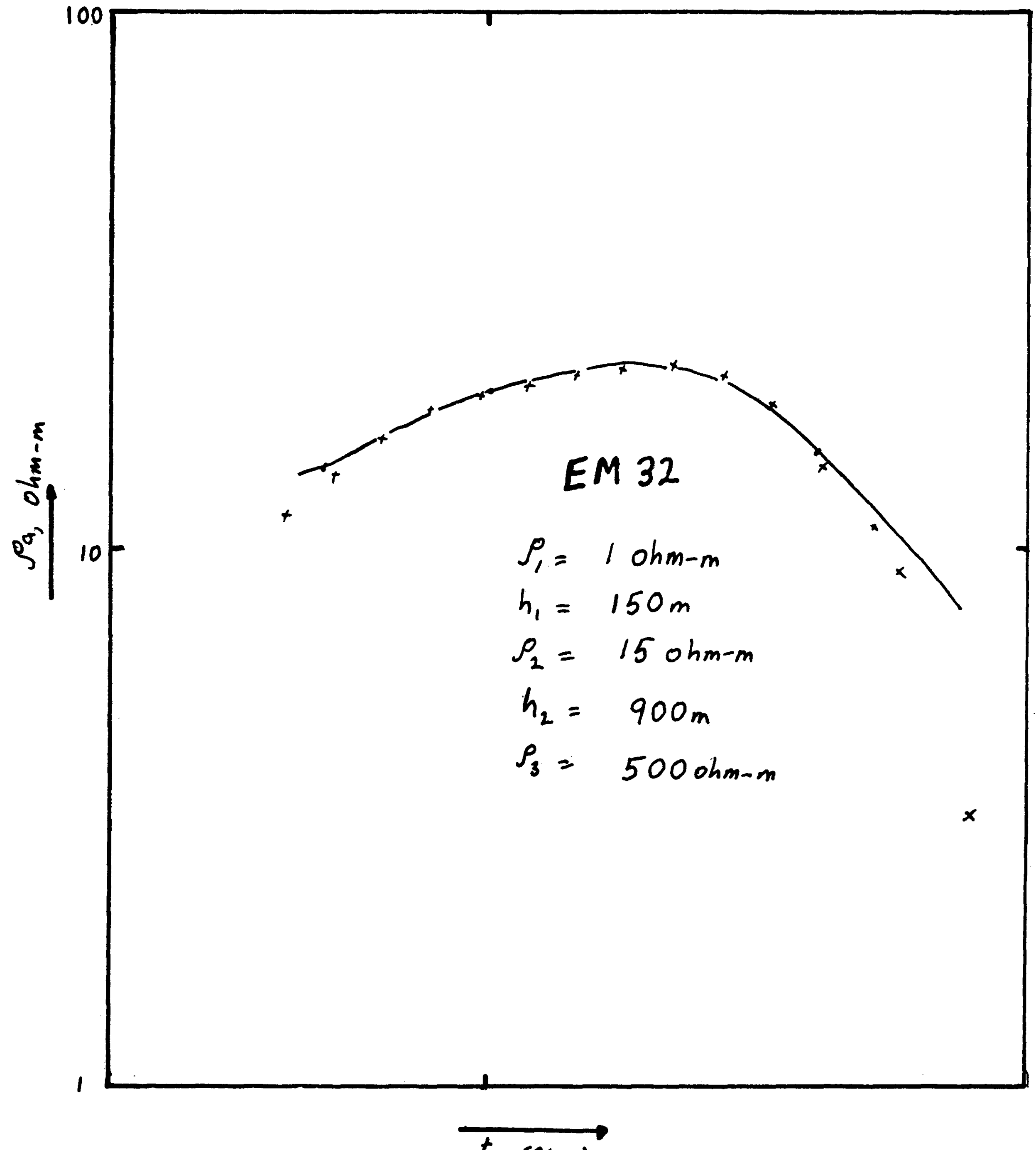

Deconvolved field curve and theoretical match, Station EM32.

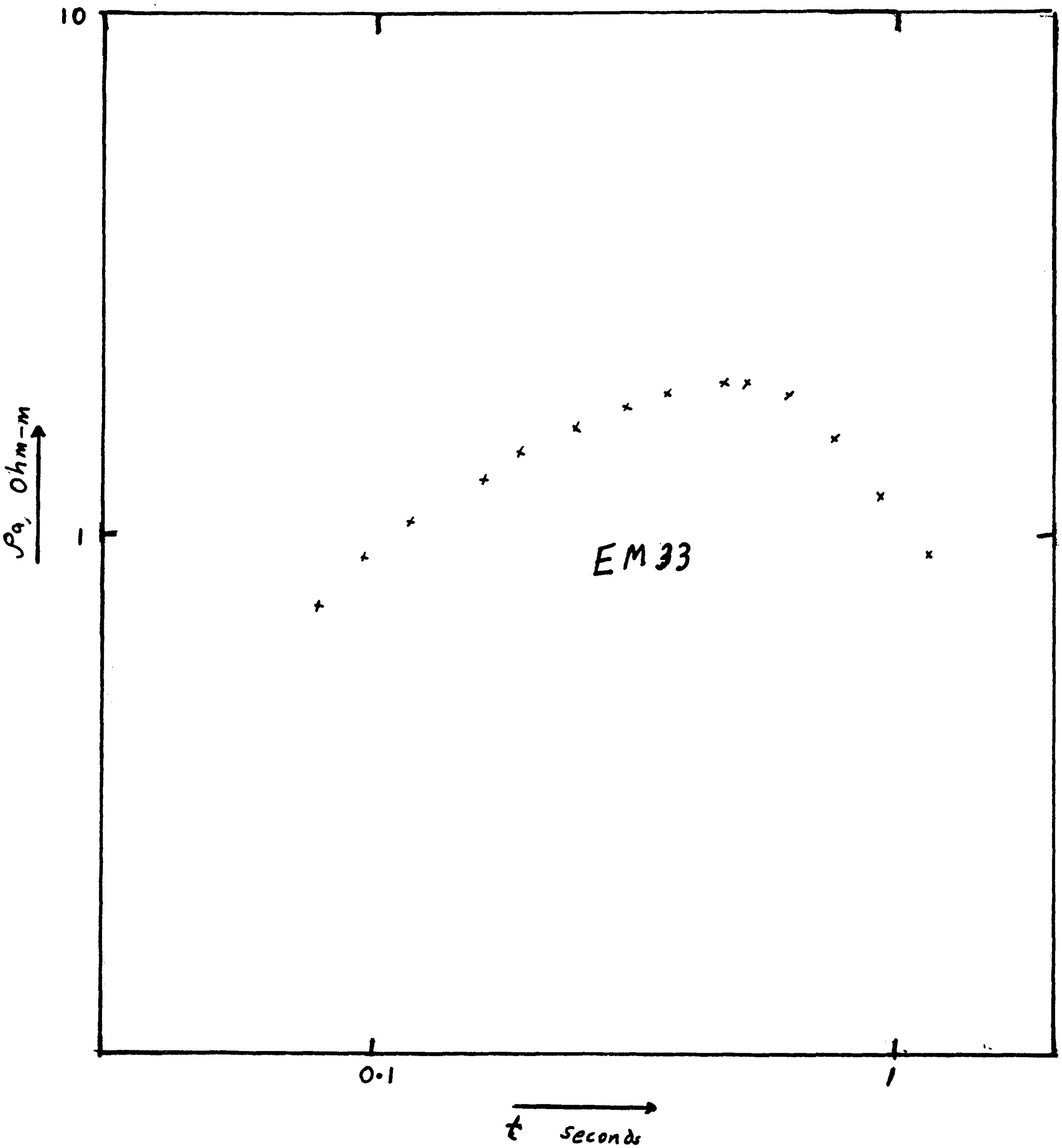

Deconvolved field curve, Station EM33.

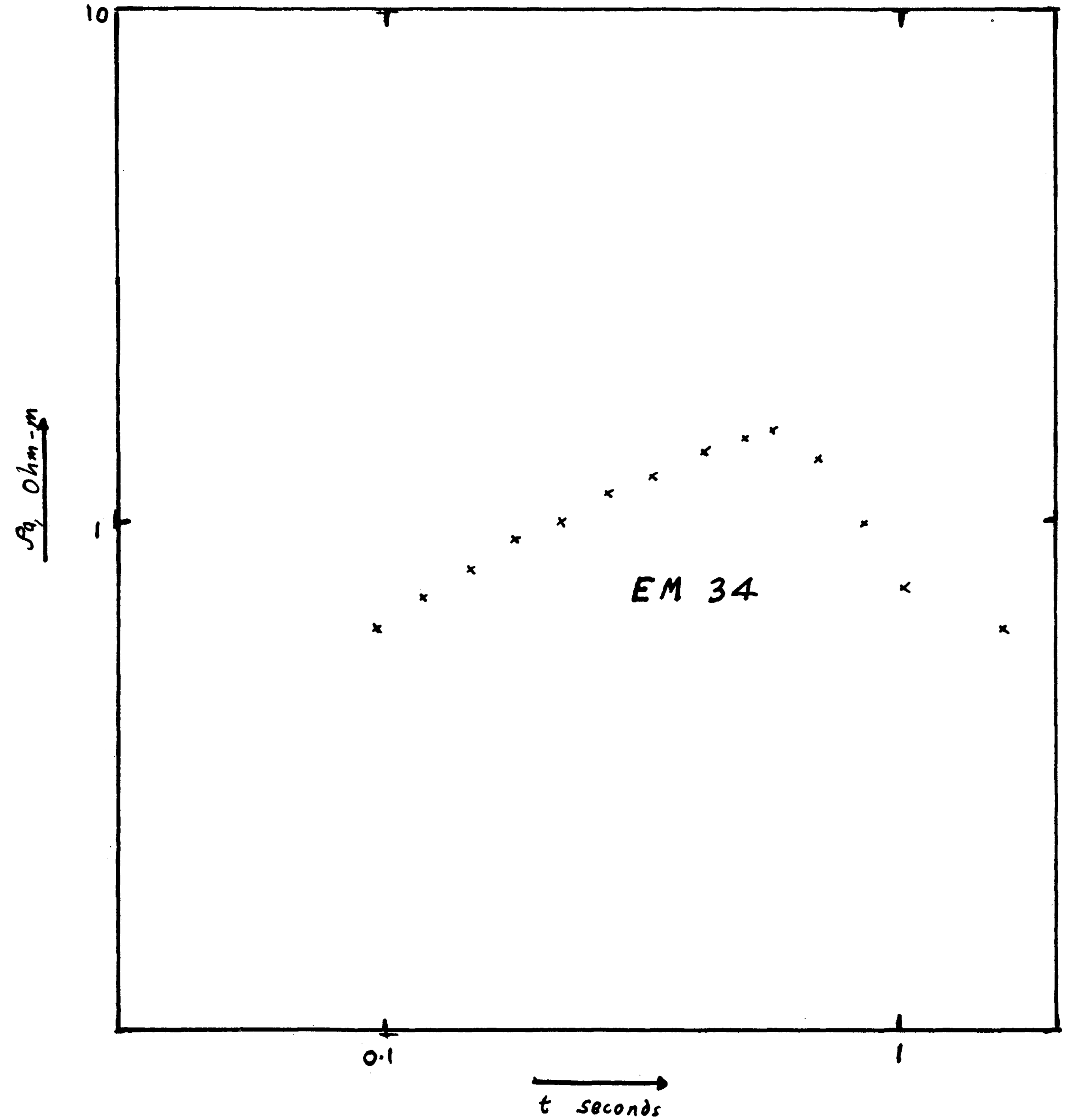

Deconvolved field curve, Station EM34.

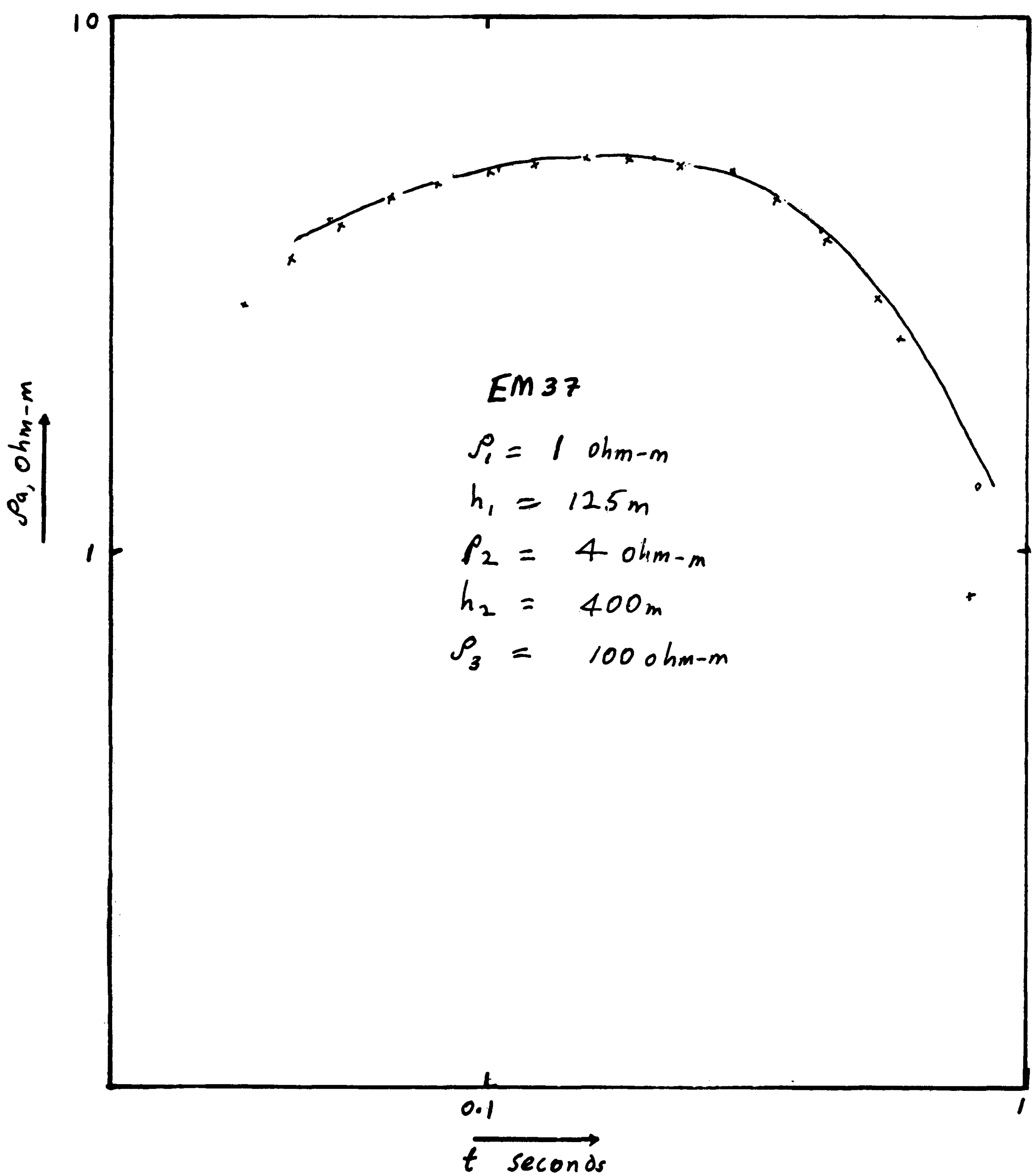

Deconvolved field curve and theoretical match, Station EM37.

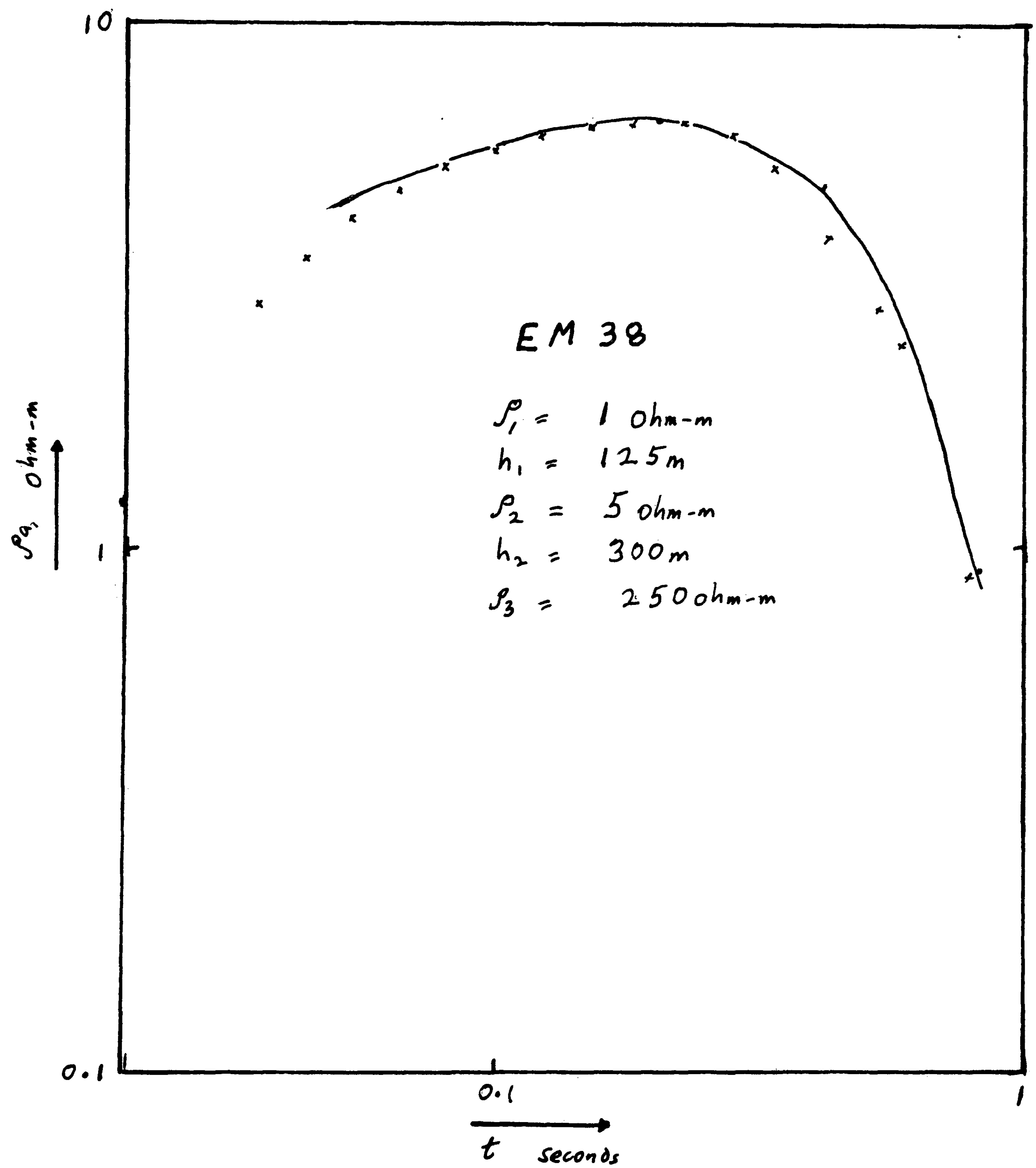

Deconvolved field curve and theoretical match, Station EM38.

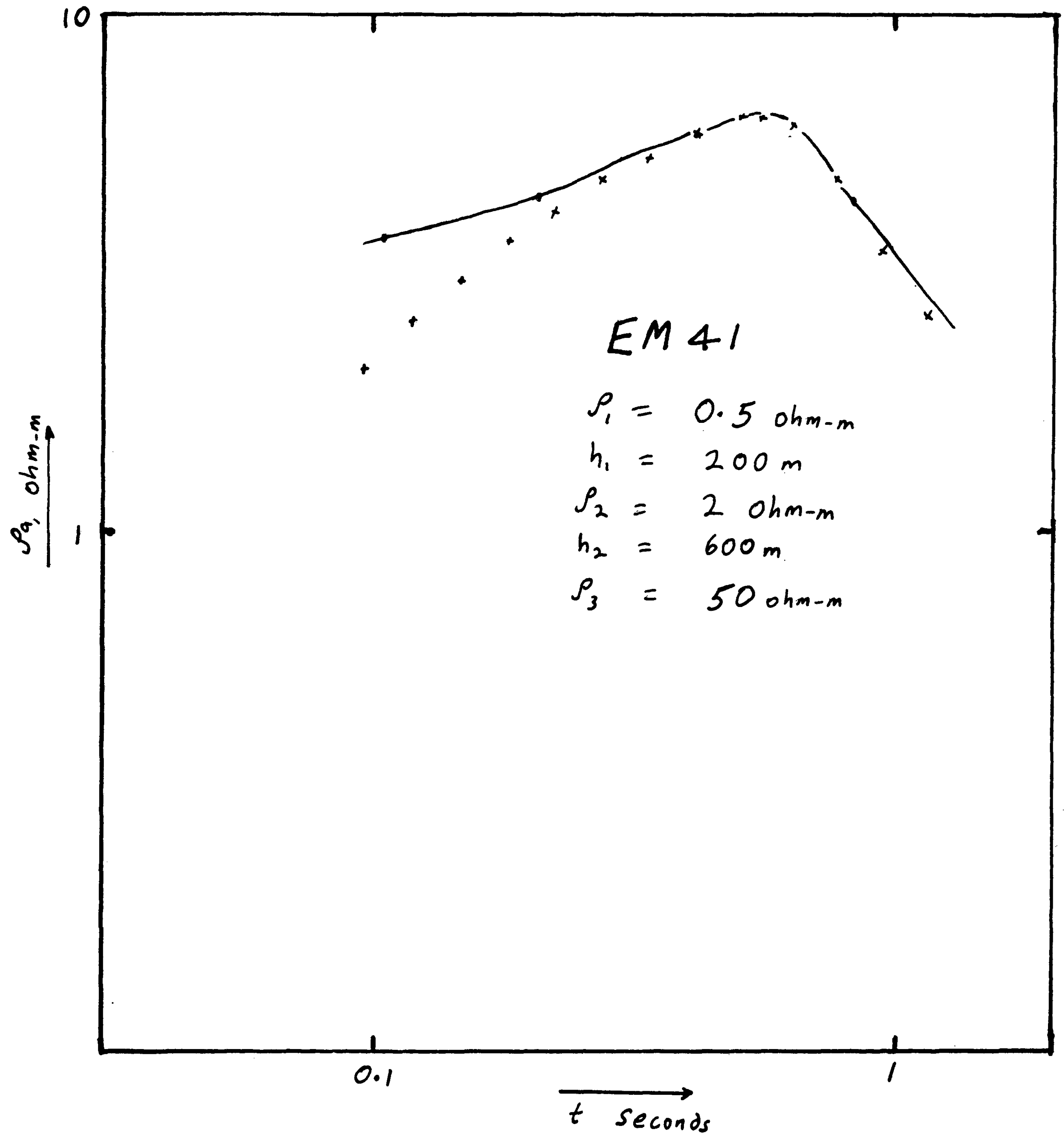

Deconvolved field curve and theoretical match, Station EM41.

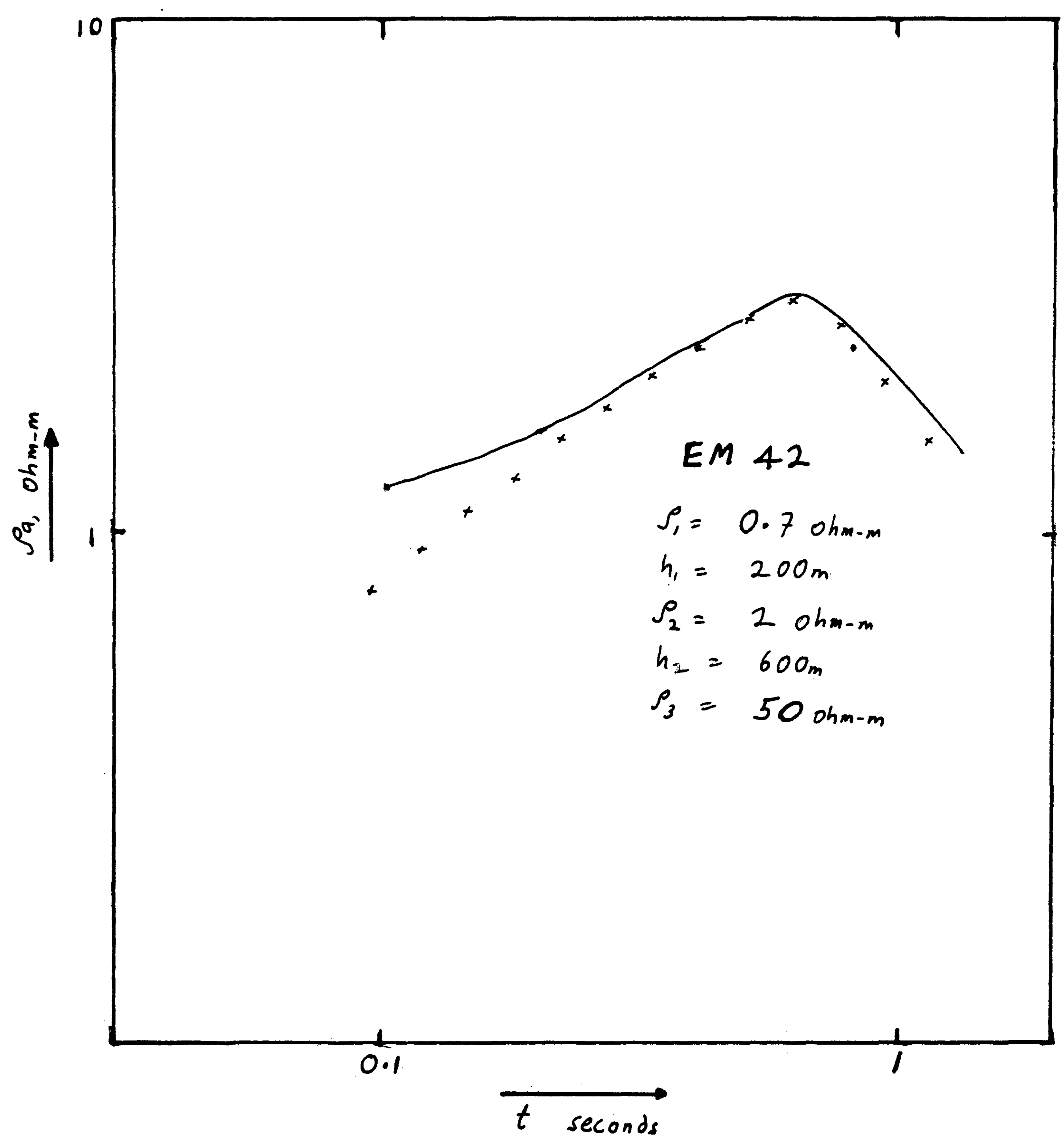

Deconvolved field curve and theoretical match, Station EM42.

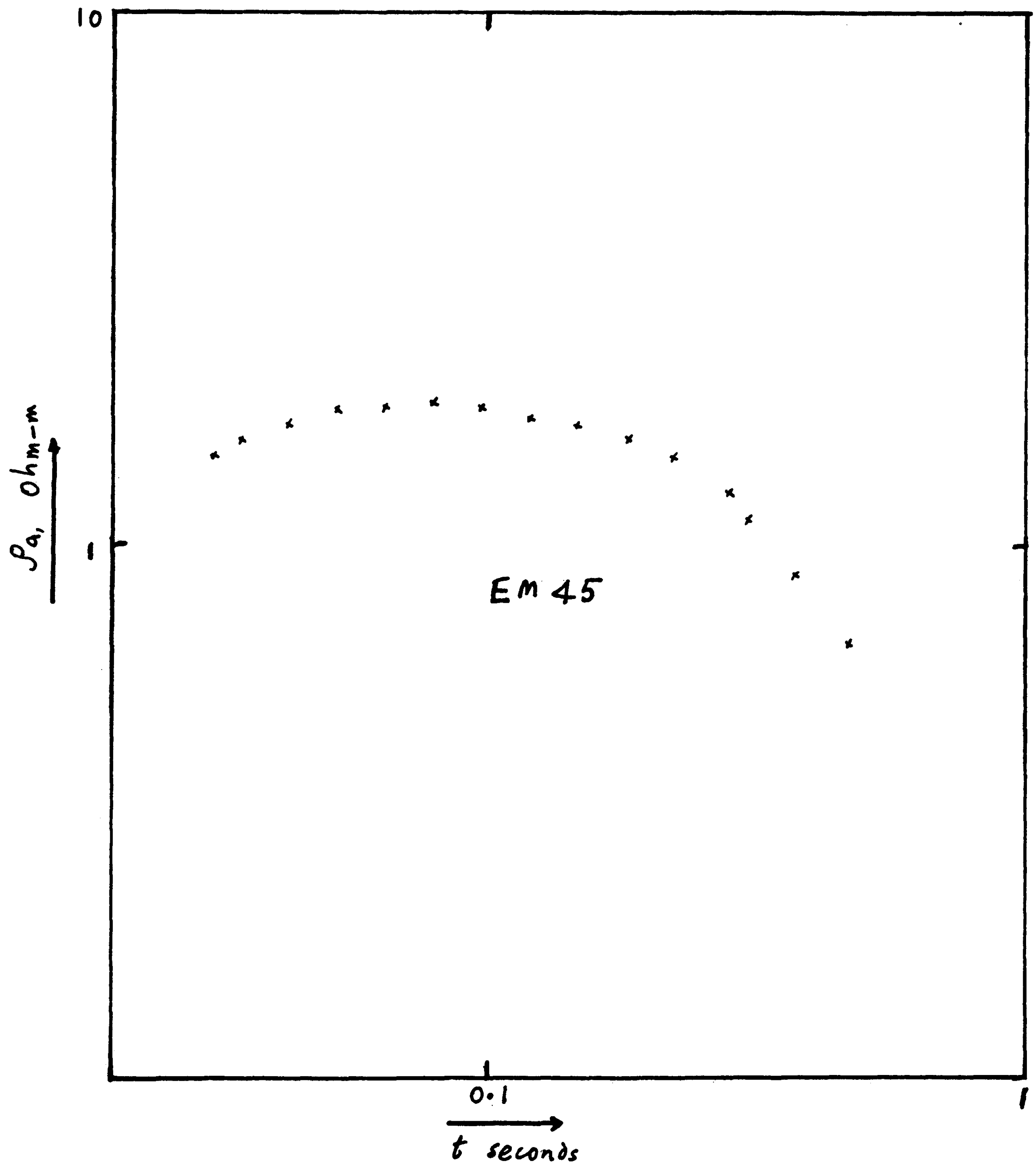

Deconvolved field curve, Station EM45.

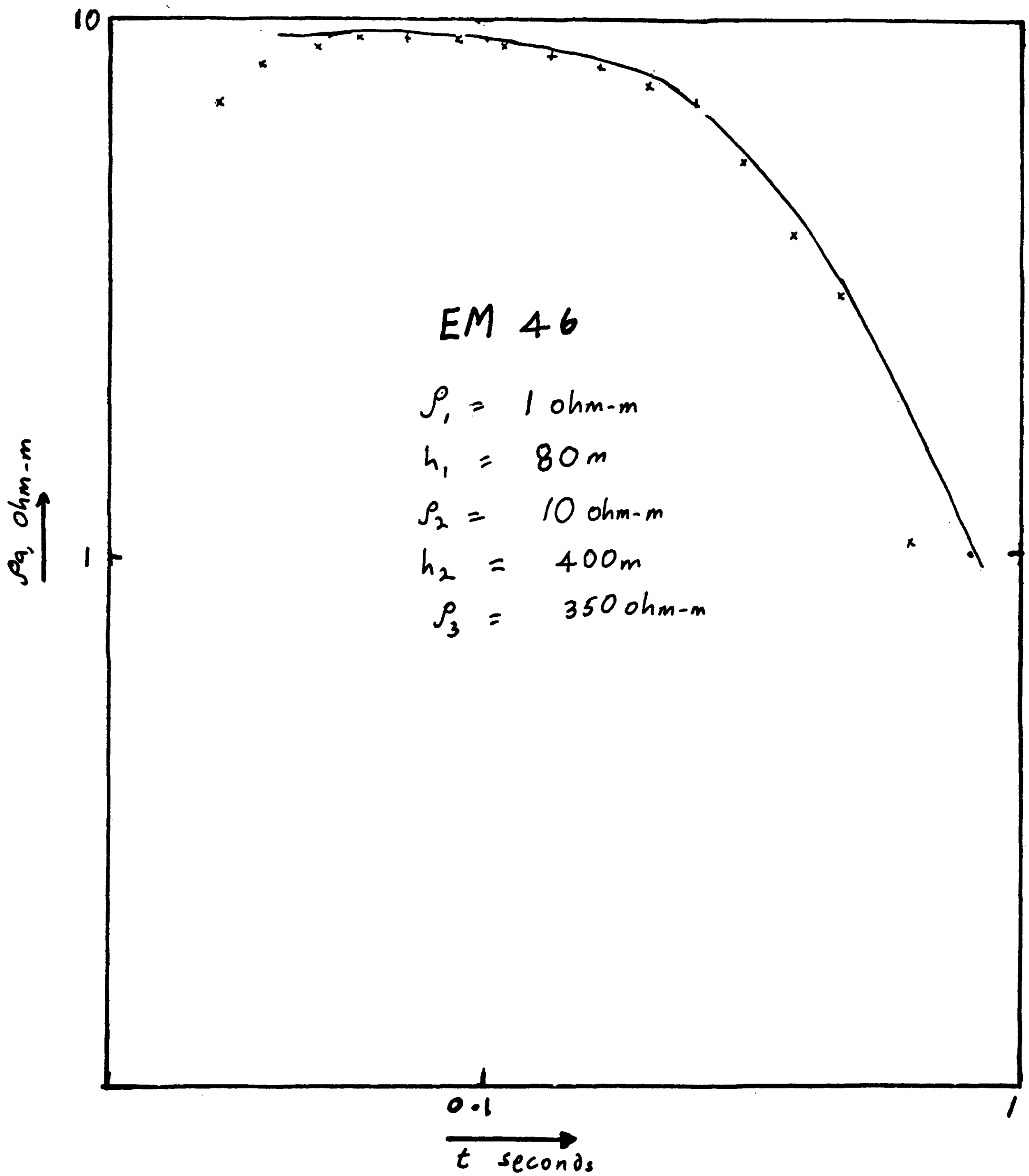

Deconvolved field curve and theoretical match, Station EM46.

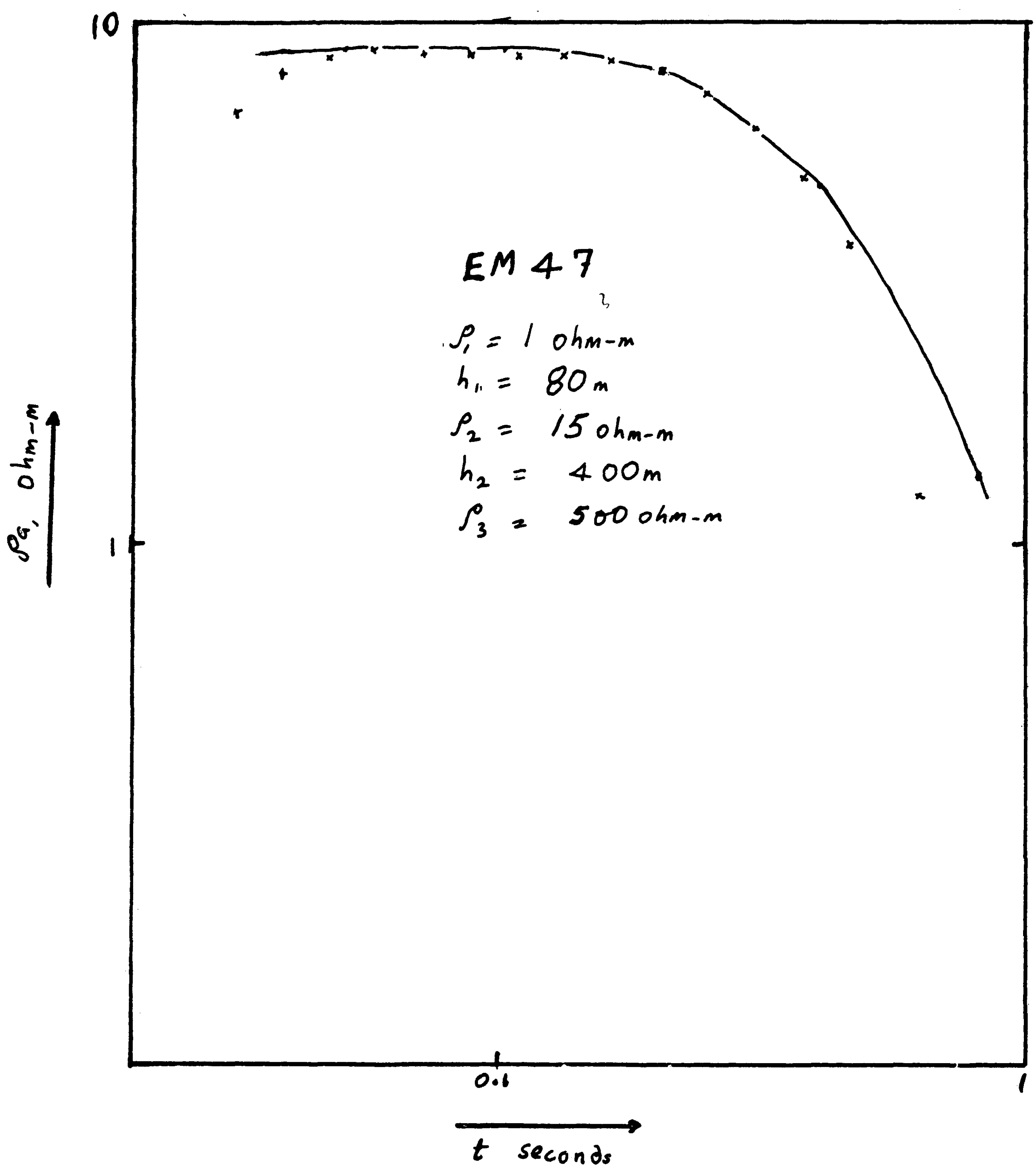

Deconvolved field curve and theoretical match, Station EM47.

APPENDIX B

Computer programs.

All programs are in the Fortran IV language.

SYSTEM .F4

This program generates the system response function used in the deconvolution of the field data.

```
COMMENT   SYSTEM FUNCTIONS
C      THIS PROGRAM GENERATES THE AMPLITUDE CORRECTION FACTOR
C       AND THE PHASE CORRECTION FACTOR WHICH ARE USED IN THE
C       DECONVOLUTION PROCESS IN THE PROGRAM STACK5.
C
C        ORIGINALLY PROGRAMMED BY DR. G. V. KELLER
C        MODIFIED BY OFIAFATE OFREY
C            MARCH,  1975.
C
C
      DIMENSION Z(100),Y(100),AR(100),C(100),PHC(100),AI(100)

          IN=17
          IOUT=18

  33  READ(IN,77) NUM,DT
   2  READ(IN,1)(Y(I),I=1,NUM)
   1  FORMAT(10F)
  77  FORMAT(I,F)
       SCALE=0.04
       DO 333 I=1,NUM
       Y(I)=(Y(I)-Y(NUM))*SCALE/18.*(1.0E-02)/(4.*3.1416)
 333   CONTINUE
      DO 444 I=1,NUM-1
       Y(I)=(Y(I)-Y(I+1))/DT
 444  CONTINUE
       NUM=NUM-1

      WRITE(IOUT,200) NUM
      IF(Y(1).LT.0.0) GO TO 1400
      IF(NUM.LT.41) GO TO 1300
1300   CONTINUE
      M=NUM
      DO 3008 J=1,M
      DW=3.1416*FLOAT(J)/FLOAT(M)
      C1=COS(DW)
      S1=SIN(DW)
      S2=S1
      C2=C1
      AR(J)=0.
      AI(J)=0.
      DO 3007 K=1,M
      AR(J)=AR(J)+Y(K)*C2
      AI(J)=AI(J)+Y(K)*S2
      C3=C2*C1-S2*S1
      S3=S2*C1+C2*S1
      S2=S3
3007  C2=C3
3008  AI(J)=-AI(J)
      AMP=SQRT(AR(1)*AR(1)+AI(1)*AI(1))
      DO 3009 I=1,M,2
      AM=SQRT(AR(I)*AR(I)+AI(I)*AI(I))
      PH=ATAN2(AI(I),AR(I))
      C(I)=AMP/FLOAT(I)/AM
      PHC(I)=1.5708-PH

3009   CONTINUE

      DO 16 I=1,M
```

```
      WRITE(IOUT,3001) C(I),PHC(I)
   16 CONTINUE
 1400 CONTINUE

      IF(Y(1).LT.0.0) WRITE(IOUT,400)
C       GO TO 33
 200  FORMAT(I3)
 300  FORMAT(20F4.0)
 400   FORMAT(' -1')
 3001 FORMAT(2E12.5)
      CALL EXIT
      END
```

STACK5.F4

This program does the stacking of the field records, carries out the deconvolution process and gives equally spaced data in the logarithm domain.

```
COMMENT FILE K7.F4 IS INTENDED FOR STACKING OF EM TRANSIENTS
COMMENT        INDEX1 IS NEGATIVE FOR WIRE TO WIRE COUPLING
COMMENT        INDEX1 IS ZERO FOR WIRE TO LOOP COUPLING
COMMENT        INDEX1 IS POSITIVE FOR LOOP TO LOOP COUPLING
COMMENT       FOR01,DAT IS THE FILE FOR INPUT DATA
C                   I.E  DIGITISED DATA
COMMENT       FOR02,DAT IS THE FILE FOR OUTPUT DATA
COMMENT             I.E.  STACKED DATA
COMMENT       FOR03,DAT IS THE FILE WITH SYSTEM RESPONSE
COMMENT      FOR08,DAT IS THE FILE CONTAINING DECONVOLVED FIELD DATA
COMMENT PROGRAM K7 CALLS K1003 AND K1005 AS SUBPROGRAMS
C
C
C
C             THIS IS A MODIFIED VERSION OF THE PROGRAM
C             STACK2,F4 BY DR. G. V. KELLER.
C                     OFIAFATE OFREY,
C                      MARCH, 1975.
C
C
C
C
      DIMENSION XX(20),X(20,100),A5(16),I(100),AV2(100),S(100),
     1A3(6),AV(100),RLATE(100),REARLY(100),Y2(100),C(100)
     2,PHC(100),JXX(100)
      I1=1
      I2=2
      I3=3
C       NPNT= NUMBER OF DIGITISED POINTS
C       C(I)=AMPLITUDE CORRECTION FACTOR
C       PHC= PHASE CORRECTION FACTOR
C       R = SOURCE RECEIVER SEPARATION IN METERS
C       A1 NOT USED
C       A2 NOT USED
C       CUR = CURRENT IN AMPERES
C       THETA = ANGLE DESCRIBING SOURCE - RECEIVER ORIENTATION
C       STN = STATION NUMBER
C       DT= DIGITISING INTERVAL OF FIELD RECORDS
C       SCALA = SCALE OF RECORD
C       MCASE=NUMBER OF DIGITISED RECORD PER STATION
        I44=8
       INDEX1=0
      NPNT=40
      DO 605 I=1,NPNT-1
  605 READ (I3,606) C(I),PHC(I)
  606 FORMAT(2E12.5)
 1019 FORMAT(I3,I2,F6.3)
      READ(I1,1005)R,A1,A2,CUR,THETA,BETA
 1005 FORMAT(6F)
      READ(I1 1009) (XX(I),I=1,3)
 1009 FORMAT(3F)
      SCALE=XX(3)/(XX(2)-XX(1))
C          THE FOLLOWING SECTION DOES THE STACKING OF THE
C                RECORDS    **************
 9999  READ(I1,1070)IN,STN,DT,SCALA,MCASE
      IF(IN.EQ.-1) STOP
 1070  FORMAT(I2,A4,2X,F5.3,2X,F4.2,2X,I1)
      WRITE(I44,1010) STN
 1010  FORMAT(4X,A4)
      NCASE=1
```

```
      SCALE=ABS(SCALE)
    2 NPNT=0
    3 CONTINUE
 1102 FORMAT(20(I3,1X))
      READ(I1,1102) (JXX(I),I=1,40)
      DO 1212 JK=1,40
      XX(JK)=FLOAT(JXX(JK))
 1212 CONTINUE
    9 DO 10 I=1,40
      NPNT=NPNT+1
   10 X(NCASE,NPNT)=XX(I)
       IF(NCASE.EQ.MCASE) GO TO 7
    8 CONTINUE
      NCASE=NCASE+1
      GO TO 2
    7 CONTINUE
      IF(INDEX1)20,21,21
   20 N4=NPNT-1
      DO 22 I=1,NPNT
      DO 22 J=1,NCASE
   22 X(J,I)=(X(J,I)-X(J,1))*SCALE*.000001
      DO 24 I=1,NCASE
      IF(X(I,3)) 25,24,24
   25 DO 27 J=1,NPNT
   27 X(I,J)=-X(I,J)
   24 CONTINUE
      GO TO 34
   21 CONTINUE
 1002 FORMAT(20F4.0)
      DO 32 I=2,NPNT
      DO 32 J=1,NCASE
   32 X(J,I)=X(J,I)-X(J,40)
      DO 33 I=2,NPNT
      DO 33 J=1,NCASE
   33 X(J,I)=X(J,I)*(SCALA/18.0)*(1.0E-02)/(4.0*3.1416)
      DO 34 I=1,NCASE
      IF(X(I,3))35,36,36
   35 DO 37 J=2,NPNT
   37 X(I,J)=-X(I,J)
   36 CONTINUE
   34 CONTINUE
      Z=FLOAT(NCASE)
      DO 310 JPNT=2,NPNT
      AV(JPNT)=0
      DO 309 JCASE=1,NCASE
  309 AV(JPNT)=AV(JPNT)+X(JCASE,JPNT)
  310 AV(JPNT)=AV(JPNT)/Z
      DO 312 JPNT=2,NPNT
      S(JPNT)=0
      DO 311 JCASE=1,NCASE
  311 S(JPNT)=S(JPNT)+(X(JCASE,JPNT)-AV(JPNT))**2
  312 S(JPNT)=SQRT(S(JPNT)/Z)
      WRITE(I2,1007) STN
      DO 315 JPNT=2,NPNT
      N(JPNT)=0
      AV2(JPNT)=0
       TEST1=2.*S(JPNT)
      DO 322 JCASE=1,NCASE
      TEST2=ABS(X(JCASE,JPNT)-AV(JPNT))
 1007 FORMAT(1H1,//2X,'EDITED AND STACKED DATA',4X,'STATION ' A4//,
```

```
      25X,'TIME',3X,'NUMBER',4X,'AVERAGE',6X,'ST. DEV.')
       IF(TEST2-TEST1)321,321,322
  321  AV2(JPNT)=AV2(JPNT)+X(JCASE,JPNT)
       N(JPNT)=N(JPNT)+1
  322  CONTINUE
  315  AV2(JPNT)=AV2(JPNT)/FLOAT(N(JPNT))
C
C       END OF THE STACKING PROCESS
C
       CALL K1001(R,A1,A2,CUR,THETA,BETA,INDEX1,FACTOR,SCALE
      2,XPNT1,XPT2)
       DO 333 JPNT=2,NPNT
  800  FORMAT(10X,'INDEX1=',I,/)
       IF(INDEX1) 601,602,602
  601  DCLEV=(AV2(NPNT-4)+AV2(NPNT-3)+AV2(NPNT-2))/3.
       REARLY(JPNT)= FACTOR*(AV2(JPNT)-DCLEV)
       RLATE(JPNT)= SCALE/(((AV2(JPNT)-DCLEV)*FLOAT(JPNT-1)
      1*DT)**XPNT1)
       GO TO 603
  602  CONTINUE
       REARLY(JPNT)=FACTOR*AV2(JPNT)
       RLATE(JPNT)=SCALE/(AV2(JPNT)*(FLOAT(JPNT-1)*DT)**XPNT1)
  603  CONTINUE
       IF(RLATE(JPNT))334,334,335
  334  RLATE(JPNT)=0
       GO TO 333
  335  RLATE(JPNT)=RLATE(JPNT)**XPT2
  333  CONTINUE
         DO 101 JPNT=2,NPNT
       TIME=FLOAT(JPNT-1)*DT
       WRITE(I2,1008) TIME,N(JPNT),AV2(JPNT),S(JPNT)
 1008  FORMAT(3X,F4.3,4X,I2,2(4X,E10.3))
  101  CONTINUE
         DO 2101 I=1,NPNT-1
 2101   AV2(I)=(AV2(I)-AV2(I+1))/DT
C       NPNT=NPNT-1
       CALL K1003(AV2,NPNT,Y2,C,PHC)
       IF(INDEX1) 701,702,702
  701  DO 704 J=2,NPNT
       DCDLEV=(Y2(NPNT-4)+Y2(NPNT-3)+Y2(NPNT-2))/3.
  704  Y2(J)=Y2(J)-DCDLEV
  702  CONTINUE
       DO 401 I=2,NPNT
       TIME=FLOAT(I-1)*DT
       R1=FACTOR*Y2(I)
       R2=SCALE/(Y2(I)*TIME**XPNT1)
       IF(R2)402,402,403
  402  R2=0
       GO TO 404
  403  R2=R2**XPT2
  404  CONTINUE
  401  CONTINUE
C       WRITE(I2,1015) (A5(I),I=1,10)
       DO 501 JPNT=30,NPNT
  501  Y2(JPNT)=AV2(JPNT)
       N3=NPNT-1
       DO 502 JPNT=1,N3
  502  Y2(JPNT)=Y2(JPNT+1)
 1015  FORMAT(/////,2X,10A5)
       CALL K1005(Y2,NPNT,DT,FACTOR,SCALE,2.5,.667,A3)
```

```
       GO TO 9999
      STOP
      END
COMMENT PROGRAM TO GNERATE GEOMETRIC FACTORS
C     NOT REQUIRED FOR THIS INTERPRETATION
C
C**************************************************************
      SUBROUTINE K1001(R,A1,A2,CUR,THETA,BETA,INDEX1,FACTOR
     2,SCALE,XPNT1,XPT2)
      IF(INDEX1)10,20,30
   10  XPNT1=1.5
      XPT2=2.0
      X=40.
      SCALE=X**1.5*1.E-12*CUR*A1*A2/12.
      FACTOR=(6.2832*R**3*COS(BETA/57.3))/((3.*SIN(THETA/57.3)**2
     2-2.)*CUR*A1*A2)
      GO TO 100
   20 XPNT1=2.5
      A1=A1*1000000.
      XPT2=.667
      FACTOR=6.2832*R**4/(A1*A2*CUR*COS(THETA/54.))/3.
      SCALE=A1*A2*CUR*.0793E-17
     2*R
      GO TO 100
   30 XPNT1=2.5
      A1=A1*1000000.
      A2=A2*1000000.
      XPT2=.667
      SCALE=CUR*A1*A2*15.9E-18
      FACTOR=6.2832*R**5*COS(BETA/54.)/9./CUR/A1/A2
  100 CONTINUE
      RETURN
      END
COMMENT SUBROUTINE DECON2
C      THIS SUBROUTINE CARRIES OUT THE DECONVOLUTION PROCESS
C      C IS THE AMPLITUDE CORRECTION FACTOR
C      PHC IS THE PHASE CORRECTION FACTOR
C      X IS THE STEP RESPONSE FUNCTION
C      NPNT IS THE NUMBER OF POINTS
C**************************************************************
      SUBROUTINE K1003 (X,NPNT,Y2,C,PHC)
                DIMENSION C(100),PHC(100),X(100),A(100),B(100),
     2PHX(100),V(100),Y2(100)
      X(1)=0.
      NUMBER=NPNT
      DO 7 J=1,NUMBER
      W=3.1416*FLOAT(J)/FLOAT(NUMBER)
      C1=COS(W)
      S1=SIN(W)
      C2=C1
      S2=S1
      A(J)=0
      B(J)=0
      DO 6 K=1,NUMBER
      A(J)=A(J)+X(K)*C2
      B(J)=B(J)+X(K)*S2
      C3=C2*C1-S2*S1
      S3=C2*S1+S2*C1
      C2=C3
      S2=S3
```

```
    6 CONTINUE
      B(J)=-B(J)
      PHX(J)=ATAN2(B(J),A(J))
      V(J)=SQRT(A(J)*A(J)+B(J)*B(J))
    7 CONTINUE
      DO 8 I=1,NUMBER,2
      V(I)=V(I)*C(I)
      PHX(I)=PHX(I)+PHC(I)
      A(I)=V(I)*COS(PHX(I))
    8 B(I)=V(I)*SIN(PHX(I))
      M2=NUMBER-1
      DO 3012 I=2,M2,2
      I2=I-1
      I3=I+1
      A(I)=(A(I2)+A(I3))/2.
 3012 B(I)=(B(I2)+B(I3))/2.
      DO 1  J=1, UMBER
      W=3.1416*FLOAT(J)/FLOAT(NUMBER)
      C1=COS(W)
      S1=SIN(W)
      C2=C1
      S2=S1
      Y2(J)=0
      DO 9 K=1,NUMBER
      Y2(J)=Y2(J)+B(K)*S2
      C3=C2*C1-S2*S1
      S3=C2*S1+S2*C1
      C2=C3
      S2=S3
    9 CONTINUE
      Y2(J)=Y2(J)/FLOAT(NUMBER)*2.
   10 CONTINUE
      RETURN
COMMENT SUBROUTINE TO CONVERT A TRANSIENT TO THE LOG DOMAIN
C        AND SMOOTH.
      END
C        V IS THE TRANSIENT
C        NPNT IS THE NUMBER OF POINTS IN THE TRANSIENT AT FIRST
C        DELTAT IS THE DIGITIZING INTERVAL IN SECONDS
C        FACTOR IS THE EARLY TIME GEOMETRIC FACTOR
C        SCALE IS THE LATE TIME GEOMETRIC FACTOR
C          XPNT1 IS THE EXPONENT ON TIME FOR LATE RESISTIVITY
C          XPT2 IS THE ROOT FOR LATE RESISTIVITY
C            WIRE/LOOP  XPNT1=2.5, XPT2=.6667, CALL K1006
C            WIRE/WIRE  XPNT1=1.5, XPT2=.6667, CALL K1007
C            LOOP/LOOP
C*****************************************************************
      SUBROUTINE K1005(V,NPNT,DELTAT,FACTOR,SCALE,XPNT1,XPT2,A5)
      DIMENSION V(100),T(100),X(400),Y1(100),A5(10)
     1,ABCD(16)
     1,SINT(100),DELTA(100)
      I22=2
      I44=8
      NUMBER=NPNT-1
      DO 1 I=1,NPNT
    1 T(I)=FLOAT(I)*DELTAT
      SHIFT=0
      VMAX=V(40)
      VMIN=VMAX
      DO 710 I=2,NUMBER
```

```
      IF(V(I)-VMIN)702,702,701
 701  VMAX=V(I)
 702  IF(V(I)-VMIN)703,710,710
 703  VMIN=V(I)
 710  CONTINUE
      SHIFT=0
      IF(VMIN) 711,713,713
 711  SHIFT=.01*(VMAX-VMIN)-VMIN
      DO 712 I=1,NUMBER
 712  V(I)=V(I)+SHIFT
 713  CONTINUE
      DT=ALOG(T(NUMBER)/T(NUMBER-1))
      RANGE=ALOG(T(NUMBER)/T(1))
      NEED =AINT(RANGE/DT)
      DO 11 I=1,NUMBER
      T(I)=ALOG(T(I))
  11  V(I)=ALOG(V(I))
      DO 21 I=1,NEED
      XI=FLOAT(I)
      TIME=XI*DT+T(1)-DT*.99
      J=1
  12  IF(TIME-T(J))14,14,13
  13  J=J+1
      IF(J-NUMBER)12,14,14
  14  J=J-1
      IF(J-2)15,15,16
  15  X(I)=0
      DO 151 K1=1,3
      TERM=V(K1)
      DO 153 K2=1,3
      IF(K1-K2) 154,153,154
 154  TERM=TERM*(TIME-T(K2))/(T(K1)-T(K2))
 153  CONTINUE
 151  X(I)=X(I)+TERM
      GO TO 21
  16  IF(J-NUMBER+2) 18,17,17
  17  X(I)=0
      N1=NUMBER-2
      DO 171 K1=N1,NUMBER
      TERM=V(K1)
      DO 173 K2=N1,NUMBER
      IF(K1-K2) 174,173,174
 174  TERM=TERM*(TIME-T(K2))/(T(K1)-T(K2))
 173  CONTINUE
 171  X(I)=X(I)+TERM
      GO TO 21
  18  X(I)=0
      N1=J-1
      N2=J+1
      DO 181 K1=N1,N2
      TERM=V(K1)
      DO 183 K2=N1,N2
      IF(K1-K2)184,183,184
 184  TERM=TERM*(TIME-T(K2))/(T(K1)-T(K2))
 183  CONTINUE
 181  X(I)=X(I)+TERM
  21  CONTINUE
      N3=NEED-4
      I2=1
      DO 6655 I=4,N3,4
```

```
      N4=I-3
            N5=I+3
      Y1(I2)=0
      DO 7655 I3=N4,N5
 7655 Y1(I2)=Y1(I2)+X(I3)
      Y1(I2)=Y1(I2)/7.
 6655 I2=I2+1
      SINT(1)=1./Y1(1)
      DO 6656 I=2,I2
      DELTA(I)=(2.*EXP(FLOAT(4*I+1)*DT+T(1)))/.1256E-09/Y1(I)
      DELTA(I)=SQRT(ABS(DELTA(I)))/100.
      SINT(I)=(DELTA(I)/Y1(I)-DELTA(I-1)/Y1(I-1))/(DELTA(I)-DELTA(I-1))
 6656 CONTINUE
      INDEX1=-1
      INDEX=1
      NCX=3
      NCY=3
      D=3.33
      XZERO=.01
      YZERO=.1
      IFLAG=
      WRITE(I22,1020)
 1020 FORMAT(1H1,2X,'ELECTROMAGNETIC INTERPRETATION:
     2NON-LINEAR FILTERING'//)
      WRITE(I22,4444)
C      WRITE (I44,998)NCX,NCY,D,XZERO,YZERO
      LASTPL=1
      IGRID=0
      IPOS=1
      INEG=2
C      WRITE(I44,910)LASTPL,IGRID,IPOS,INEG
  910 FORMAT(4I2)
 4444 FORMAT(3X,'TIME    EARLY     LATE        DELTA        DELTA',/
     211X,'RESIS.    RESIS.      DEPTH      CONDUCTANCE',//)
  998 FORMAT(2I10,3F10.0)
    7   FORMAT(2X,E13.5,3X,E13.5)
      DO 911 I8=1,16
  911 ABCD(I8)=0
C      WRITE(I44,912) (ABCD(I8),I8=1,16)
  912 FORMAT(16A5)
C      WRITE(I44,912) (A5(I),I=1,16)
      WRITE (I44,913) I2
  913 FORMAT(I3)
  997 FORMAT(5A5,I10)
  909 FORMAT(E12.5)
  908 FORMAT(I1)
      DO 7656 I=1,I2
      TIME=EXP(FLOAT(4*I+1)*DT+T(1))
      VOLT=EXP(Y1(I))-SHIFT
      RATIO=FACTOR*VOLT
      IF(VOLT)301,302,302
  301 VOLT=-VOLT
      RHO=(SCALE/(VOLT*TIME**XPNT1))**XPT2
      RHO=-RHO
      GO TO 303
  302 RHO=(SCALE/(VOLT*TIME**XPNT1))**XPT2
  303 CONTINUE
      WRITE (I44,7) TIME,VOLT
 7656 WRITE (I22,7657) TIME,RATIO,RHO,DELTA(I),SINT(I)
 7657 FORMAT(5X,F6.3,2(5X,F6.2),2(3X,E10.3))
```

```
RETURN
END
```

RHOA.F4

This program reads the output from STACK5.F4 and multiplies it by the geometric factor to obtain apparent resistivities.

```
COMMENT   THIS PROGRAM READS IN THE DECONVOLVED FIELD DATA
C       AND MULTIPLIES BY THE GEOMETRIC FACTOR
C
C       INPUT FILE = FOR08.DAT,FOR07.DAT
C       OUTPUT FILE =FOR01.DAT
C
C           OFIAFATE OFREY
C              MARCH 1975.
C
C
C
C
        DIMENSION T(50),H(50),RHOA(50)

         IN=8
          IN2=7
          IOUT=1

  1     READ(IN,10) N,STN
 10      FORMAT(I2,2X,A4)
         IF(N.EQ.-1)STOP
         READ(IN,20)NPNT
 20      FORMAT(I3)
         READ(IN2,30) SL,SI,R,THETA
 30      FORMAT(4F)
         PHI=22./7.
         SUS=4.*PHI*(1.0E-07)
         AN=PHI*THETA*2./360.
         SR=3.*SI*SL*COS(AN)
         FR=2.*PHI*SUS*(R**4.)
         FACTOR=(FR/SR)
         READ(IN,40)(T(I),H(I),I=1,NPNT)
C        WRITE(4,40)(T(I),H(I),I=1,NPNT)
 40      FORMAT(2X,E13.5,3X,E13.5)
         DO 50 I=1,NPNT
         RHOA(I)=FACTOR*H(I)
 50      CONTINUE
         DO 60 I=2,NPNT-1
 60      RHOA(I)=RHOA(I)+RHOA(I-1)/2.+RHOA(I+1)/2.
         DO 70 I=4,NPNT-3
 70      RHOA(I)=RHOA(I)/7.+RHOA(I-1)/7.+RHOA(I-2)/7.+RHOA(I-3)/7.
      1+RHOA(I+1)/7.+RHOA(I+2)/7.+RHOA(I+3)/7.
         WRITE(IOUT,80) NPNT
 80      FORMAT(I2)
         WRITE(IOUT,90) STN
 90      FORMAT(4X,A4)
        WRITE(IOUT,40)(T(I),RHOA(I),I=1,NPNT)
       GO TO 1
         END
```

EMFWD8.F4

The program computes theoretical curves for the vertical component of the electromagnetic field in the frequency domain.

```
COMMENT**********
C       PROGRAM TO GENERATE FREQUENCY-DOMAIN COUPLING CURVES FOR
C       A VERTICAL-AXIS LOOP RECEIVER AND A HORIZONTAL GROUNDED-
C       WIRE SOURCE.
C            INPUT FILE IS FOR09.DAT
C            OUTPUT FILE IS FOR11.DAT
C****************
        DIMENSION FREQ(100),Z(100),RH(10),TH(10),ALPHA(20)
        COMPLEX H(100)
        INDATA=9
        IOUT=11
      1 NLAYER=1
        READ(INDATA,1091)STN
   1091 FORMAT(A4)
        WRITE(IOUT,1091)STN
        READ (INDATA,1000) R
        WRITE(IOUT,3091)R
   3091 FORMAT(F7.1)
   1000 FORMAT (F)
   1001 FORMAT (2F)
   2001 FORMAT (//,2X,'FREQUENCY COUPLING BETWEEN GROUNDED WIRE AND LOOP')
   2002 FORMAT (2X,'LAYER',I2,' HAS RESISTIVITY OF ',F5.1,' AND
      & THICKNESS OF ',F6.1,/)
   2003 FORMAT (2X,'LAST LAYER HAS RESISTIVITY OF ',F5.1,/)
   2004 FORMAT (5X,'FREQUENCY',4X,'REAL',10X,'IMAGINARY',4X,'MAGNITUDE',/)
   2005 FORMAT (4(3X,E10.3))
      4 READ (INDATA,1001) RH(NLAYER),TH(NLAYER)
        IF (TH(NLAYER)) 6,5,5
      5 NLAYER=NLAYER+1
        GO TO 4
      6 CONTINUE
        FACTOR=SQRT(2.)
        FREQ(1)=0.001
        DO 8 I=2,30
      8 FREQ(I)=FACTOR*FREQ(I-1)
        NDATA=30
        CALL CURVE (NDATA,FREQ,NLAYER,RH,TH,H,R)
C        WRITE (IOUT,2001)
C        WRITE (IOUT,2000) R
   2000 FORMAT (/,2X,'SOURCE RECEIVER SEPARATION IS ',F7.1,/)
        DO 11 I=1,NLAYER-1
     11 WRITE(IOUT,2091)RH(I),TH(I)
   2091 FORMAT(4X,F5.1,2X,F6.1)
        WRITE(IOUT,2092)RH(NLAYER)
   2092 FORMAT(4X,F6.1)
C        DO 10 I=1,NLAYER-1
C   10 WRITE (IOUT,2002) I,RH(I),TH(I)
C        WRITE (IOUT,2003) RH(NLAYER)
C        WRITE (IOUT,2004)
        DO 12 I=1,NDATA
        X2=(REAL(H(I)))**2+(AIMAG(H(I)))**2
        X2=SQRT(X2)
     12 WRITE (IOUT,2005) FREQ(I),H(I),X2
C        GO TO 1
        STOP
        END
C**************
C       PROGRAM TO COMPUTE FREQUENCY DOMAIN COUPLING BETWEEN A
C       WIRE SOURCE AND A VERTICAL-AXIS LOOP RECEIVER, FROM J. DANIELS.
C**************
```

```
      SUBROUTINE CURVE (NFW,FF,N,RH,HP,H,R)
      DIMENSION HPP(1Ø),HP(1Ø),FF(1ØØ),D(1Ø),RK(1Ø),RH(1Ø)
      COMPLEX H(1ØØ),H2
C************************ VARIABLES *******************
C
C NFW= THE NUMBER OF FREQUENCIES TO BE CALCULATED
C R= SOURCE-RECEIVER SEPERATION
C FF=FREQUENCY IN HERTZ
C F=ANGULAR FREQUENCY
C N= THE NUMBER OF LAYERS
C HP(I)= LAYER THICKNESS
C RH(I)= LAYER RESISTIVITY
C CE(I)= COEFFICIENTS FOR CALCULATING THE JØ HANKEL TRANSFORM
C YE(I)= ABSSCISSA VALUES FOR CALCULATING CE(I)
C*****************************************************************
      COMMON /CV/ CI,DS,ANG,F,X,YH(48),CH(48),TM
      DATA
     &YH/-4.5327316E Ø,-4.3024731E Ø,-4.0702146E Ø,-3.8399561E Ø,
     &   -3.6096976E Ø,-3.3794391E Ø,-3.1491806E Ø,-2.9189221E Ø,
     &   -2.6886636E Ø,-2.4584051E Ø,-2.2281466E Ø,-1.9978881E Ø,
     &   -1.7676296E Ø,-1.5373711E Ø,-1.3071126E Ø,-1.0768541E Ø,
     &   -8.4659563E-1,-6.1633713E-1,-3.8607863E-1,-1.5582013E-1,
     & 7.4438359E-2,   3.0469687E-1,  5.3495537E-1, 7.6521387E-1,
     &    9.9547237E-1, 1.2257309E Ø, 1.4559894E Ø, 1.6862479E Ø,
     &   1.9165064E Ø, 2.1467649E Ø, 2.3770234E Ø, 2.6072819E Ø,
     &    2.8375404E Ø, 3.0677989E Ø,  3.2980574E Ø, 3.5283159E Ø,
     &    3.7585744E Ø, 3.9888329E Ø, 4.2190914E Ø, 4.4493499E Ø,
     &    4.6796084E Ø, 4.9098669E Ø, 5.1401254E Ø, 5.3703839E Ø,
     &    5.6006424E Ø, 5.8309009E Ø, 6.0611594E Ø, 6.2914179E Ø/
      DATA
     &CH/3.1410561E-6, 1.8802098E-5, 5.4019540E-5, 9.2891602E-6,
     &    1.5523239E-4, 3.0344652E-5, 3.5338744E-4, 1.4798022E-4,
     &    7.7342377E-4, 5.3570857E-4, 1.7170605E-3, 1.6387239E-3,
     &    3.9257683E-3, 4.5796505E-3, 9.2110468E-3, 1.2130467E-2,
     &    2.1938415E-2, 3.0853660E-2, 5.1973594E-2, 7.4661566E-2
     &    1.1775455E-1, 1.6353574E-1, 2.3127545E-1, 2.7368461E-1,
     &    2.0259285E-1, 1.2875840E-1, -1.5380437E-1,-4.5659951E-1,
     &   -3.6077766E-2, 4.2985683E-1,-2.1506075E-1,-2.3624312E-1,
     &    8.9316746E-2,-7.4344283E-2, 4.8572965E-2,-3.0089872E-2,
     &    1.8846544E-2,-1.2158687E-2, 8.0708759E-3,-5.4706275E-3,
     &    3.7554604E-3,-2.5929707E-3, 1.7909426E-3,-1.2320277E-3,
     &    8.4095286E-4,-5.6749747E-4, 3.7718405E-4,-1.5891635E-4/
      TM=12.566371E-7
      DO 2 JJ=1,N
    2 RK(JJ)=RH(1)/RH(JJ)
COMMENT RK IS RATIO OF LAYER RESISTIVITY TO RHO-1
      DO 21 I=1,NFW
      F=6.2831853*FF(I)
COMMENT IS FREQUENCE IN RADIANS PER SECOND
      DEL=SQRT(2.*RH(1)/(TM*F))
COMMENT DEL  IS THE WAVE NUMBER (REAL PART) IN LAYER 1
      DO 6  JJ=1,N
    6 D(JJ)=2.*HP(JJ)/DEL
COMMENT D(JJ) IS THE THICKNESS OF LAYER JJ IN TERMS OF FIRST-LAYER
C          SKIN DEPTHS
      X=ALOG(R/DEL)
COMMENT X IS THE LOGARITHM OF THE OFFSET DISTANCE MEASURED IN
C        SKIN DEPTHS IN THE FIRST LAYER
       CALL FV(RH,H2,RK,N,DEL,R,D)
      H(I)=H2
```

```
COMMENT TRAN IS THE REAL PART OF THE VERTICAL MAGNETIC FIELD
C        IN THE FREQUENCY DOMAIN
   20 CONTINUE
      RETURN
      END
C***********************
COMMENT    END OF SUBROUTINE CURVE
C************************
COMMENT SUBROUTINE FV(ALUE) IS USED IN SUBROUTINE CURVE TO COMPUTE
C        THE CONVOLUTION SUM OF THE HZ FIELD COMPONENT
C************************
      SUBROUTINE FV (RH,H,RK,N,DEL,R,D)
      DIMENSION RK(10),RH(10),D(10)
      COMMON /CV/ CI,DS,ANG,F,X,YH(48),CH(48),TM
      COMPLEX H,V1,F1,SUM,H1,C1,C2
      SUM=CMPLX(0.0,0.0)
      BB=EXP(X)
      C1=CMPLX(0.0,1.0)
      C2=CMPLX(1.0,1.0)
      DO 8 J=1,48
COMMENT DO LOOP TO DO CONVOLUTION OF BESSEL FILTER WEIGHTS FOR J1
      Y=EXP(-(X-YH(J)))
      CALL CALC(F1,V1,Y,RK,N,DEL,R,D)
      H=Y*Y*V1*(1.-F1)
      H=H/((Y+V1*F1)*(Y+V1))
      SUM=SUM+CH(J)*H
    8 CONTINUE
      H=SUM*C1*TM*F*R**3/3./DEL
      H1=3.-(3.+3.*C2*BB+2.*C1*BB**2)*CEXP(-C2*BB)
       H1=RH(1)*H1/3.
      H=H+H1
      RETURN
      END
C***********************
COMMENT SUBROUTINE TO CALCULATE THE LAYERED EARTH CORRECTION
C         FUNCTION, ALSO KNOW AS THE STEFANESCU FUNCTION OF THE
C         FIRST KIND
C***********************
      SUBROUTINE CALC(F1,V1,Y,RK,N,DEL,R,D)
      DIMENSION RK(10),RH(10),D(10)
      COMPLEX V1,F1,V2,AEX
      Y2=Y*Y
      T=2.*RK(N)
      V2=CSQRT(CMPLX(Y2,T))
      DO 9 LL=2,N
      IF(LL.GT.2) GO TO 4
      F1=CMPLX(1.0,0.0)
    4 I=N-LL+1
      DD=D(I)
      T=2.*RK(I)
      V1=CSQRT(CMPLX(Y2,T))
      AEX=(1.-CEXP(-V1*DD))/(1.+CEXP(-V1*DD))
      F1=(V2*F1+V1*AEX)/(V1+V2*F1*AEX)
    9 V2=V1
      RETURN
      END
```

TRANS3.F4

This program Fourier transforms the curves computed by EMFWD8.F4 into time domain using the polygonal approximation method and also calculates the step response.

```
C::::::::::::::::::::::::::::::::::::::::::::::::::::::::::::::::::::::::::::::
C        THIS PROGRAM CALCULATES THE COSINE TRANSFORM OF THE REAL PART
C   OF ANY FUNCTION, A POLYGONAL-APPROXIMATION TRANSFORM
C   METHOD IS USED.  THE STEP RESPONSE IS ALSO CALCULATED.
C:::::::
C   INPUT FILE -- FOR01.DAT       OUTPUT FILE -- FOR02.DAT
C::::::::::::::::::::::::::::::::::::::::::::::::::::::::::::::::::::::::::::::
      DIMENSION R(25),D(25),XX(200),YY(200),W(200),F(200),S(200)
  3       READ(11,2093)STN
      READ(11,2095)SR
 2095 FORMAT(F7.1)
 2093 FORMAT(A4)
      WRITE(2,2094)STN
      WRITE(2,2096)SR
 2096 FORMAT(/'SOURCE-RECEIVER SEPARATION IS',1X,F7.1,'METERS')
 2094 FORMAT('STATION NUMBER IS ',4X,'****',A4,'****')
      READ(11,2091)R(1),D(1)
      READ(11,2092)R(2)
 2091 FORMAT(4X,F5.1,2X,F6.1)
 2092 FORMAT(4X,F6.1)
102   FORMAT(3(3X,E10.3))
101   FORMAT(5F)
      PI=3.1415926
      WRITE(2,71)
      N=2
      WRITE(2,1003) (R(I),D(I),I=1,N)
1003   FORMAT(20X,' RESISTIVITY=',E10.2,5X,'THICKNESS=',E10.3)
C      I=1
37      READ(11,102)(W(I),XX(I),YY(I),I=1,30)
C      IF(W(I).GT.20.0) GO TO 38
C      I=I+1
C      GO TO 37
71    FORMAT(//' TIME-DOMAIN CURVE FROM COSINE TRANSFORM OF H(J)',5X,
     1'STEP RESPONSE OF THE TIME CURVE')
38    WRITE(2,72)
72    FORMAT(//6X,'TIME',8X,'AMPLITUDE',30X,'TIME',8X,'AMPLITUDE')
      T=0.0
      FZERO=0.
C  CALCULATE THE ZERO-TIME VALUE
      DO 4  N=1,I-1
4     FZERO = FZERO +((1.0/PI)*(XX(N+1)-XX(N))*(W(N+1)-W(N)))
7     FORMAT(2E15.7,22X,2E15.7)
C  CALCULATE THE TIME-DOMAIN CURVE
      T=.0001
      DO 6  K=1,1000
      F(K)=0.0
      DO 5  J=1,I-1
5     F(K)=F(K)+(2.0/(PI*T**2))*((XX(J)-XX(J+1))/(W(J+1)-W(J)))*
     1(COS(W(J)*T)-COS(W(J+1)*T))
       F(K)=ABS(F(K))
      T=T*2.0
      IF(T.GT.1000.) GO TO 100
6     CONTINUE
C  CALCULATE THE STEP RESPONSE
100   DO 18  JJ=1,I
18    XX(JJ)=XX(JJ)/(-1.0*W(JJ))
      T=0.0
      SZERO=0.0
      DO 14  N=1,I-1
14    SZERO=SZERO+((1.0/PI)*(XX(N+1)-XX(N))*(W(N+1)-W(N)))
```

```
      WRITE(2,7)T,FZERO,T,SZERO
      T=.0001
      DO 16  K=1,1000
      S(K)=0.0
      DO 15  J=1,I-1
15    S(K)=S(K)+(2.0/(PI*T**2))*((XX(J)-XX(J+1))/(W(J+1)-W(J)))*
     1(COS(W(J)*T)-COS(W(J+1)*T))
      S(K)=ABS(S(K))
      WRITE(2,7) T,F(K),T,S(K)
      T=T*2.0
      IF(T.GT.1000.) GO TO 103
16    CONTINUE
  103 CONTINUE
C      GO TO 3
1000  STOP
      END
```

REFERENCES

1. Boham, H.F. (1969), Geology and Mineral Deposits of Washoe and Storey Counties, Nevada. Bull 70, Nevada Bureau of Mines.

2. Clarke, John (1974), Josephson Junction Detectors, Science: Vol. 184, No. 4143.

3. Daniel, J.J. (1974), Interpretation of Electromagnetic Sounding Using a Layered Earth Model. Ph.D. Thesis 1627, Colorado School of Mines.

4. Frischknecht, F.C. (1967), Field about an oscillating magnetic dipole over a two-layer earth and application to ground and airborne electromagnetic survey. Colorado School of Mines Quarterly, Vol. 62, No. 1.

5. Keller, G.V., and Grose, L.T. (1974), The Colorado School of Mines Nevada Geothermal Study - Report of Progress for the Period May 1 - July 31, 1974.

6. Keller, G.V (1968), Electrical prospecting for oil. Colorado School of Mines Quarterly, Vol. 63, No. 2.

7. _____ and Frischknecht, F.C. (1966), Electrical Methods in Geophysical Prospecting. London Pergamon Press.

8. King, C.A. (1971), Time-domain Electromagnetic Coupling, M.Sc. Thesis 1427, Colorado School of Mines.

9. Papoulis, A. (1962), The Fourier Integral and Its Applications, New York, McGraw-Hill Book Co.

10. Pritchard, J I. (1971), The Theory of Electromagnetic Soundings in the Frequency Domain, Ph.D. Thesis 1364, Colorado School of Mines.

11. Silva, R. (1969), Two Layer Master Curves for Electromagnetic Sounding, M.Sc. Thesis 1250, Colorado School of Mines.

12. Skokan, C.K. (1974), A Time Domain Electromagnetic Survey of the East Rift Zone, Kilauea Volcano, Hawaii. Ph.D. Thesis 1700, Colorado School of Mines.

13. Wait, J.R. (1961), The Electromagnetic Fields of a Horizontal Dipole in the Presence of a Conducting Half Space. Can. J. of Physics, V. 39, p. 1017-1027

14. _____ (1966a), Electromagnetic Fields of a Dipole Over an Isotropic Half Space. Can. J. of Physics, V. 44, p. 2387-2401.

15. _____ (1966b), Fields of a Horizontal Dipole Over a Stratified Anisotropic Half Space, IEEE Trans. Ant. and Prop., V. 14, No. 6.

16. Willden, R. (1964), Geology and Mineral Deposits of Humboldt County, Nevada, Bull. 59, Nevada Bureau of Mines.

17. Vanyan, L.L. et al (1967), Electromagnetic Depth Soundings, New York Consultants Bureau.